DESIGN AND IMPLEMENTATION OF A MICROPROCESSOR-BASED ADAPTIVE PROTECTION FOR A DISTRIBUTION NETWORK

A Thesis

Submitted to the College of Graduate Studies and Research

in Partial Fulfilment of the Requirements

for the Degree of

Doctor of Philosophy

in the

Department of Electrical Engineering

University of Saskatchewan

by

BIJOY CHATTOPADHYAY

Saskatoon, Saskatchewan

June 1993

In the fond memory of
my father

COPYRIGHT

ACKNOWLEDGEMENTS

The author expresses his appreciation and gratitude to Dr. M.S. Sachdev for his supervision of this work. His advice and assistance in the preparation of this thesis is thankfully acknowledged.

The author also acknowledges the help of Dr. T.S. Sidhu in procuring the equipment and providing assistance in many ways. The author is thankful to Dr. M. Hojati of Department of Finance and Management Science at the University of Saskatchewan for many valuable discussions on optimization.

The author wishes to express his deepest gratitude to his wife, Sujata, and daughter, Arhana, for their constant encouragement and support. Special thanks are extended to his mother, parents-in-law and to all other family members for their support in making this project a reality.

The author is also thankful to Dr. P. Pramanick, T. Adu, W. Guttormson and R. Das for their helps in the preparation of the thesis. Financial assistance provided by the University of Saskatchewan through its Graduate Scholarship and by the NSERC is thankfully acknowledged.

UNIVERSITY OF SASKATCHEWAN

Electrical Engineering Abstract 93A379

DESIGN AND IMPLEMENTATION OF A MICROPROCESSOR-BASED ADAPTIVE PROTECTION FOR A DISTRIBUTION NETWORK

Student: Bijoy Chattopadhyay Supervisor: Dr. M.S. Sachdev

Ph.D. Thesis Submitted to the
College of Graduate Studies and Research
June 1993

ABSTRACT

The development of microprocessor-based relays started in early 1970's. Many researchers have had the view that long range economic trend favours the use of microprocessors in protective relays. As a result, for the last 25 years an extensive research has been carried out on digital protection. The research, design and economics of microprocessor-based relays reached to a stage where commercial production began in the early 1980's.

While microprocessor-based relays are being used by many utilities, the protection philosophy remains the same. In the present practice, abnormal operating conditions are analyzed *a priori* and relays are set considering all contingencies. Since it is difficult to identify all operating conditions in advance, and determine a set of relay settings that are optimum for all operating states, compromises are made in determining the settings. This results in the relays having inadequate selectivity, higher operating times and even failure to operate in some conditions. Researchers are now investigating whether the capabilities of microprocessor based relays can be fully utilized and dynamic conditions of power systems can be included in the protection system. This approach, known as adaptive protection, allows the utility engineers to change the settings of relays as the system conditions change.

The work reported in this thesis includes the designs of two major software packages developed for adaptive protection of a distribution network. One software

package is for performing the relaying tasks and the other software package is for relay settings and checking coordinations. The relaying software was implemented on TMS320C25 DSP microprocessors and relay setting and coordination software was implemented in a personal computer. Also, two communication application softwares were developed; these softwares used two commercial packages for communication between the relays, station controller and a central control computer. A small scale prototype was designed and built in the power system laboratory at the University of Saskatchewan.

The thesis also examines the improvement that can be achieved by applying the adaptive protection approach to a distribution network. Results reported in the thesis demonstrate that the use of adaptive protection minimizes relay operating times and improves coordination between relays.

Table of Contents

List of Figures

List of Tables

1. INTRODUCTION

1.1. Background

An electric power system generates, transmits and distributes electric energy. It is composed of electrical equipments, such as generators, transformers, lines, switchgear and associated devices. Abnormalities and faults can severely damage the system equipment and can cause severe reduction of voltage, loss of synchronism, prolonged outages of the equipment and consequently substantial loss of revenue. Therefore, it is necessary to protect all power system components to limit damage due to faults.

1.2. Power System Protection

The protection of a power system is accomplished by using relays and circuit breakers. The relays recognise the existence of a fault, determine its location and initiate opening of circuit breakers for isolating the faulted equipment. While protective relays must respond to abnormal operating conditions without delay, they should not operate during the normal operation of the system. Therefore, the success of a protection system depends on its sensitivity and selectivity.

Figure 1.1 shows a power system which is divided into several zones for protection purposes [1]. Each zone covers one or more components of the system. The neighbouring zones overlap so that no part of the system is unprotected. Each zone is protected by dedicated relays, circuit breakers and associated equipment. During abnormal conditions, relays identify this condition and then send trip signals to appropriate circuit breakers which open to isolate the affected zone from the power system.

Two sets of relays, primary and backup, are usually provided for each zone of

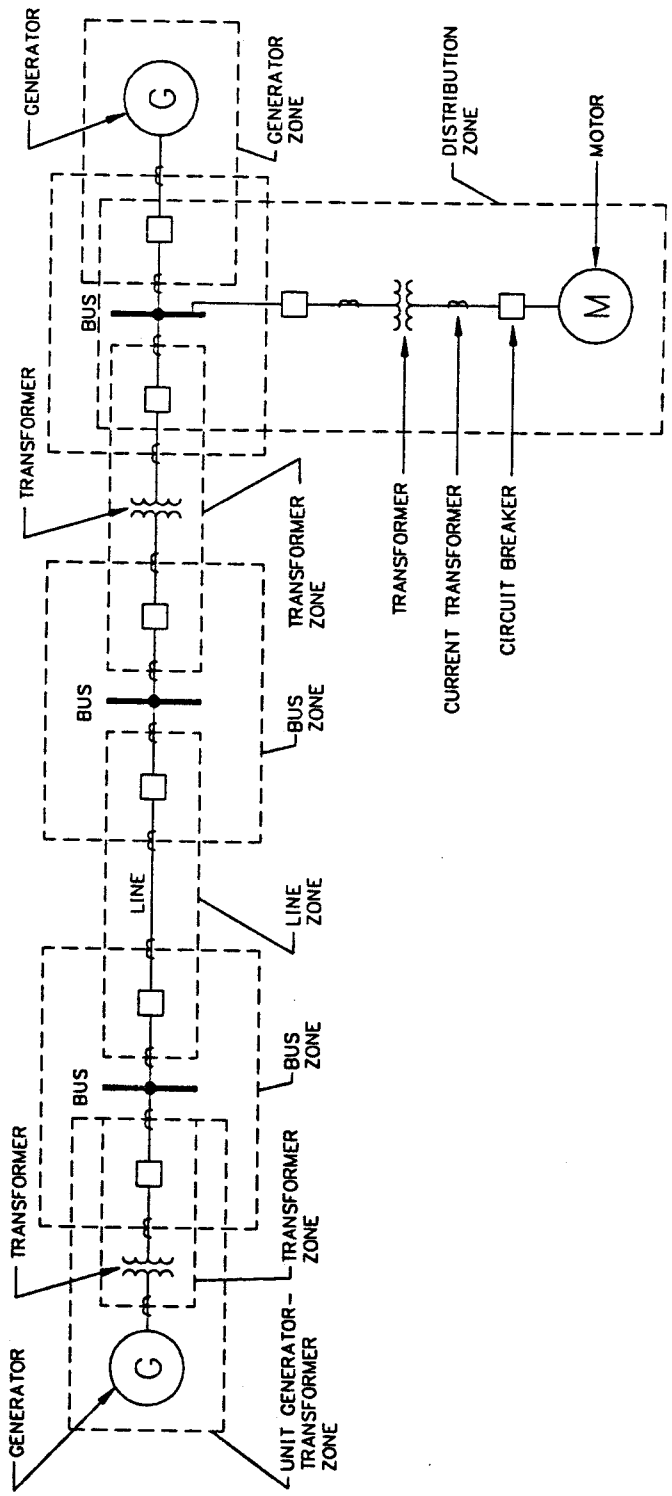

Figure 1.1: Typical zones for primary protection in a power system.

protection [2]. The purpose of a primary relay is to detect a fault in its zone of protection and initiate control actions for isolating the faulted zone as quickly as possible. If a primary relay fails, backup relays operate after a predetermined time-delay and isolate the faulted zone as well as the adjoining zone(s).

1.3. Past and Present Trends in Power System Protection

Fuses were the first automatic devices used for isolating the faulted equipment from the system. It is effective but suffers from the disadvantage that it must be replaced after every operation. Also, a fuse cannot discriminate faults on its line side from those on its bus side.

A significant improvement in power system protection was achieved with the introduction of automatic circuit breakers and the development of electromechanical relays that initiate tripping of circuit breakers when pre-specified operating conditions were encountered. Protective devices with greater sensitivity, better selectivity and faster speed were gradually developed for applications in power systems which became increasingly complex with the passage of time.

The development of solid state electronic relays started in the 1950's. In the early stages, these relays were not generally accepted by the users because of high failure rates of electronic components and inappropriate relay designs. Today, several kinds of solid state relays are used in power systems.

The complexity of modern power systems requires that protective relays be reliable and accurate. To achieve these characteristics in electromechanical and solid state devices requires that high-precision analog components be used. Recent developments in the field of digital electronics have made it possible to build microprocessor-based relays which provide a viable alternative to the presently used electromechanical and solid state devices. Microprocessor based relays use software for interpreting signals and implementing logic. Memory storage capabilities of these relays are used to save useful information concerning pre and post-fault currents and voltages. This information can be examined and analysed later for developing improved operating practices and relay design.

G.D. Rockefeller [3] presented one of the earliest papers that examined the feasibility of using a digital computer for protecting equipment in a major substation and transmission lines emanating from it. The intention was to use two main frame computers, a main and a standby, for performing all protection functions. This concept has been discarded in favour of using an individual microprocessor or a combination of microprocessors for each relaying task.

The first digital relay was installed at the Tesla substation of the Pacific Gas and Electric Company (PG & E) as a joint venture between the Westinghouse Electric Corporation and PG & E [4]. Many researchers have been of the view for many years that the long range economic trend favours the use of microprocessors in protective relay designs. Because of this reason, extensive research on digital protection has been carried out for the last 25 years. The research, design and economics of microprocessor-based relays reached to a level where commercial production began several years ago.

1.3.1. Adaptive Protection as a Future Trend

Although microprocessor based relays are presently being used by many utilities, the protection philosophy remains the same. In the present practice, abnormal operating conditions are analyzed a priori. The relay settings, that would maintain coordinations between all primary and backup relays, are then determined. Two major difficulties are encountered in this practice; firstly, identifying all contingencies of concern in advance and secondly determining a set of relay settings that would be optimum for all normal and abnormal operating conditions. This results in inadequate selectivity and higher operating times, and even failure to operate during some operating conditions. Several attempts have been made in the past to alleviate such problems but only partial success has been achieved. The bottle neck has been the type of technology used to design and manufacture relays.

With the development of microprocessor-based relays [5, 6], it has become feasible to design a system that can adapt to the system changes because digital relays can collect information, handle complex logic, and communicate with other relays and control devices. Hence, it is possible to continuously monitor the state of a power system,

analyze it in real-time, and change the relay settings to those most appropriate at that time. This approach, classified as adaptive relaying, has become a challenge to many researchers.

In recent years, several proposals on adaptive relaying have been reported. Sachdev and Wood [7] described the concept of adaptive relaying applied to a distribution system. Rockefeller et al. [8] illustrated the philosophy of adaptive protection for transmission lines. They indicated that most of the concepts require a hierarchical computer structure to process power system information and determine new settings. Horowitz et al. [9] investigated adaptive reclosing which would eliminate the possibility of reclosing into multiphase faults. They have also illustrated some benefits in transformer protection when adaptive approach is considered. Monitoring the transformer tap and using the correct turns ratio in computing the trip and restraint currents, a digital relay could use smaller pickup and slope settings than normally required.

Shah et al. [10] proposed the use of different characteristics of overcurrent relays for different system operating conditions. They also discussed the technical feasibility and economic viability of adaptive protection. A cost comparison of adaptive protection with respect to benefits reported in that paper, indicates benefit-to-cost ratio of 4.3 to 33. Jampala et al. [11] described some software aspects of adaptive transmission protection. They suggested that a multiprocessing concept would be suitable in adaptive protection for real time computation of relay settings and coordination.

1.4. Objectives of the Thesis

The work reported in this thesis has the following major objectives.

- To develop the software necessary for implementing an adaptive protection system. The software is developed in such a manner that the adaptive relaying concept can be applied to the distribution system of the 'City of Saskatoon'.

- To design, build and test a small scale prototype system in the laboratory.

1.5. Outline of the Thesis

The thesis is organised in ten chapters and seven appendices. The first chapter introduces the subject of the thesis and describes its organization. The present protection philosophy is outlined and future trend of using adaptive relaying is discussed.

Chapter 2 describes a typical distribution system and provides a brief review of the protection schemes used for distribution networks. Microprocessor based overcurrent relay algorithms consist of three software segments: modelling time-current characteristics, estimating phasors of the fundamental frequency currents and voltages and implementing trip logic. Chapter 3 reviews the presently available techniques for modelling the time-current characteristics, and estimating current and voltage phasors.

Chapter 4 discusses some of the present protection problems experienced in distribution systems. The areas where adaptive relaying would benefit most are identified. The functions of adaptive protection for a typical substation have also been included in that chapter. The adaptive relaying concept has been applied to a distribution system which is a reduced version of the 'City of Saskatoon' network. The selected network is described in Chapter 4. This network requires specific instrumentation which is identified. Some details of current transformers and analog-to-digital converters are also discussed in that chapter.

Two major software packages are required to design an adaptive protection system, one for the relaying and the other for calculating appropriate settings. The presently available algorithms for overcurrent relays were modified for use in the adaptive application. The necessary modifications and additions along with the development of relaying software are described in Chapter 5. The implementation of the software on a TMS 320C25 DSP microprocessor is also outlined.

The relay setting and coordination software is discussed in Chapter 6. This software consists of four modules: network topology detection, state estimation, fault analysis and determining appropriate relay settings. The mathematical development of each module is

described in that chapter. The software, developed in Chapters 5 and 6, were implemented and a prototype system was put together in the Power Systems Laboratory at the University of Saskatchewan. Chapter 7 discusses the hardware and the implementation of the laboratory model.

Chapter 8 reports the results obtained from system studies for which four different operating conditions were considered. The results show that using the adaptive approach reduces the relay operating times considerably. Also, selectivity in relay coordination improves. In some cases, failure to operate the relays are alleviated by the adaptive approach.

Chapter 9 provides a summary of the thesis and draws conclusions from the work reported in the thesis. The main conclusions are that the adaptive approach improves system protection by lowering the relay operating times and maintains coordination among the relays at the operating conditions studied during the work for this thesis. A list of references is given in Chapter 10.

This thesis also contains seven appendices. Appropriate selection of current transformers is important both for instrumentation and relaying. Appendix A describes the method used for calculating the ratings of current transformers. Auxiliary transformers are needed for reducing analog signal levels before they are provided to analog-to-digital converters. Appendix B describes the procedure for selecting the ratings of auxiliary transformers. Since the noise in a signal affects its measurement, the impact of the noise on the selected algorithm must be considered. Appendix C discusses these aspects for the selected nonrecursive filter. The decoupled load flow technique is described in Appendix D. Simplex method has been used to develop the relay coordination algorithm. Appendix E describes the simplex method. In developing a communication software for exchanging information between relays and substation control computer, a commercially available record management software has been used. Some details of this software are provided in Appendix F. Some of the test results are illustrated in Appendix G.

The specific contributions made by this project includes the following:

1. High ratio of fault current to load current causes difficulties in selecting current transformers and analog-to-digital converters. Techniques to alleviate these problems are discussed in Chapter 4.
2. The software necessary for the functioning of adaptive relays were developed and are reported in Chapter 5.
3. A technique for setting and coordinating relays adaptively was developed and is described in Chapter 6.
4. A microprocessor based adaptive protection system was designed, implemented and tested. The details are reported in Chapter 7.

2. PROTECTION OF DISTRIBUTION SYSTEMS

2.1. Introduction

Distribution networks of an electric power system link bulk sources of energy to customers' facilities. To perform this task, distribution networks include lines, transformers, buses, reactors, capacitors, circuit breakers and switches. If an outage occurs on a distribution circuit, supply to the customers is interrupted. It is estimated that 80% of all interruptions occur due to failures in distribution systems [12]. It is, therefore, important that systems used for protecting a distribution network be secure and dependable.

This chapter first describes a typical distribution system and then presents techniques used for protecting it.

2.2. A Typical Distribution System

A typical distribution system is shown in Figure 2.1. It includes subtransmission circuits, substations, feeders, transformers, secondary circuits and services to customers' premises. The subtransmission circuits transport energy from bulk power sources to the distribution substations over voltages that ranges from 12 to 245 kv. A distribution substation includes power transformers, buses, reactors, capacitors, circuit breakers and switches. The transformers reduce the voltages from the subtransmission levels to lower levels for local distribution. Three-phase primary distribution feeders, which operate at voltages ranging from 4.16 to 34.5 kv, distribute energy to load centres. From there, the circuits branch into three-phase subfeeders and single phase laterals.

Distribution transformers of 10 to 500 kva size are usually installed on primary feeders and subfeeders. They reduce the distribution voltage to the utilization level.

Secondary circuits facilitate distribution of energy from distribution transformers to the customers through service drops.

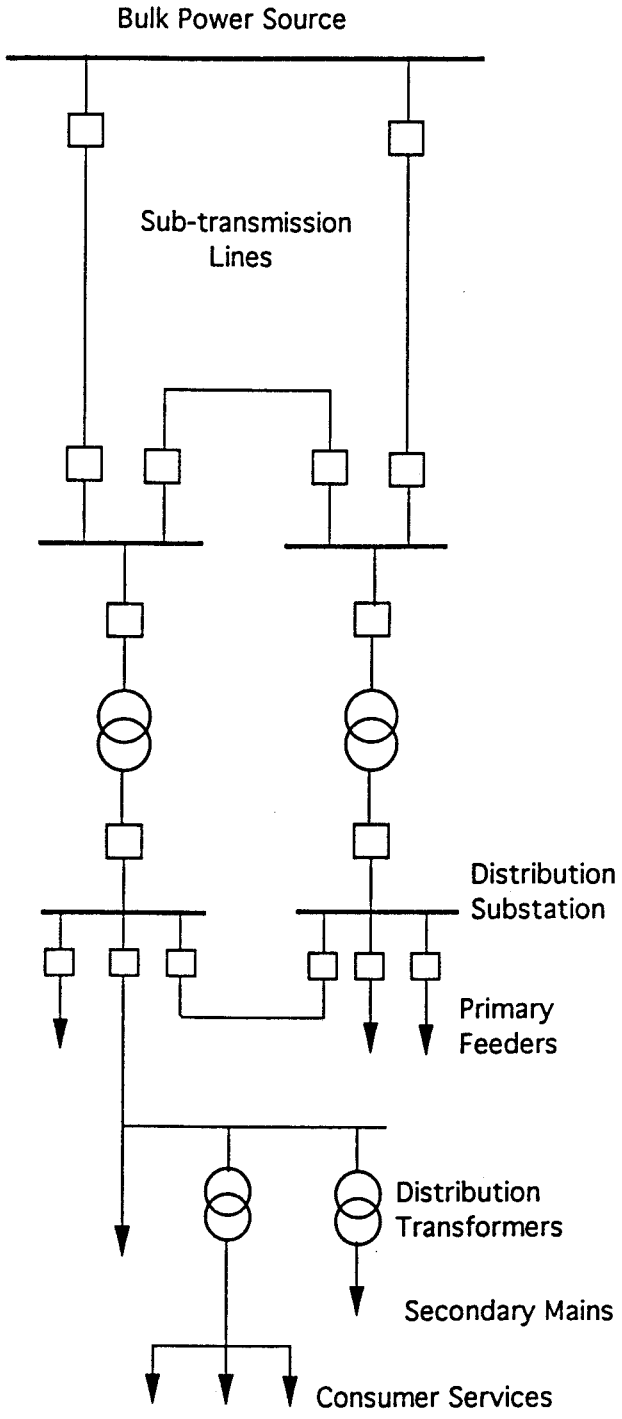

Figure 2.1: A typical distribution network.

2.3. Protecting Distribution Systems

The most commonly used techniques for detecting faults and isolating the faulted circuits are

1. time overcurrent relaying,
2. instantaneous overcurrent relaying,
3. directional overcurrent relaying,
4. distance protection and
5. pilot relaying.

2.3.1. Time-Overcurrent Protection

The most popular techniques to protect distribution systems are the time-overcurrent schemes. These are based on the principle that currents flowing in a line during a fault are more than the normal load currents. The techniques include the time-graded, current-graded or time-current graded methods.

2.3.1.1. Time-Graded Protection

Time-graded protection is applied to radial circuits which have a few line sections in series. To ensure selectivity of operation, the relays closest to the source are set to operate with maximum time delays. The delay is decreased as the location of a relay moves away from the source. Definite time delay relays are generally used in these applications. Figure 2.2 illustrates the principle of time-graded overcurrent protection of a radial feeder. As the number of relays increases, the operating time of the relay nearest to the source increases. When this form of protection is used, faults near the source which have large current magnitudes, are cleared after larger time delays compared to the faults at remote locations which have relatively small magnitudes of currents flowing in them. This application is preferred for systems in which levels of fault currents do not vary substantially with the fault locations.

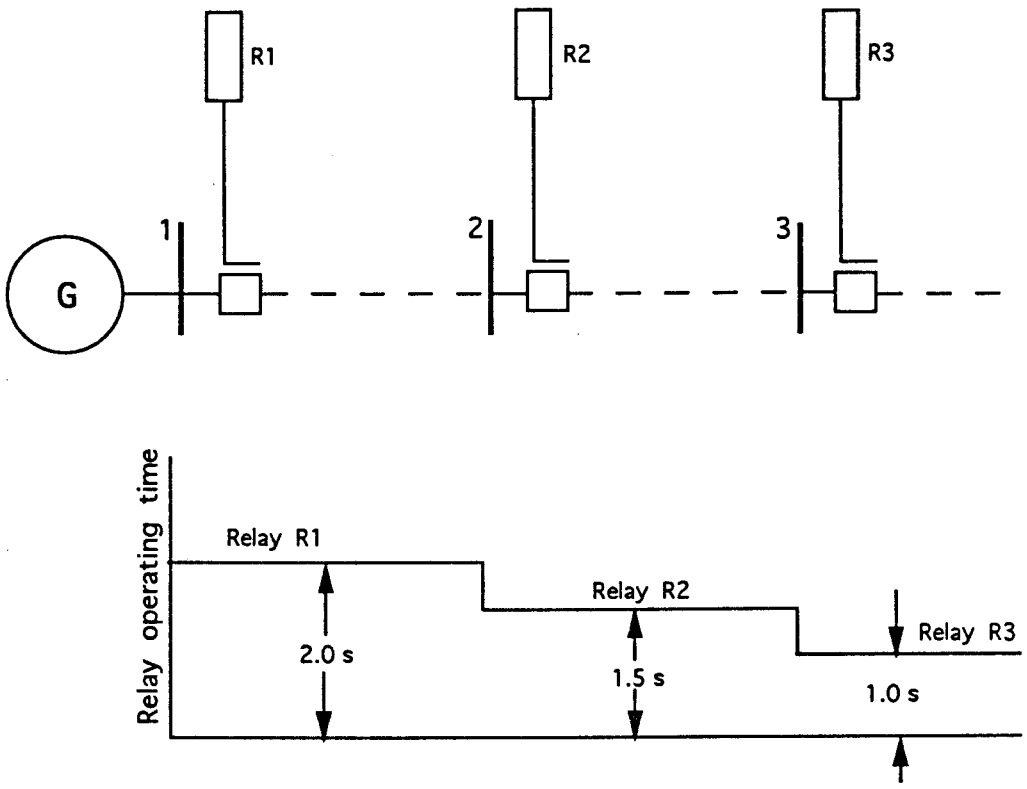

G: Generator

Figure 2.2: Time-graded overcurrent relaying scheme for protecting a radial circuit.

2.3.1.2. Current-Graded Protection

Short-circuit currents for faults along the length of a protected circuit decrease as the distance from the source to the fault increases. If the relays closer to the source are set to pickup at a progressively higher current, the disadvantage of long time delays that occur with time grading can be partially overcome. This approach, known as current grading, is used in distribution systems. These relays are known as high set overcurrent relays.

Figure 2.3 illustrates the simple current-graded scheme. Each relay is set to pickup at a progressively higher current towards the source. The settings of relays R_1, R_2, R_3 are such that relay R_1 operates for faults on the line from bus 1 to bus 2, the relay R_2 for faults from bus 2 to bus 3, relay R_3 for faults beyond bus 3. Although discrimination is achieved in this manner, the following difficulties are encountered:

1. The relay cannot distinguish faults between two sides of the bus because the fault current magnitudes are the same.
2. Small difference in source impedance may cause problem in relay operation because of change in fault current.

2.3.1.3. Current-Time Scheme

Both, time and current graded protection methods have serious disadvantages. A time-graded scheme clears more severe faults after long time delays. A current-graded scheme can be applied only if the impedance of the circuit, between the two adjacent relays, are substantial. To alleviate these problems, relays with inverse time-current characteristics are used. These characteristics are represented by a family of curves showing the contact closing time of the relay versus the current in the relay. Figure 2.4 shows the current-time characteristics for an overcurrent relay. To achieve a desired contact closing time for a specified current, an appropriate time dial setting is selected. Although, infinite operating characteristics can be achieved by adjusting the time dial setting, a finite number of curves are used in practice.

The inverse time overcurrent relays have shorter operating times for faults near the power source compared to operating times for remote faults. Figure 2.5 shows that these relays provide faster clearing than definite-time relays.

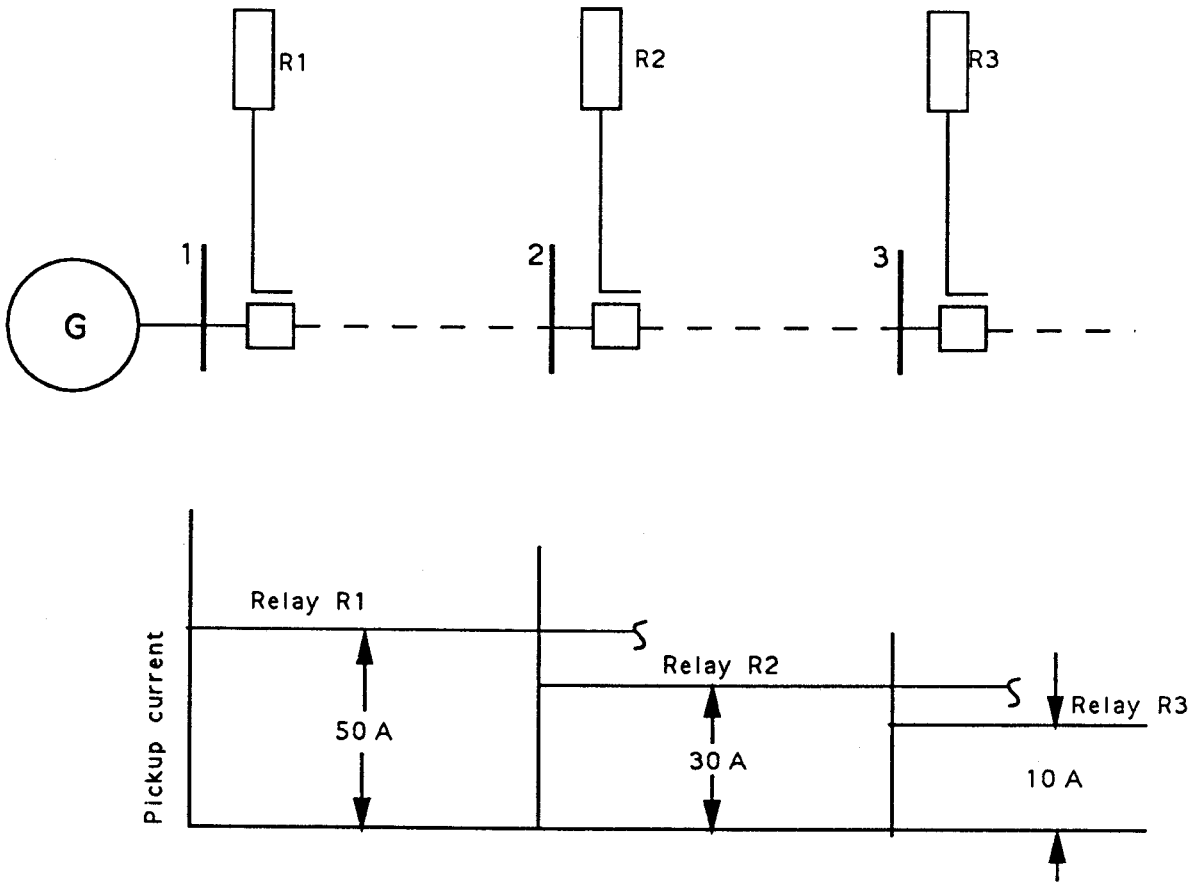

Figure 2.3: Current-graded protection for a radial circuit.

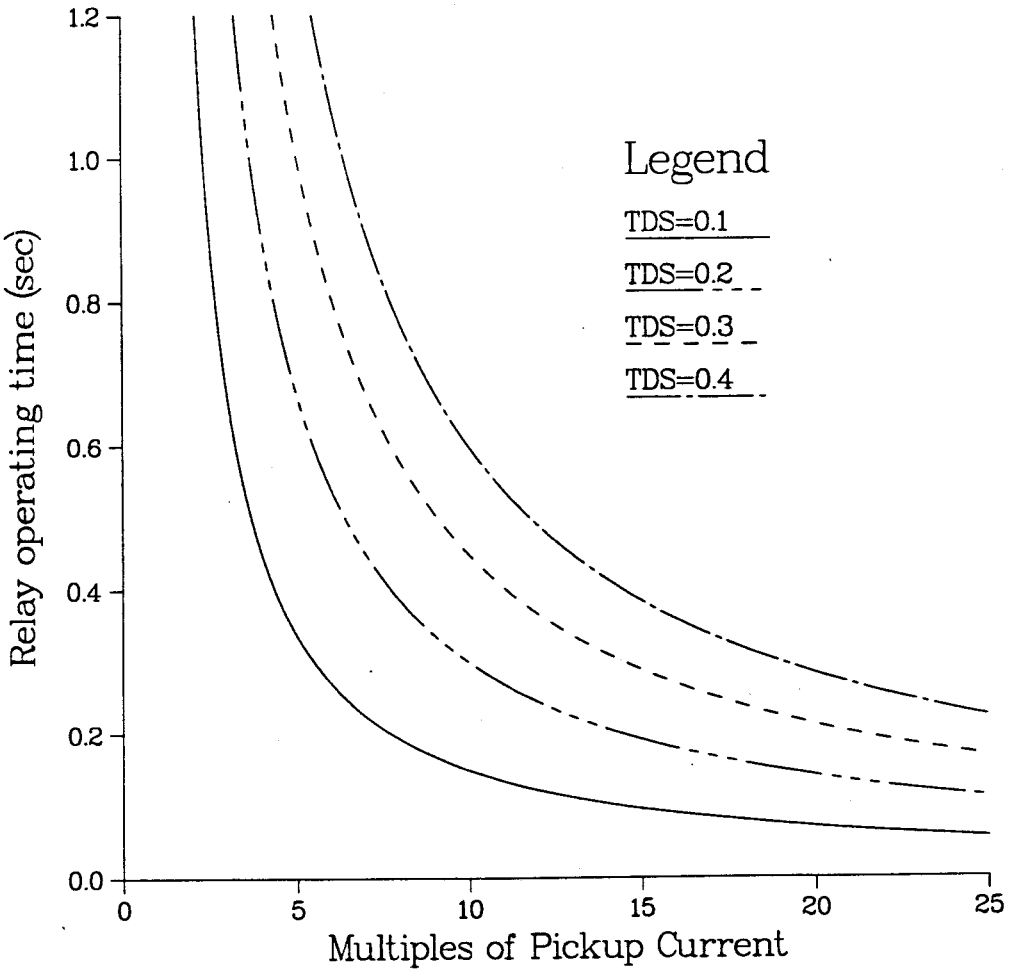

Figure 2.4: Typical current-time characteristics of an overcurrent relay.

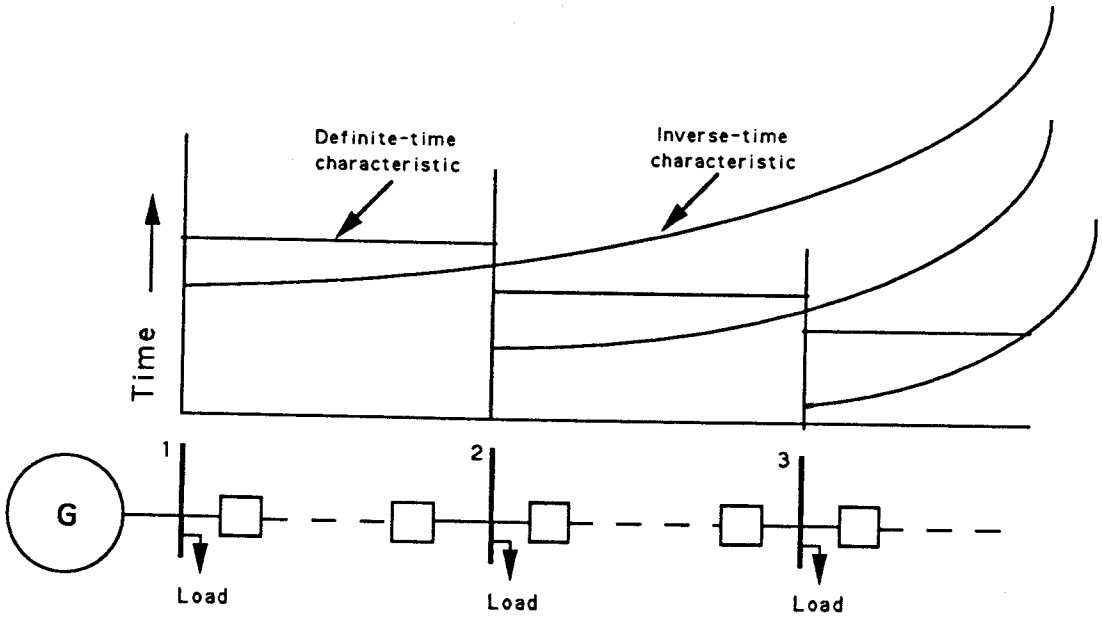

Figure 2.5: Definite-time and inverse-time relays for protecting a radial circuit.

2.3.2. Directional Overcurrent Protection

It is not possible to achieve relay coordination based on current magnitude alone if the distribution system consists of looped circuits. Figure 2.6 illustrates a simple loop network. For a fault at F, both relays R_m and R_n experience the same fault current except that the directions of current flow are different. If the relays are not directional, relays R_m and R_n would operate and open circuit breakers B_m and B_n. The operation of B_m disconnects the unfaulted line between bus 1 and 2 from bus 2 which is undesirable. To protect loop circuits, overcurrent protection must, therefore, include an additional feature to ensure proper discrimination. In such cases, a directional element is used in conjunction with each overcurrent relay so that it operates only if the fault is on the line side of the relay.

2.3.2.1. Directional Operation

Traditionally, electromechanical directional relays develop operating torque when the fault is on the line side of the relay. The torque, T, is expressed as

$$T = k_1 |V| |I| \cos(\theta - \tau) - k_2, \tag{2.1}$$

where:

V	is the voltage phasor,
I	is the current phasor,
θ	is the angle between I and V,
τ	is the maximum torque angle,
k_1	is the relay constant and
k_2	is the restraining torque.

When the relay is on the verge of operation, the torque is about zero; Equation 2.1 provides

$$|V| |I| \cos(\theta - \tau) > \frac{k_2}{k_1}. \tag{2.2}$$

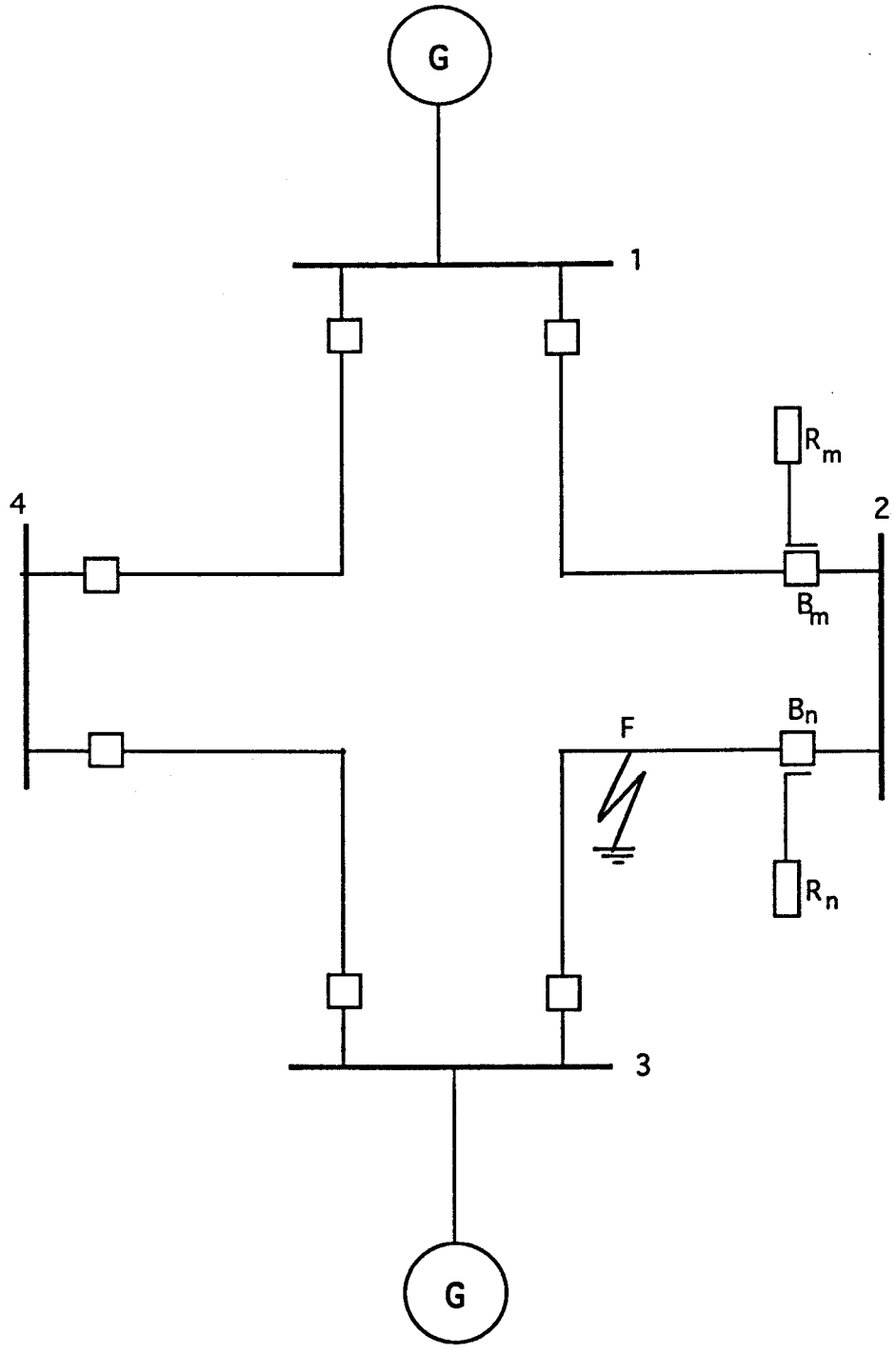

Figure 2.6: A simple loop distribution circuit.

Figure 2.7 shows the operating characteristic of the directional relay with the voltage as reference; voltage is called the polarizing quantity. The relay operating characteristic, determined from Equation 2.2, is a straight line. The relay picks up when the current phasor is in the positive torque region. For a specified current magnitude, the torque is maximum if the current phasor is along the maximum torque line which is shifted from the reference phasor by the maximum torque angle τ.

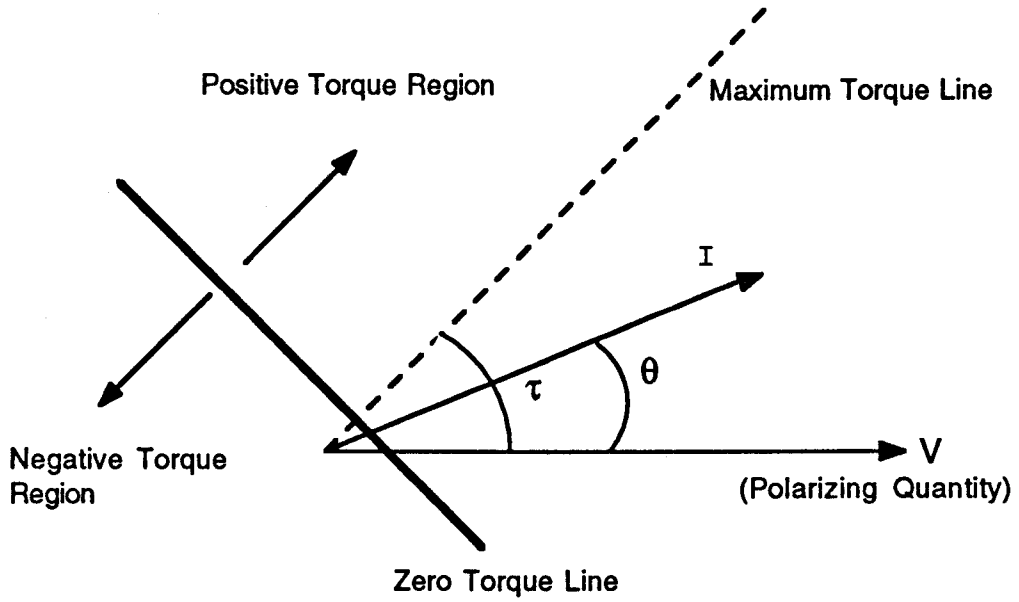

Figure 2.7: The operating characteristic of a directional relay.

2.3.2.2. Relay Connection Angle

To obtain the desired torque during faults, the selection of suitable polarizing voltage and maximum torque angle is important. The polarizing voltage during faults must not be too low and its phase angle should remain fairly constant. This is generally accomplished by selecting appropriate current-voltage combinations, which are identified as relay connection angles. The four relay connection angles, shown in Table 2.1, generally used are the 30 °, 60 ° delta, 60 ° wye and 90° connections. The suitability of the connections can be determined by checking the torque developed by the relay for different types of faults and during overload conditions. Fault currents lag their unity power factor position by large angles and it is, therefore, desirable that a directional relay develop sufficient torque in these conditions. While the most versatile connection is the 90°, other connections are used for specific applications. Each relay connection is described in the following sections.

Table 2.1: Relay connection angles for directional relay.

Connection	Phase A		Phase B		Phase C		Recommended Maximum Torque Angle
	I	V	I	V	I	V	
30 0	I a	Vac	Ib	Vba	Ic	Vcb	0 0
60 0 delta	Ia-Ib	Vac	Ib-Ic	Vba	Ic-Ia	Vcb	0 0
60 0 wye	Ia	-Vc	Ib	-Va	Ic	-Vb	0 0
90 0	Ia	Vbc	Ib	Vca	Ic	Vab	30 0/45 0

I. The 30 Degree Connection

In this connection, *A* phase element of the relay is supplied with current I_a and voltage V_{ac}, $(V_a - V_c)$. Therefore, the maximum torque occurs when the current lags the system phase to neutral voltage by 30°. It provides an operating zone from 60° leading to 120° lagging currents, as shown in Figure 2.8(a).

II. The 60 Degree Delta Connection

Figure 2.8(b) illustrates the 60° delta connection where *A* phase element of the relay is supplied with current I_{ab} and the voltage V_{ac}. This results in maximum torque being produced when current lags the unity power factor line by 60°. This connection that uses V_{ac} voltage with delta current, produced by subtracting phase *A* and phase *B* currents at unity power factor, gives a current leading the voltage V_{ac} by 60°. This provides a correct directional operating zone over a current range of 30° leading to 150° lagging.

III. The 60 Degree Wye Connection

Figure 2.8(c) illustrates the 60° wye connection where *A* phase element of the relay is supplied with current I_a and voltage $-V_c$. This results in maximum torque being produced when the current lags the system phase to neutral voltage by 60°. This connection provides a correct directional operating zone over a current range of 30° leading to 150° lagging. Although the most suitable maximum torque angle for this connection is 0°, there is a risk of incorrect operation of relays for all types of faults excepting three-phase faults. Hence, this connection type is generally not recommended.

IV. The 90 Degree Connection

There could be two different operating characteristics in 90 degree connections depending upon maximum torque angle of 30° or 45°. With 30° maximum torque angle, *A* phase element of the relay is supplied with the current I_a and the voltage V_{bc}, displaced by 30° in an anti-clockwise direction, as shown in Figure 2.9(a). This results in maximum torque being produced when the current lags the system phase to neutral voltage by 60°. This connection provides a correct directional operating zone over a current range of 30° leading to 150° lagging.

When maximum torque angle of 45° is used, *A* phase element of the relay is supplied with the current I_a and the voltage V_{bc}, displaced by 45° in an anti-clockwise direction as shown in Figure 2.9(b). This results in maximum torque being produced

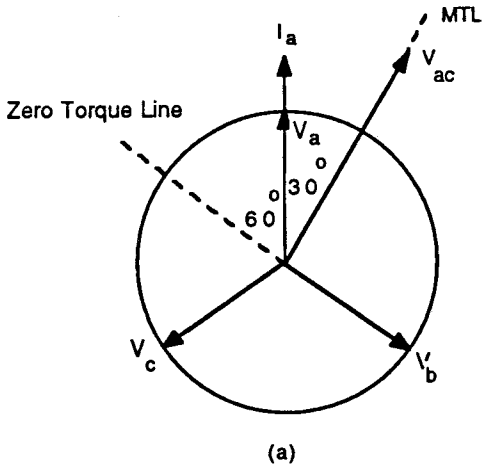

(a)

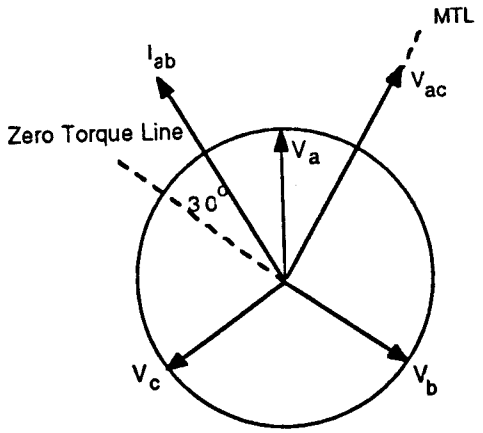

(b)

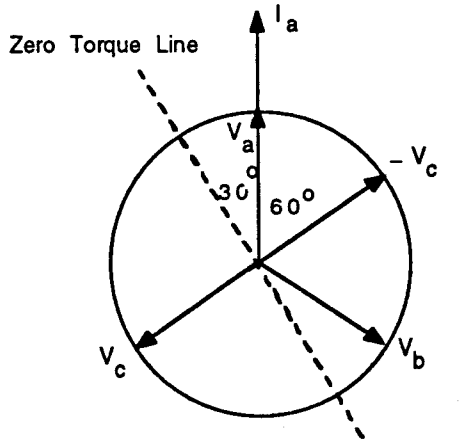

(c)

Figure 2.8: Phasor diagrams for (a) 30°, (b) 60° delta connection and (c) 60° wye connection.

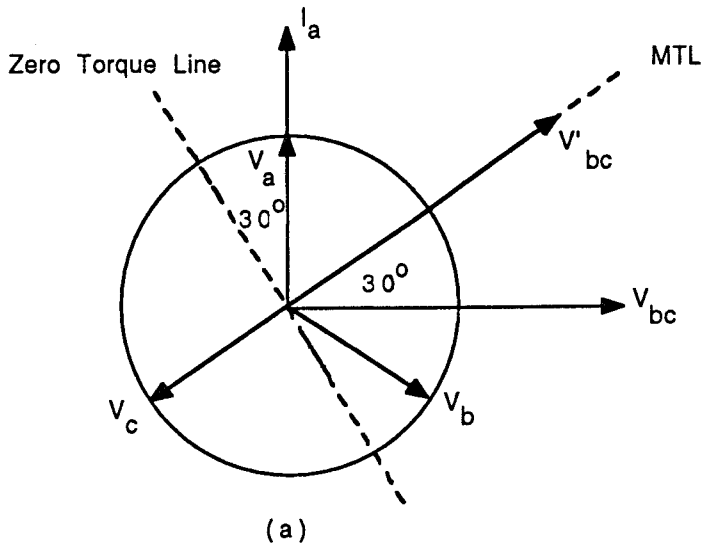

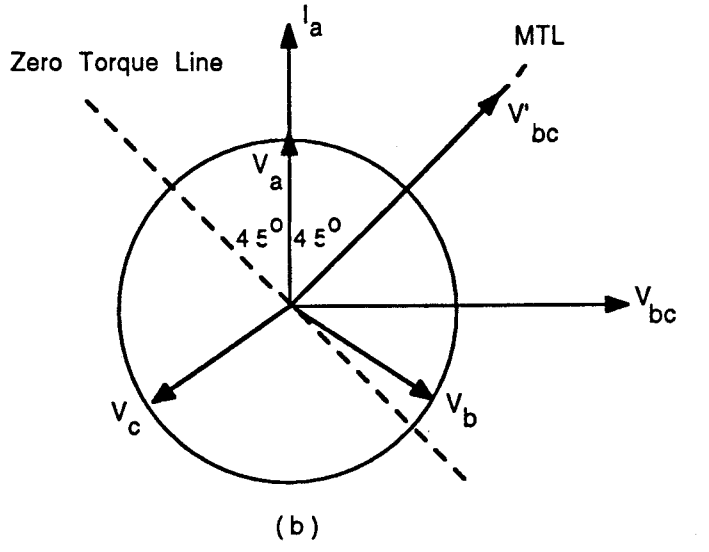

Figure 2.9: Phasor diagrams for (a) 90°-30° operating characteristic and (b) 90°-45° operating characteristic.

when the current lags the system phase to neutral voltage by 45°. This connection provides a correct directional operating zone over a current range of 45° leading to 135° lagging. This connection is recommended for the protection of transformer feeders having zero sequence source in front of the relay. The 90°- 45° connection is essential in case of parallel transformers or transformer feeders to ensure correct relay operation for faults beyond the star/delta transformer.

2.3.3. Instantaneous Overcurrent Protection

An instantaneous overcurrent unit in conjunction with an overcurrent relay provides high speed operation for near-end faults. In some cases it may also permit relays in the adjacent sections to be set for faster operation. Figure 2.10 shows that the instantaneous overcurrent relays reduce the clearing times for near-end faults.

2.3.3.1. Reach of an Instantaneous Relay

When there are sufficient differences between the near-end and far-end fault currents, instantaneous elements are used along with overcurrent relays. In distribution circuits, instantaneous units are used if the ratio of near-end fault (maximum and/or minimum) and far-end fault (maximum) is on the order 1.15 to 1.3 or more [13]. The part of the line protected by an instantaneous unit is given by

$$n = \frac{K_s(1-K_i)+1}{K_i}, \tag{2.3}$$

where:

- n is the normalized length of the line protected by the instantaneous unit,
- K_i is the ratio of the pickup current of the instantaneous unit and maximum far-end fault current and
- K_s is the ratio of the source and line impedances.

The pickup current of an instantaneous unit is, therefore, given by

$$I_{IT} = K_i \times I_{FF}, \tag{2.4}$$

where:

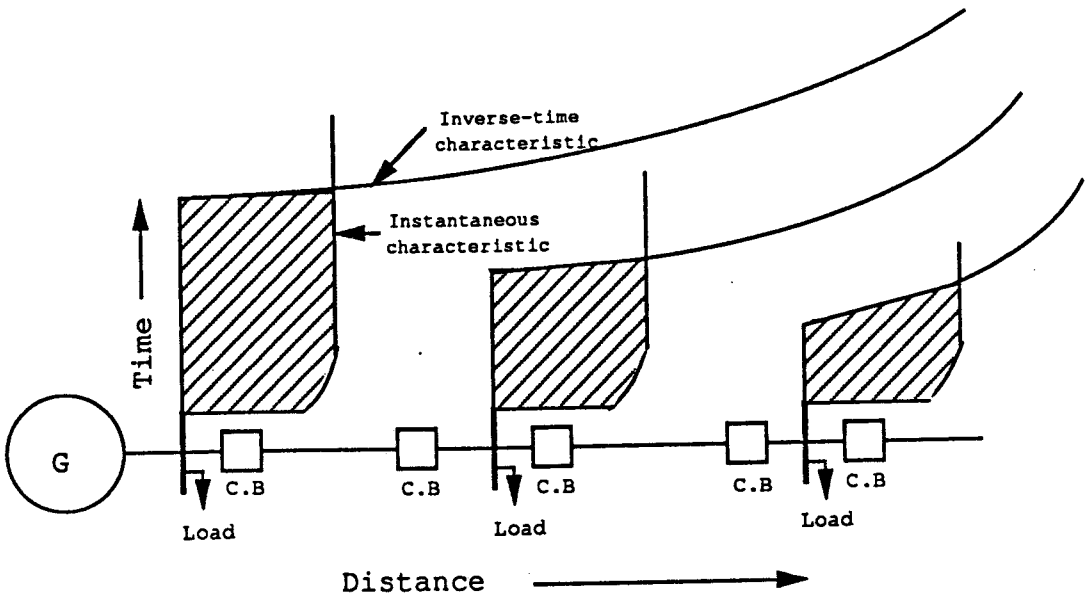

Figure 2.10: Reducing relay operating times by using instantaneous overcurrent relays.

I_{IT} is the pickup setting of the instantaneous pickup current and
I_{FF} is the far-end fault current.

A simplified relation of the line protected by an instantaneous unit is given by [13]

$$100\frac{I_{C1}-I_{IT}}{I_{C1}-I_{FB}}\%, \tag{2.5}$$

where:

I_{C1} is the near-end fault current,
I_{FB} is far-end fault current and
I_{IT} is the instantaneous unit setting.

2.3.4. Distance Protection

Distance relays are generally applied for phase fault protection of lines at 69 kv and above to achieve high speed of operation. These relays use voltage at the relay location and current in the protected line to measure the line impedance from the relay location to the fault. Since this impedance is proportional to the distance from the relay to the location of the fault, decisions are made considering the measured values of the magnitude and phase angle of the impedance.

2.3.4.1. Zone of Protection

The impedance and time settings of the distance relays are selected in such a way that a protection scheme is divided into several zones. Figure 2.11 shows three radial lines, 12, 23 and 34 between buses 1 and 4. The lines are protected by distance relay protection systems R_{11}, R_{12}, R_{21}, R_{22}, R_{31}, R_{32}, R_{41}, R_{42}. Loads L_1, L_2, L_3 and L_4 are connected to the buses, 1, 2, 3 and 4 respectively.

The settings and time delays of the relays are generally selected to accomplish three zone distance protection at each relay location. Each protection system, R_{11} etc., has three relays set to operate in times t_1, t_2 and t_3 for zone one, two and three faults respectively. Zone 1 relay, R_{22}, is set to trip instantaneously if the distance of the fault from bus 2 is less than 80% of the length of line 23. The zone two relay provides backup

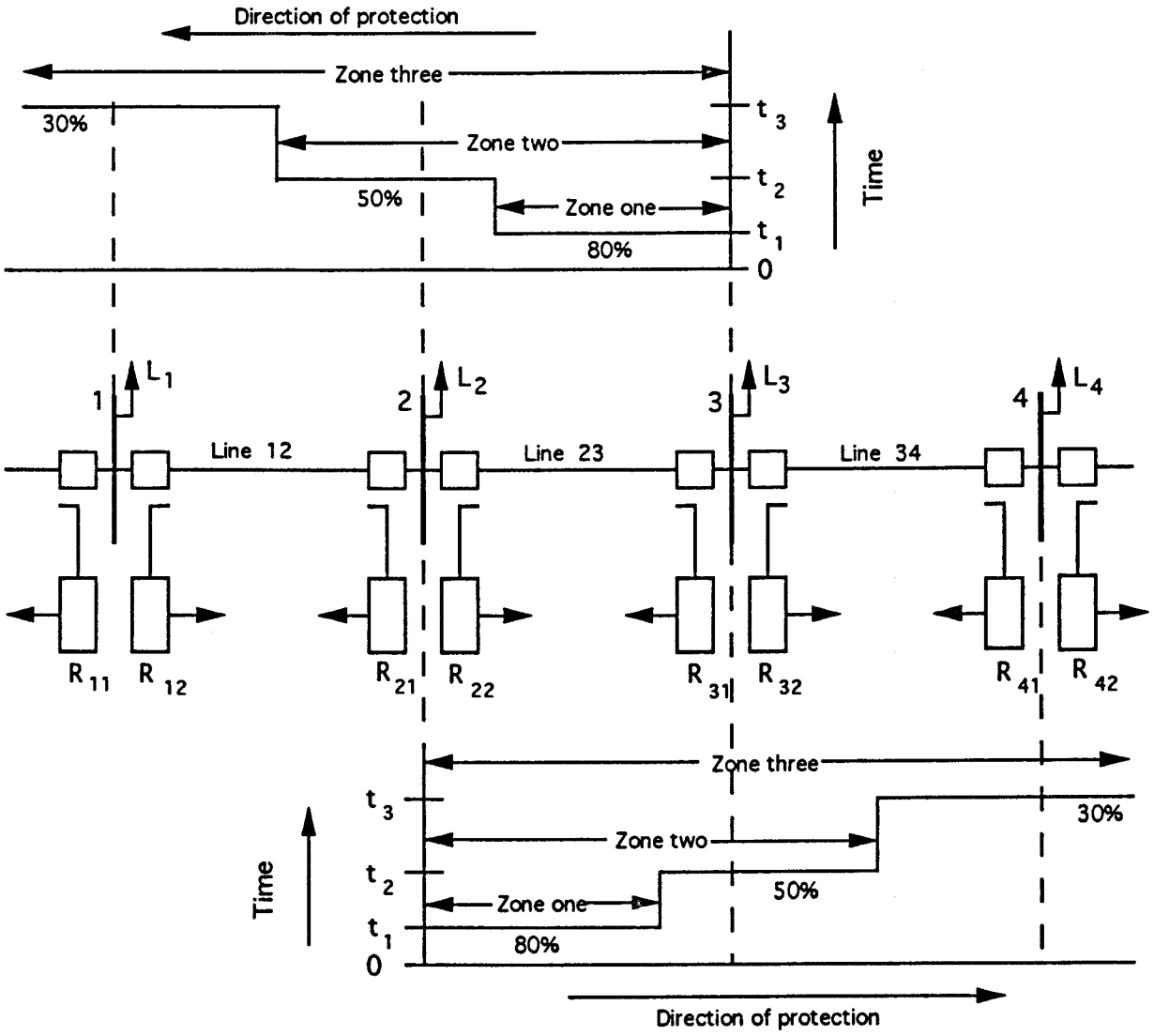

Figure 2.11: Time-distance characteristic of a three-zone distance protection.

protection for the first 80 % of the line 23, primary protection for the remaining 20% of the line and backup protection for the first 20-50% of the line 34. The relay opens the circuit breaker after a time delay which is usually set to be from 0.25 s to 0.40 s. Zone three relay provides back up protection for the lines 23 and 34, and 20-30% of the line beyond bus 4. This relay is set to operate after a time delay of about 0.80 s. The relays at bus 3, that protect line 23, perform similar functions except that they measure distance in the direction from bus 3 to bus 2 and beyond. Similar arrangements are implemented at the other relaying locations.

2.3.5. Pilot Protection

Distance relays provide high speed protection for only 70 to 85 percent of the protected line. To obtain selective high speed clearing of faults for 100 percent of the line, pilot protection is applied. Two major schemes, directional comparison and phase comparison are used for this purpose. The implementation of the schemes requires a communication circuit that compares system conditions at the terminals of the line. Four types of communication channels commonly used are pilot wire, power line carrier, microwave and fiber optic communications. A pilot wire circuit is used for short lines and compares the operating parameters using dc, 50 to 60 Hz or audio frequency signals. The pilot wire circuits are either owned by the utility or are rented from telephone companies. Carrier-current schemes, used on long lines, transmit low voltage, radio frequency signals of 30 to 300 kHz range over the power lines. Microwave pilots are applied when the number of services needing pilot channels is beyond the technical or economic capabilities of a carrier-current scheme. Radio signals in 2 to 12 GHz range are used in this application. More recently fiber optic communication links have been used to transmit information using light modulated signals. This approach eliminates the problems of electromagnetic noise corrupting the transmitted signals.

2.4. Summary

A typical distribution system has been described in this chapter. The relaying schemes used for protecting the distribution system are reported. The limitations of time-graded and current-graded protection schemes are discussed. The most commonly used inverse-time protection scheme and its advantages are outlined. Instantaneous elements are generally used when the ratio of near-end and far-end fault current is high. This unit ensures high speed clearing of near-end faults and reduces overall operating times.

Distance and pilot relaying schemes are also briefly discussed. The primary zone of a distance protection scheme provides high speed protection of 70 to 85 percent of the line. Pilot protection is used for high speed clearing of all faults on the line.

3. OVERCURRENT RELAYING ALGORITHMS

3.1. Introduction

Overcurrent relays are used to protect the selected distribution network. The operating principles of these relays and their application to distribution systems have been discussed in Chapter 2. This chapter describes algorithms that have been previously proposed for designing microprocessor-based overcurrent relays.

The design of a microprocessor-based overcurrent relay consists of modelling the relay characteristics, estimating current and voltage phasors, and developing the relay decision logic. Mathematical equations used to model the relay characteristics are, therefore, reviewed. Some techniques for estimating current and voltage phasors from their sampled values are also outlined.

3.2. Modelling Current-Time Characteristic

The current-time characteristics of inverse-time overcurrent relays are usually expressed as families of curves corresponding to several values of time dial settings. Several mathematical equations, expressing relay operating times as functions of relay currents, have been suggested in the past for modelling the characteristics. These equations can be classified in two categories; exponential equations and polynomial equations. Some of the suggested equations are presented in this section.

3.2.1. Exponential Equations

A. R. van C. Warrington [2] proposed the following equation to express the contact closing time of an inverse-time overcurrent relay as a function of the operating current:

$$t = c + \frac{k \times TDS}{I^n - 1}, \tag{3.1}$$

where:

t	is the relay operating time,
I	is the relay current in multiples of the pickup current,
TDS	is the time dial setting,
k	is the design constant and
c, n	are constants which define the relay characteristic.

This equation provides a good mathematical model of the characteristics of inverse-time overcurrent relays marketed by European manufacturers. It is possible to find the coefficients of Equation 3.1 for a relay using a curve fitting technique.

J.E. Hieber [14] proposed the following empirical equation for defining the relay operating time as a function of current:

$$t = c + \frac{k}{(I - h + wI^{-2I})^q} - b\left(\frac{I}{50}\right)^n, \tag{3.2}$$

where b, h, q and w are constants.

Hieber suggested that the constants used in this equation be determined at maximum and minimum time dial settings. He also suggested that the relay characteristics at intermediate time dial settings be obtained by non-linear interpolations. Although Equation 3.2 is suitable for modelling the relay characteristics, finding the coefficients is quite involved.

The International Electrotechnical Commission (IEC) Standard 255.4 [15] suggests that the characteristics of inverse-time overcurrent relays correspond to the following formula:

$$t = \frac{k}{I^n - 1}, \tag{3.3}$$

where:

t	is the relay operating time,
k	is a constant characterising the relay,
n	is an index characterising the algebraic function and
I	is the relay current in multiples of the pickup current.

Appropriate values of k and n are chosen to achieve standard inverse, very inverse and extremely inverse characteristics. The values suggested in the IEC standard [15] are given in Table 3.1.

Table 3.1: Coefficients for modelling inverse-time overcurrent relay characteristics suggested in the IEC standard 255.4 [15].

Item	Standard Inverse	Very Inverse	Extremely Inverse
k	0.14	13.5	80.0
n	0.02	1.0	2.0

3.2.2. Polynomial Equations

Polynomial equations have been suggested by several investigators for modelling the current-time characteristics of inverse-time overcurrent relays. Albrecht et al. [16] suggested that the operating time of an overcurrent relay can be expressed as a polynomial in two variables, time dial settings and current. He proposed the equation,

$$t_r = [\sum_{j=1}^{m} \sum_{i=1}^{n} c_{ji} \times (TDS)^j (I)^i]^k, \quad (3.4)$$

where:

t_r	is the relay operating time,
c_{ji}, m, n and k	are constants and
TDS	is the time dial setting.

G.E. Radke [17] expressed the relay operating time as a polynomial in logarithms of the relay current.

$$\log(t_r - d_c) = c_0 + c_1(\log I) + c_2(\log I)^2 + c_3(\log I)^3 + c_4(\log I)^4, \quad (3.5)$$

where:

t_r	is the relay operating time and
d_c, c_0, c_1, c_2, c_3 and c_4	are constants.

Each time dial setting is modelled by assigning a suitable value to constant c_0. The disadvantages of using Equations 3.4 and 3.5 are that the charcateristics provided by them are not asymptotic to the pickup current and relay operating time does not decrease monotonically as the current increases. These models, therefore, do not adequately represent the desired relay characteristics.

Singh et al. [18] examined polynomials, reproduced as Equations 3.6 through 3.10 for representing the characteristics of overcurrent relays. The characteristics described by these equations are asymptotic to the pickup current and the minimum operating time.

$$log(t_r) = c_0 + \frac{c_1}{log\ I} + \frac{c_2}{(log\ I)^2} + \frac{c_3}{(log\ I)^3} \cdots \quad (3.6)$$

$$t_r = c_0 + \frac{c_1}{I-1} + \frac{c_2}{(I-1)^2} + \frac{c_3}{(I-1)^3} \cdots \quad (3.7)$$

$$t_r = c_0 + \frac{c_1}{I-1} + \frac{c_2}{I^2-1} + \frac{c_3}{I^3-1} \cdots \tag{3.8}$$

$$t_r = c_0 + \frac{c_1}{I-1} + \frac{c_2 I}{(I-1)^2} + \frac{c_3 I^2}{(I-1)^3} \cdots \tag{3.9}$$

$$t_r = c_0 + \frac{c_1}{I-1} + \frac{c_2 I}{I^2-1} + \frac{c_3 I^2}{I^3-1} \cdots \tag{3.10}$$

These equations can be used for modelling characteristics of inverse-time overcurrent relays for a selected time dial setting. A composite model was also suggested for obtaining the characteristics at other time dial settings. The approach used for developing a composite model consists of the following three steps:

1. Develop a model of the relay characteristic in the form of time as a function of relay current at a selected time dial setting, say 4 or 5.
2. Develop a polynomial model of the relay operating times versus time dial settings for a selected relay currents, say 3 or 4 times the current setting. The following polynomial was suggested for this purpose.

$$t_r = b_0 + b_1(TDS) + b_2(TDS)^2 + b_3(TDS)^3. \tag{3.11}$$

3. Combine the two models for calculating the relay operating time for the selected relay operating current and time dial setting.

Finally, Damborg et al. [19] combined Equations 3.9 and 3.11 to obtain the following composite equation:

$$t_r = c_1 + c_2(TDS) + \frac{c_3\,(TDS)}{(I-1)^2} + \frac{c_4\,(TDS)^2}{I-1} + \frac{c_6\,(TDS)}{(I-1)^3} + \frac{c_7\,(TDS)^2}{(I-1)^4}. \tag{3.12}$$

The relay operating times for all time dial settings are used in Equation 3.12 and the coefficients c_1 through c_7 are calculated using the least squares curve fitting technique [20].

The mathematical models of the relay characteristics described by Equations 3.6 to 3.11 were exhaustively tested by Singh et al. [18]. The published data of the relay operating times were first used to obtain the coefficients of the equations using the least squares curve fitting technique. The accuracy of the equations was then tested by computing the relay operating times for currents that were increased from two to thirty times of the pickup value. Errors between the relay operating times published in the literature [21] and those computed by the equations were calculated. Reference [18] reported that Equations 3.1 to 3.3, and 3.6 to 3.11 represent the relay characteristics adequately. The times computed by these equations were within 3 cycles of 60 Hz of the published relay operating times for small operating times and within 5% for large operating time.

Any one of the twelve equations, reproduced in this section, can be used in a microprocessor-based inverse-time overcurrent relay. Two factors important in selecting an equation for this application are

1. the accuracy with which the equation can represent a relay characteristic and
2. the ease with which the equation can be implemented on a microprocessor.

3.3. Estimating of Current and Voltage Phasors

The design of microprocessor-based relays requires that current and voltage phasors be estimated from the sampled data. Currents and voltages usually contain transient components, such as exponentially decaying dc, harmonic and non-harmonic components in addition to the fundamental frequency components. The transient components are suppressed by filters and the fundamental frequency components are computed using signal processing techniques [20, 22, 23]. Some of the techniques are briefly described in this section.

3.3.1. Fourier Algorithms

These algorithms assume that the waveform of a current $i(t)$ has a finite energy in the interval $(0,T)$ and the current can be expressed as

$$i(t) = a_0 + \sqrt{2}a_1\sin(2\pi t/T) + \sqrt{2}a_2\cos(2\pi t/T) + \ldots\ldots\ldots \quad (3.13)$$

In this equation, a's are the Fourier coefficients and T is the time period of the fundamental frequency component. The peak value of the fundamental frequency component of $i(t)$ can be computed from Fourier coefficients as

$$I_1 = \sqrt{2(a_1^2 + a_2^2)}. \quad (3.14)$$

Researchers proposed different approaches for obtaining the Fourier coefficients. The correlation and discrete Fourier techniques, which are commonly used for this purpose, are discussed in the following sections.

3.3.1.1. Correlation Algorithms

A signal can be correlated with itself, with other signals or with mathematical functions. The objective is to extract the real and imaginary parts of the fundamental frequency phasor representing the signal. Ramamoorty [24] suggested that the required information can be extracted from an observed signal by correlating one cycle of data sampled at prespecified intervals with sine and cosine waves sampled in the manner in which the signal was sampled. This is commonly known as the Fourier technique and can be expressed mathematically as

$$V_r = \frac{2}{m}\sum_{n=0}^{m-1} V_{k+n-m+1}\sin\frac{2\pi n}{m}, \quad (3.15)$$

$$V_i = \frac{2}{m}\sum_{n=0}^{m-1} V_{k+n-m+1}\cos\frac{2\pi n}{m}, \quad (3.16)$$

where:

m is the number of samples per second,

V_r is the real part of the fundamental frequency phasor representing the signal and

V_i is the imaginary part of the fundamental frequency phasor representing the signal.

After evaluating Equations 3.15 and 3.16, the peak value and phase angle of the signal can be determined from the following equations:

$$V_p = \sqrt{V_r^2 + V_i^2}, \tag{3.17}$$

$$\theta_v = \text{arctg}\frac{V_i}{V_r}. \tag{3.18}$$

Implementing the correlation approach, Phadke et al. [25] used a data window of one half cycle plus one sample.

Another group of functions that use the correlation approach are odd and even rectangular waves shown in Figure 3.1 [26]. In mathematical form, they are expressed as

$$W_r(t) = signum(\sin \omega_0 t), \tag{3.19}$$

$$W_i(t) = signum(\cos \omega_0 t), \tag{3.20}$$

where:

$signum(x)$ = -1 for $x < 0$,
= 0 for $x = 0$,
= 1 for $x > 0$,

$W_r(t)$ is the odd rectangular wave and

$W_i(t)$ is the even rectangular wave.

The real and imaginary components of the fundamental frequency phasor can be calculated by the following equations:

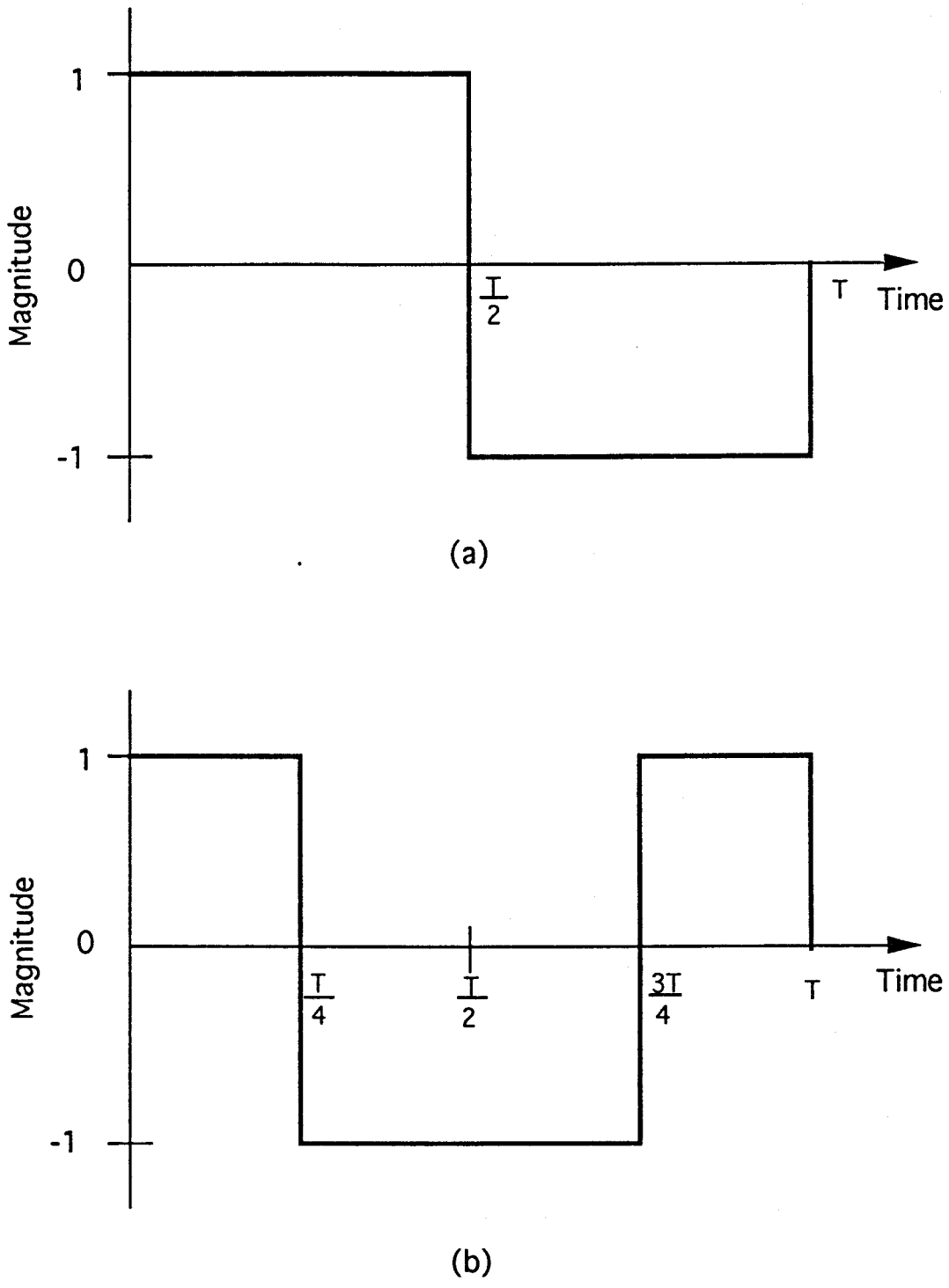

Figure 3.1: Rectangular waves of the fundamental frequency: (a) odd wave and (b) even wave.

$$V_r = \frac{1}{A}\sum_{n=0}^{m-1} V_{k+n-m+1}\, signum(\sin\frac{2\pi n}{m}), \tag{3.21}$$

$$V_i = \frac{1}{A}\sum_{n=0}^{m-1} V_{k+n-m+1}\, signum(\cos\frac{2\pi n}{m}), \tag{3.22}$$

where:

A is a scaling factor.

Since the weighting factors are either +1, 0 or -1, the computations involved are additions and subtractions only. This makes the technique very attractive. Schweitzer et al. [27] used this approach to calculate the phasors of the fundamental and harmonic frequency components. Hope et al. [28] used cross-correlation and auto-correlation of currents and voltages. The procedure they suggested is based on the following fundamental equations:

$$\psi_1(\tau) = \frac{1}{N}\sum_{k=1}^{N} i_k\, i_{k+\tau}, \tag{3.23}$$

$$\psi_2(\tau) = \frac{1}{N}\sum_{k=1}^{N} i_k\, v_{k+\tau}, \tag{3.24}$$

where:

$\psi_1(\tau)$ is the auto-correlation function,
$\psi_2(\tau)$ is the cross-correlation function and
τ is the lag.

In the above equations, voltage and current signals, $v_{k+\tau}$ and $i_{k+\tau}$, are delayed by $2\pi\tau/N$ radians from the voltage and current signals v_k and i_k respectively. The sums of the products in Equations 3.23 and 3.24 can be formed on a digital computer by a running sum technique. The running sum is calculated by adding the newest product for an incoming sample and subtracting the oldest from the sum of the sample products over one period. Thus the corresponding quantities measured during a particular sampling period need only be multiplied together to compute the values of the correlation functions.

3.3.1.2. Recursive Caculations for Discrete Fourier Algorithm

Phadke et al. [29] suggested a recursive procedure for implementing the discrete Fourier transform (DFT) algorithm to compute phasors. A brief mathematical developments of the technique is given in this section.

The DFT of a current provides an estimate of a signal that can be expressed as

$$I_n(p-1) = \frac{2}{N}\sum_{k=0}^{N-1} i(p-1-k)\exp(-j\frac{2\pi}{N}nk), \tag{3.25}$$

where:

n	is the order of harmonic component,
p	is the data window number and
N	is the number of samples in a data window.

The phasor, $I_n(p-1)$, is estimated using the $i(p-N),....,i(p-1)$ samples. The data window containing these samples can be classified as $(p-1)^{th}$ window. A new sample is obtained ΔT seconds later and the p^{th} data window that contains the $i(p-N+1),....,i(p)$ samples is formed. The discrete Fourier transform of this data provides a new estimate of the phasor, $I_n(p)$, which can be expressed as

$$I_n(p) = \frac{2}{N}\sum_{k=0}^{N-1} i(p-k)\exp(-j\frac{2\pi}{N}nk). \tag{3.26}$$

The authors of Reference [29] calculated the phasor $I(p)$ using the Fourier coefficients that are displaced by a phase angle $2\pi/N$ radians. Therefore, Equation 3.26 becomes

$$I_n(p,2\pi/N) = \frac{2}{N}\sum_{k=0}^{N-1} i(p-k)\ \exp(-j\frac{2\pi}{N}(k-1)n). \tag{3.27}$$

In this equation, $I_n(p,2\pi/N)$ refers to the phasor obtained using the p^{th} data window and

the Fourier coefficients displaced by an angle $2\pi/N$. Equation 3.27 can be rewritten with the term corresponding to the latest sample, $i(p)$, ($i.e.\ k=0$) outside the summation.

$$I_n(p,2\pi/N) = \frac{2}{N} i(p)\exp(j\frac{2\pi n}{N}) + \frac{2}{N}\sum_{k=1}^{N-1} i(p-k)\exp(-j\frac{2\pi}{N}(k-1)n). \quad (3.28)$$

It is also possible to rewrite Equation 3.28 with the term corresponding to the oldest sample, $i(p-N)$, ($i.e.\ k=N-1$) outside the summation as follows:

$$I_n(p-1) = \frac{2}{N} i(p-N)\exp(j\frac{2\pi}{N}n) + \frac{2}{N}\sum_{k=0}^{N-2} i(p-1-k)\exp(-j\frac{2\pi}{N}nk). \quad (3.29)$$

Replacing $k+1$ by l, Equation 3.29 can be rewritten as

$$I_n(p-1) = \frac{2}{N} i(p-N)\exp(j\frac{2\pi n}{N}) + \frac{2}{N}\sum_{l=1}^{N-1} i(p-l)\ \exp(-j\frac{2\pi}{N}(l-1)n). \quad (3.30)$$

Using Equations 3.28 and 3.30, the phasor computed from the p^{th} window and the displaced Fourier coefficients can be expressed as

$$I_n(p,2\pi/N) = I_n(p-1)+\frac{2}{N}[i(p)-i(p-N)]\ \exp(j\frac{2\pi n}{N}). \quad (3.31)$$

This equation shows that the phasor using the p^{th} window can be computed from the phasor computed from the $(p-1)^{th}$ window by using a recursive procedure. In progressing from the $(p-1)^{th}$ data window to the p^{th} data window, one sample, *i(p-N)*, is discarded and one sample, *i(p)*, is added to the data set. This procedure takes advantage of the *2(N-1)* multiplications and *2(N-2)* additions that use the part of the data common to the old and new windows. This procedure reduces the number of computations required to obtain an estimate.

3.3.2. Least Error Square Algorithms

Luckett et al. [22] proposed the use of the least squares approach for estimating amplitudes and phase angles of voltages and currents. Brooks [23] then used this approach in distance protection. He assumed that a current is composed of a dc component and a fundamental frequency component. Sachdev and Baribeau [20] further developed this method and suggested that most of the computations can be done off-line before acquiring the data. Later, Sachdev and Shah [30] applied this technique for differential protection of transformers. They assumed that a differential current contains a decaying dc component and components of the fundamental frequency and the second and third harmonics. A current signal composed of several frequencies can be represented as follows:

$$i(t) = I_0 e^{-t/\tau} + \sum_{m=1}^{K} I_m \sin(m\omega_0 t + \theta_m), \tag{3.32}$$

where:

I_0	is the magnitude of the decaying dc component at $t=0$,
τ	is the time constant of the dc component,
K	is the order of the highest harmonic component in the current,
I_m	is the magnitude of the m^{th} harmonic component,
ω_0	is the fundamental frequency of the system and
θ_m	is the phase angle of the m^{th} harmonic.

Equation 3.32 can be expanded using well known trigonometric identity $\sin(\alpha \pm \beta) = \sin\alpha\cos\beta \pm \cos\alpha\sin\beta$ and by approximating the decaying dc component by the first two terms of its Taylor series expansion.

$$i(t) = I_0 - (I_0/\tau)t + \sum_{m=1}^{K} I_m[\sin(m\omega_0 t)\cos\theta_m + \cos(m\omega_0 t)\sin\theta_m]. \tag{3.33}$$

With $t=t_1$ and assuming that $K=3$, Equation 3.33 can be written as

$$i(t) = I_0-(I_0/\tau)t_1+I_1\sin(\omega_0 t_1+\theta_1)+I_2\sin(2\omega_0 t_1+\theta_2)+I_3\sin(3\omega_0 t_1+\theta_3). \quad (3.34)$$

$$= I_0-(I_0/\tau)t_1+(I_1\cos\theta_1)\sin(\omega_0 t_1)+(I_1\sin\theta_1)\cos(\omega_0 t_1)$$
$$+(I_2\cos\theta_2)\sin(2\omega_0 t_1)+(I_2\sin\theta_2)\cos(2\omega_0 t_1)$$
$$+(I_3\cos\theta_3)\sin(3\omega_0 t_1)+(I_3\sin\theta_3)\cos(3\omega_0 t_1). \quad (3.35)$$

$$i(t) = a_{11}x_1+a_{12}x_2+a_{13}x_3+a_{14}x_4+a_{15}x_5+a_{16}x_6+a_{17}x_7+a_{18}x_8, \quad (3.36)$$

where:

$x_1 = I_0$ $\quad a_{11} = 1$

$x_2 = -I_0/\tau$ $\quad a_{12} = t_1$

$x_3 = I_1 cos\theta_1$ $\quad a_{13} = sin(\omega_0 t_1)$

$x_4 = I_1 sin\theta_1$ $\quad a_{14} = cos(\omega_0 t_1)$

$x_5 = I_2 cos\theta_2$ $\quad a_{15} = sin(2\omega_0 t_1)$

$x_6 = I_2 sin\theta_2$ $\quad a_{16} = cos(2\omega_0 t_1)$

$x_7 = I_3 cos\theta_3$ $\quad a_{17} = sin(3\omega_0 t_1)$

$x_8 = I_3 sin\theta_3$ $\quad a_{18} = cos(3\omega_0 t_1).$

Since the current is sampled at intervals of ΔT seconds, t_1 can be replaced by $n\Delta T$ which redefines the coefficients as follows:

$a_{11} = 1$ $\quad a_{15} = sin(2\omega_0 n\Delta T)$

$a_{12} = n\Delta T$ $\quad a_{16} = cos(2\omega_0 n\Delta T)$

$a_{13} = sin(\omega_0 n\Delta T)$ $\quad a_{17} = sin(3\omega_0 n\Delta T)$

$a_{14} = cos(\omega_0 n\Delta T)$ $\quad a_{18} = cos(3\omega_0 n\Delta T).$

The following equation can now be obtained:

$$i(n\Delta T) = a_{n1}x_1+a_{n2}x_2+a_{n3}x_3+a_{n4}x_4+a_{n5}x_5+a_{n6}x_6+a_{n7}x_7+a_{n8}x_8, \quad (3.37)$$

where:

n represents the sample number in a data window.

Because current $i(t)$ is sampled every ΔT seconds, the second sample can be expressed as

$$i(t_1 + \Delta T) = a_{21}x_1 + a_{22}x_2 + a_{23}x_3 + a_{24}x_4 + a_{25}x_5 + a_{26}x_6 + a_{27}x_7 + a_{28}x_8. \tag{3.38}$$

For a preselected time reference and sampling rate, the values of the 'a' coefficients are known. For n samples taken at ΔT second intervals, the process was expressed in the form of n equations in eight unknowns, as follows:

$$\underset{n\times 8}{[A]} \quad \underset{8\times 1}{[x]} = \underset{n\times 1}{[i]}, \tag{3.39}$$

$$\underset{8\times 1}{[x]} = \underset{8\times n}{[A]^{+}} \quad \underset{n\times 1}{[i]}, \tag{3.40}$$

where:

$[A]^{+}$ is the left pseudo-inverse of $[A]$ and is given by

$$[A]^{+} = [[A^T][A]]^{-1}[A^T]. \tag{3.41}$$

The authors of Reference [20] showed that the elements of $[A]^{+}$ can be determined in the off-line mode. Equation 3.41 suggests that the real and imaginary parts of the fundamental frequency and harmonic component can be computed using the sampled values of the signal and the elements of the third and the fourth rows of the left-pseudo inverse of [A]. The peak value of the fundamental component can then be determined by using the following equation:

$$I_1 = \sqrt{x_3^2 + x_4^2}. \tag{3.42}$$

The authors of Reference [20] designed orthogonal fundamental and second harmonic frequency filters using one cycle window and time reference coinciding with the center of the data window. They used a sampling rate of 720 Hz.

3.4. Summary

This chapter reviews the previously proposed techniques for modelling the characteritics of overcurrent relay. Implementing a polynomial equation is cumbersome because it requires excessive computations. On the otherhand, the implementation of the exponential equations is simple. Some estimation techniques for computing the currents and voltages from sampled values have been presented. The recursive form of the DFT algorithm requires fewer computations compared to the usual Fourier technique. The least squres technique can model the decaying dc component, and, therefore, is likely to provide better estimates during fault conditions.

4. AN ADAPTIVE PROTECTION SYSTEM

4.1. Introduction

Adaptive relaying is a recent concept in the area of power system protection. It consists of, among others, changing relay settings as the operating state of the power system changes. Several problems in power system protection are expected to be addressed by using this approach.

This chapter includes a definition of an adaptive protection system and provides a discussion on some of the existing protection problems. Finally, the benefits that can be derived from using adaptive relaying are illustrated. Functions of an adaptive relaying scheme for a distribution system are discussed. The selected distribution network and instrumentation needed for the application of adaptive relaying are described.

4.2. Definition of an Adaptive Protection

The IEEE definition of an adaptive system is as follows [31]:

- A system that has means of monitoring its own performance and changing its own parameters by closed-loop action to improve its performance.

From the protection point of view, adaptive protection is defined as

- A protection philosophy that continuously monitors the state of a system and makes changes which are appropriate for its improved performance.

4.3. Benefits Expected from Adaptive Protection

Relay settings are presently not updated as the operating states of a power system change. This results in several protection problems; some of these can be overcome by using an adaptive approach. These include increased sensitivity, improved selectivity, ability to cope with cold-load inrush and reduced reclosure dead-time. In this section, benefits expected from the use of adaptive protection are discussed.

4.3.1. Sensitivity

The term 'sensitivity' is frequently used in connection with relay operating times. A protective relay is said to be sensitive if the operating time of the relay is short. The sensitivity depends on the magnitude of the fault current and pickup value at which a relay is set to operate. Traditionally, the pickup and time multiplier settings are selected on the basis of maximum fault currents that are likely to be experienced in the system. As a consequence, sensitivity of the relays is low when fault levels are small. Figure 4.1(a) illustrates this phenomenon using an inverse-time overcurrent relay as an example. Consider that A–B is the operating characteristic of the selected relay. For a fault current of I_1, the relay operating time is t_1. This reduces to t'_1 if the time multiplier setting is decreased and the relay operating characteristic corresponds to A'–B'.

In some cases, a relay could become so insensitive that it may not even operate because of a high pickup setting. Figure 4.1(b) shows that for a fault current of I_2, the relay does not operate because the fault current as a multiple of the pickup current is low. The adaptive approach could resolve this problem first by reducing the pickup setting and then, if necessary, by changing the time dial setting.

4.3.2. Selectivity

During a fault, a protection system sends trip commands to circuit breakers that are closest to the fault. If one of the breakers fails to operate, the relays in the adjoining zones trip the breakers they control. This property of selective tripping is also referred to as 'coordination'.

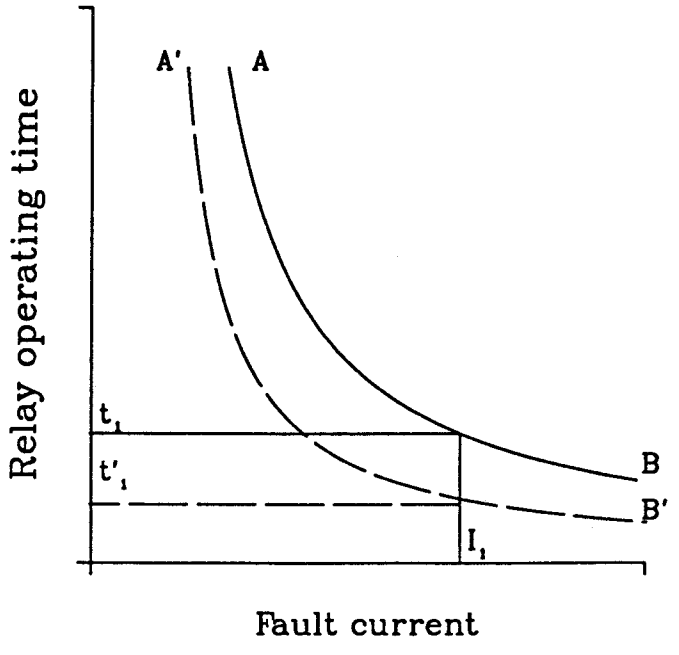

(a)

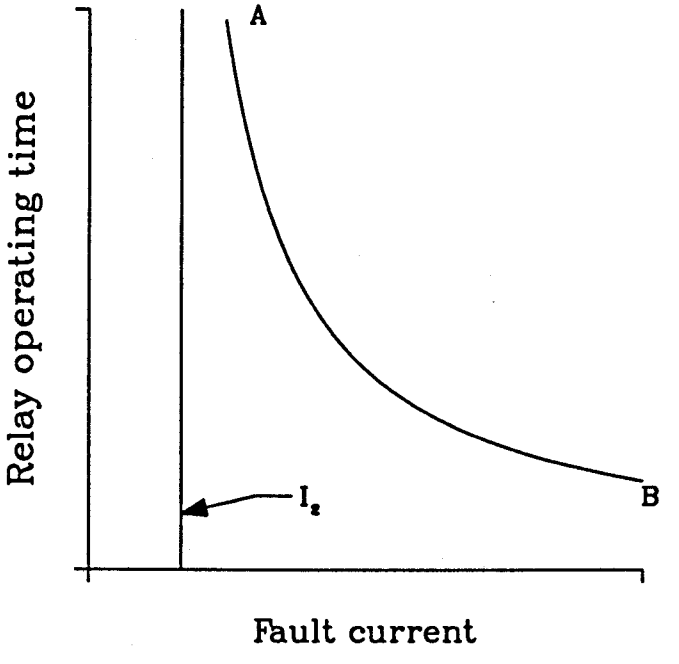

(b)

Figure 4.1: Sensitivities of an overcurrent relay: (a) a higher operating time and (b) a non-operating condition.

The present practice is that relay settings are determined by checking contingencies which are most likely to be encountered. This approach is likely to leave relays uncoordinated for some conditions. Protection engineers are usually forced to compromise in the selection of settings from the situations that are evaluated. As a result, time margins between primary and backup relays are small in some cases and relays are not coordinated in other cases. It is possible that adaptive protection would overcome these deficiencies by using appropriate settings during all operating states.

4.3.3. Cold-Load Inrush

When power on a distribution feeder is restored after a prolonged outage, the load current is substantially more than the load current normally encountered. This is caused by loss of diversity of the loads. This phenomena is known as cold-load inrush. The present practice allows an instantaneous relay to trip if the inrush current exceeds the pickup setting. Also, the setting of an inverse-time overcurrent relay is chosen in such a way that they will not operate during the inrush. In the absence of a fault, this technique works properly. But if a fault is in place, the relay will trip after a time delay during which fault currents will be large and voltage will be low. This can damage the equipment of the distribution network and that of the customers. This problem can be alleviated by changing relay settings during cold-load inrush.

4.3.4. Automatic Reclosing

The main objective of automatic reclosing of circuit breakers, after a fault is cleared, is to return the system to its normal configuration as soon as possible. A successful reclosing is, however, not guaranteed; it depends on a variety of factors, such as fault current, the secondary arc current, the recovery voltage across the arc path, the arc location and the meteorological conditions. Some delay, before a circuit breaker is reclosed, is necessary to allow for complete de-ionization of the arc to prevent it from restriking. The de-ionization time of an uncontrolled arc in free air depends on the circuit voltage, fault current, fault duration, conductor spacing, capacitive coupling from adjacent circuits and wind speed. In the case of single-phase auto-reclosing where each phase of circuit breaker is segregated, longer de-ionization time is allowed because the

capacitive coupling of the faulted phase with the healthy phases is likely to maintain the arc for some time. This delay can be made adaptive depending on the recovery voltage produced during reclosing.

4.4. A Distribution Network

A distribution network experiences variations of load over each 24-hour period. System generation changes to match the load. The network occasionally undergoes topological changes, either due to scheduled maintenance of lines, breakers etc. or because of opening of circuit breakers to isolate a fault. These changes are associated with changes of source impedance. This results in the changes of fault current levels which cause the relay operating times to change. Generally, the pickup and the time dial settings of a relay are selected considering maximum load and fault currents that are likely to be experienced. When the system load decreases, generators are taken out of the service which reduces the fault levels. As a result, relay operating times become larger during low load periods.

In an adaptive approach, load and on-line generation could be periodically monitored and system configuration could be checked by monitoring circuit breakers. The relay settings can then be determined by considering the operating state of the system. This allows the pickup and time dial settings to be changed. As a consequence of these changes, the relay sensitivity and selectivity improves.

4.4.1. Functioning of an Adaptive Relaying System

Figure 4.2 shows the functional block diagram of the adaptive relaying system designed for a typical distribution substation. Only relays and the substation's control computer are shown for the sake of clarity. Similar configurations of relays and computers are used at other substations. The relays sample bus voltages and line currents via potential and current transformers, auxiliary transformers, analog-to-digital converters and multiplexers. Each relay processes quantized samples and calculates voltage and current phasors. During normal operating conditions, each relay provides phasor measurements to the station control computer at regular intervals. The relay also

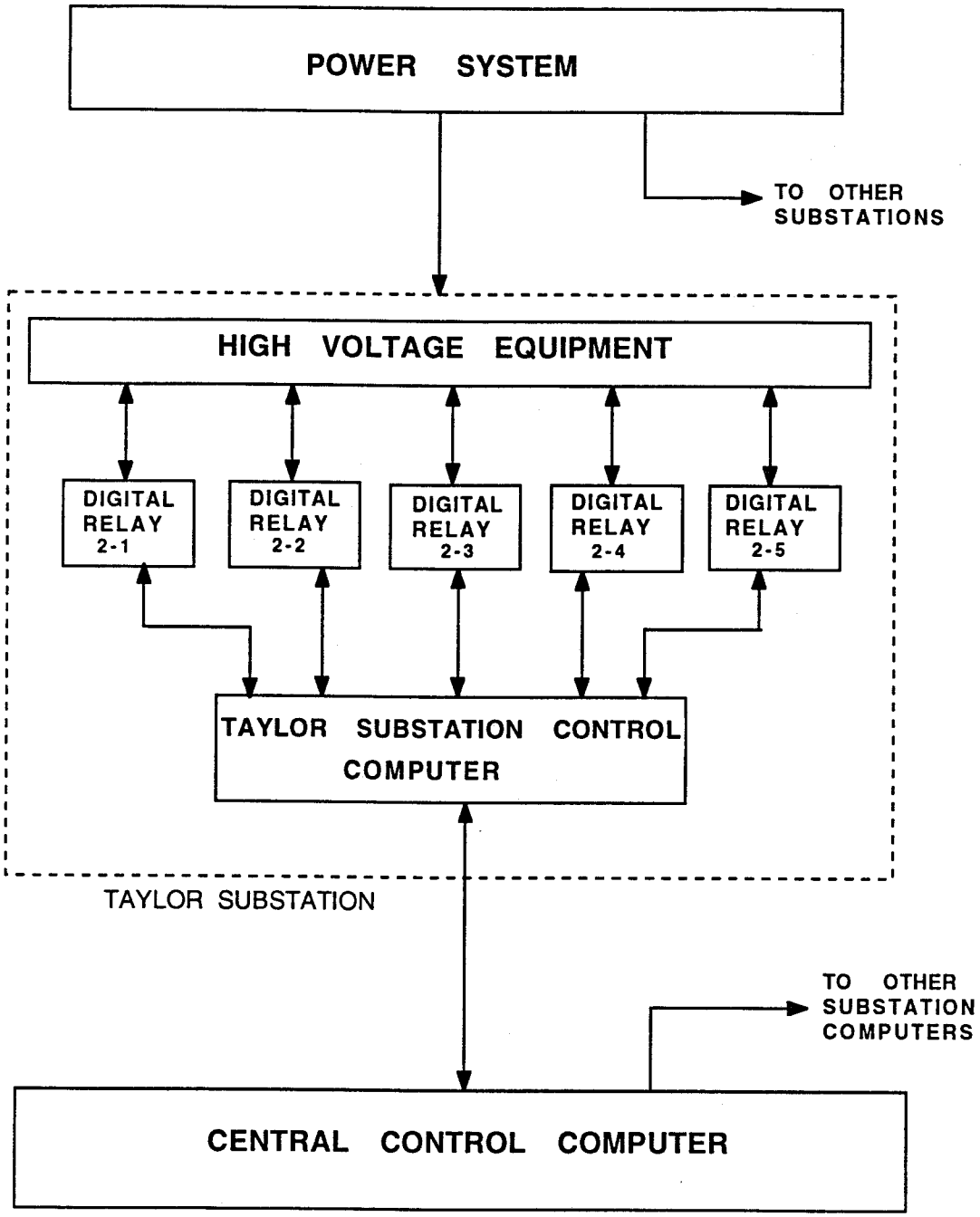

Figure 4.2: Functional block diagram of an adaptive relaying system.

checks the status of isolators and circuit breakers controlling the circuit protected by the relay and provides the information to the station computer. In addition to communicating with the relays, the station computer passes on the collected information to the central computer at pre-specified intervals, say one hour.

The central computer receive similar information from other station computers in the network, estimates the system state and decides whether the relay settings should be changed or not. If it decides that it is necessary to change the settings, it calculates them and conveys them to the relays via the station control computers. The relays implement the new settings and send confirmation messages to the central computer via the station computers. If the central computer decides not to change the settings, its decision is conveyed to the relays for sharing information and confirming that communication facilities are working properly.

When a switch is opened or closed, the relay supervising it sends the information to the central computer that analyzes the new state of the system and calculates the new relay settings.

4.5. The Selected Distribution Network

Figure 4.3 shows the distribution system, a reduced version of the 'City of Saskatoon' distribution network, which was used during the course of work presented in this thesis. The network consists of five switching stations, Avenue C, Taylor, Friebel, Cowley, and Pleasant Hill substations. Two 138 kv lines, QE-1A and QE-2A, connect the QE generating station of the Saskatchewan Power Corporation (SPC) to the Ave C substation. Three transformers, provided at the Ave C substation, step down the voltage to 14.4 kv. A 72 kv line, QE-5, connects the QE station to the Pleasant Hill substation, and another 72 kv line, QE-18, connects the QE station to the Cowley, Friebel and Taylor substations via the Bunn substation.

The substations have 72 kv/14.4 kv step down transformers which are connected to 14.4 kv buses. These buses are interconnected by lines to form the distribution network. Each line connects two substations and is protected by a circuit breaker provided at each

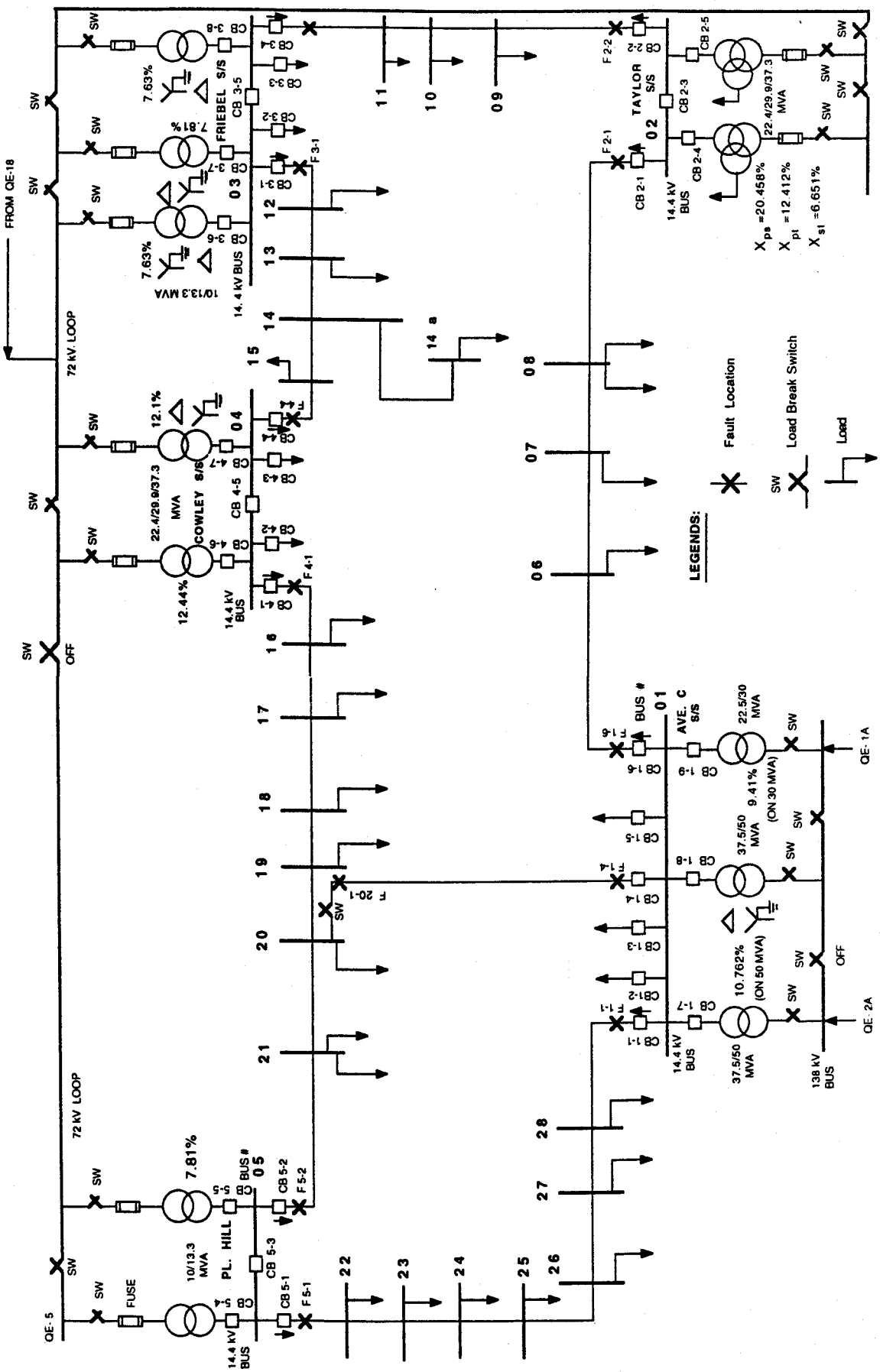

Figure 4.3: Single line diagram of the distribution network.

end. Each circuit breaker is equipped with an overcurrent or a directional overcurrent relay. All relays are also equipped with instantaneous overcurrent elements. Non-directional overcurrent relays are used for protecting 138/14.4 kv and 72/14.4 kv transformers, and load circuits emanating from the substations.

The present operating practice of the 'City of Saskatoon' is to operate each line as a radial circuit while each substation serves its local loads. In the event of loss of power at a substation, lines emanating from it are connected to other substations to restore power to the customers. However, for the studies reported in this thesis, all 14.4 kv circuit breakers are considered to be closed. The details of loads and parameters of lines are listed in Table 4.1.

4.6. Instrumentation

Instrumentation plays an important role in a protection system. Figure 4.4 shows a typical instrumentation scheme for a digital relay. Analog information concerning currents and voltages are received via current and potential transformers. The input signals are further reduced by auxiliary transformers which also electrically isolate the relays from the power system. The current inputs are then converted to voltages by current-to-voltage converters. Both the current and voltage inputs are applied to low-pass filters to limit the effects of noise and high frequency components. The filtered analog signals are sampled at time instants determined by a sampling clock. To preserve the phase of a signal, the sampling instants are precisely controlled. Also, analog-to-digital conversion requires that analog signals must be held steady during conversion. Sample and hold (S/H) amplifiers are used to perform this task. Usually, an analog multiplexer is applied to select one S/H output at a time for conversion. The filtered, scaled, sampled and selected quantity is presented to the analog-to-digital converter for conversion from a voltage to a number which can be used for further processing.

Several technical aspects must be studied before applying these devices in digital relays. The current transformers and analog-to-digital converters are the two most important devices that require consideration. These are discussed in the sections that follow.

Table 4.1: Line parameters and load levels of the distribution network.

Line Impedance			Bus Load (Maximum Loading Condition)		
Line (bus to bus)	% Resistance on 10 MVA base	% Reactance % on 10 MVA base	Bus	Real Power (MW)	Reactive Power (MVAR)
1-6	0.723	0.270	1	19.480	9.430
6-7	0.683	1.064	6	0.000	-2.400
7-8	0.243	0.374	7	10.930	5.290
8-2	1.218	0.861	8	1.350	-0.546
2-9	1.047	3.333	2	13.500	6.530
9-10	0.209	0.653	9	6.300	3.051
10-11	0.077	0.240	10	0.000	-1.200
11-3	0.591	1.841	11	0.315	0.152
3-12	0.555	1.734	3	11.020	5.336
12-13	0.663	2.160	12	0.180	0.087
13-14	0.357	1.163	13	0.810	0.392
14-15	0.149	0.463	14	5.210	2.524
15-4	1.042	3.248	15	0.000	-1.200
4-16	0.688	1.842	4	13.730	6.647
16-17	1.024	3.180	16	1.800	0.872
17-18	0.400	0.616	17	2.700	1.307
18-19	0.165	0.498	18	6.367	3.084
19-20	0.165	0.498	19	0.000	-1.200
20-21	0.804	1.759	20	1.035	0.501
21-5	0.427	1.065	21	8.704	2.415
5-22	0.536	1.241	22	2.780	1.349
22-23	0.251	0.407	23	4.500	0.984
23-24	0.337	0.653	24	0.280	0.135
24-25	0.110	0.171	25	1.620	0.784
25-26	0.173	0.266	26	0.900	0.436
26-27	0.521	0.801	27	3.303	3.997
27-28	0.464	1.402	28	2.780	1.349
28-1	0.386	1.048	-	-	-
1-20	0.585	0.817	-	-	-

Note: During minimum loading, bus loads are half of the listed loads.

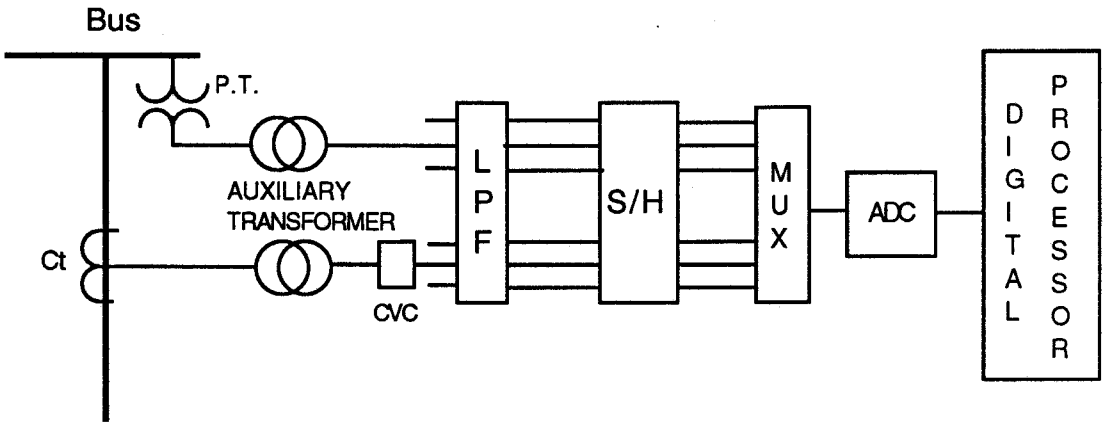

CVC: Current -to-Voltage Converter

Mux: Analog Multiplexer

LPF: Low-Pass Filter

ADC: Analog-to-Digital Converter

Figure 4.4: A typical instrumentation scheme for a digital relay.

4.6.1. Current Transformers

A current transformer secondary provides to a relay low level current which is essentially proportional to the current in its primary circuit. The performance of ct is, therefore, an important issue. Figure 4.5 shows the equivalent circuit of a current transformer. The exciting impedance of the transformer is z_e and leakage reactance is x. The resistances of the primary and secondary windings are r_p and r_s respectively. The primary quantities are reduced considering the turns ratio, n, of the transformer. The impedances of the loads are commonly called 'burden' and usually expressed in volt-amperes at a specified current or voltage. As long as a ct does not saturate, I_e can be neglected.

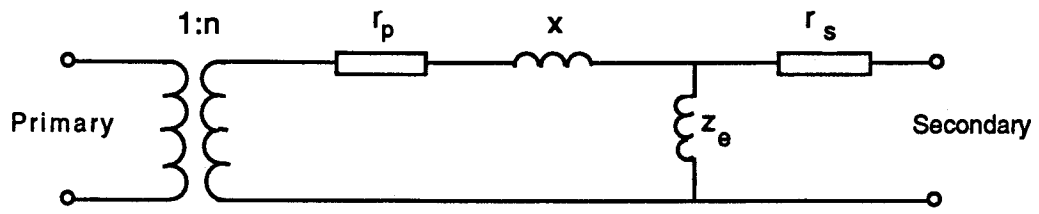

Figure 4.5: Equivalent circuit diagram of a current transformer.

4.6.1.1. Selection Criteria of Current Transformers

The selection of a ct depends on load and fault currents. The cts used for instrumentation are selected based on load currents, whereas, cts for relaying are selected considering load and fault currents. The cts used for protection should not saturate during a fault. This is checked using one of the following three methods [13].

1. Classical transformer formula.
2. Ct performance curves.
3. ANSI/IEEE standard curves.

The ANSI/IEEE standard curve technique, which is quite straight forward and assures satisfactory evaluation, is quite popular. Only this technique is, therefore, discussed in this thesis. Figure 4.6 shows the ct excitation curves reproduced from the ANSI/IEEE standard [32]. The voltage required by the burden can be expressed as

$$V_b = I_s(r_s+z_l+z_r), \tag{4.1}$$

where:

I_s is the secondary current of the ct,
r_s is the resistance of the secondary winding of the ct,
z_l is the impedance of the leads connecting the ct to the relay and
z_r is the impedance of the relay.

In this method, all burdens are first estimated and the voltage required by the burden is then calculated using Equation 4.1. The ct secondary resistance is obtained from the ANSI curve. The lead impedance depends on the size and length of cables, connecting the ct to the relay. To evaluate the relay burden, multiple of pickup current is calculated and the *VA* requirement is estimated. Once the total burden is known, the voltage required to sustain the fault current is calculated. This voltage should be less than the exciting voltage that can be produced by the chosen ct. ANSI curves provide the exciting voltages that different cts can produce. The selection of cts for this thesis is further discussed in Section 4.6.3.

4.6.2. Analog-to-Digital Converters

Analog to digital converters (ADC) are an important part of the data acquisition system. They generate strings of numbers representing analog inputs. An ADC must have sufficient precision, speed and accuracy for the application at hand. During the selection of an ADC for a relaying application, its dynamic range should be evaluated. Before discussing the dynamic range, resolution and quantizing error are discussed.

4.6.2.1. Resolution

Resolution of an ADC is a design parameter which is described as the input voltage change required to increment the output from one level to the next. An n-bit converter, therefore, has a resolution equal to 2^{-n}. A converter which has a full-scale voltage, V_{FS} volts, could resolve $V_{FS}/2^n$ volt input change. This corresponds to the size of the least significant bit (LSB).

4.6.2.2. Quantization Error

The quantization error of an ADC, which is related to its resolution, is defined as the maximum deviation from the transfer function of a perfect ADC. Figures 4.7 and 4.8 illustrate the transfer function of a three-bit ADC and its quantization error. For an input V_x, applied to an ADC of $(b+1)$ bits, the quantized value $Q(V_x)$ must not exceed the maximum value that can be stored in a word of $(b+1)$ bits.

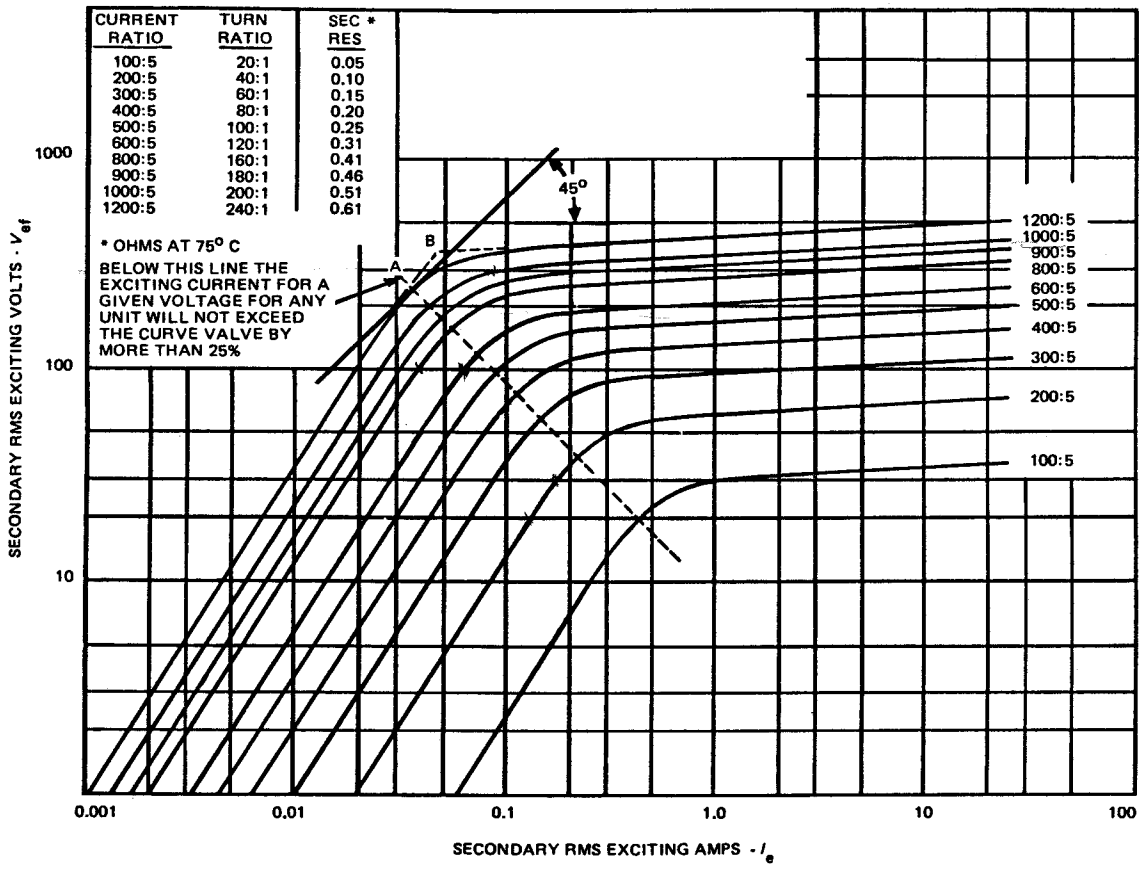

Figure 4.6: Typical excitation curves for current transformers [32].

Two methods, truncation and rounding can be applied to fit a continuous signal to generate equivalent quantized information. It is apparent that only an ADC of infinite word length would exhibit no quantization error.

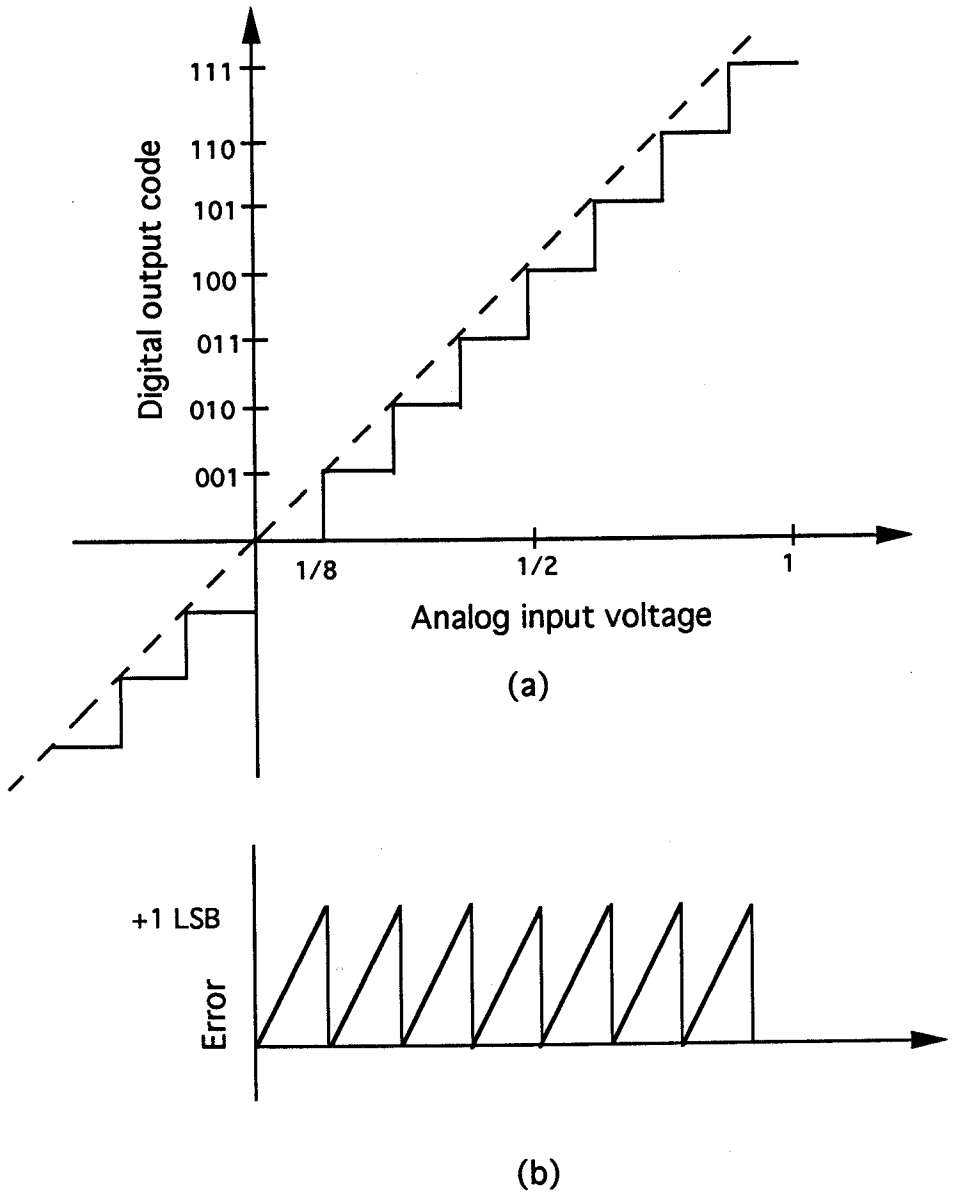

Figure 4.7: Quantization of an ideal three-bit ADC using truncation: (a) input-output relationship, (b) quantization error.

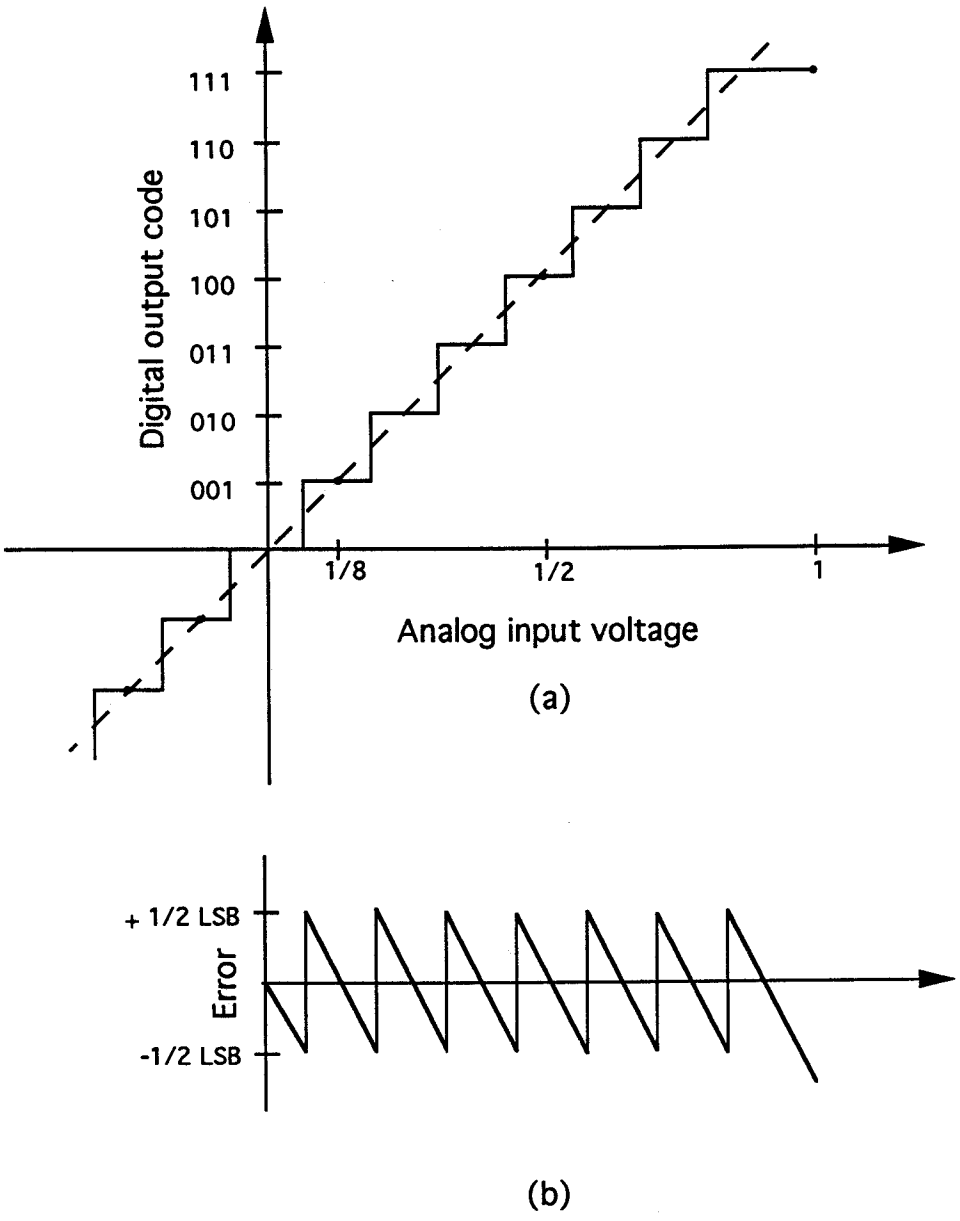

Figure 4.8: Quantization of an ideal three-bit ADC using rounding off: (a) input-output relationship, (b) quantization error.

4.6.2.3. Dynamic Range

In a relaying application, ADC of wide dynamic range is often necessary for measuring a signal which varies over a wide range. To obtain reasonable accuracy, an ADC with an exceedingly long word could be used. This is not generally done because their cost is high and the observation provided by them include system noise [33]. The noise is caused by two major factors. Firstly, changes in temperature and components used in the ADC, particularly comparators and resistors, add noise to the inputs. Noise is also generated by the electromagnetic fields of the power system and by the opening and closing of switches. As an alternative to ADC of long word, a programmable gain amplifier could be used. Figure 4.9 shows a schematic diagram of a programmable gain ADC. It first performs a trial conversion at the lowest gain. If the most significant bit (MSB) of quantized sample is zero, the gain is doubled. Another conversion is then performed and the MSB is checked, and if the MSB is still zero, the gain is doubled again until the MSB is one. Each doubling of the gain represents an addition of a bit to the resolution.

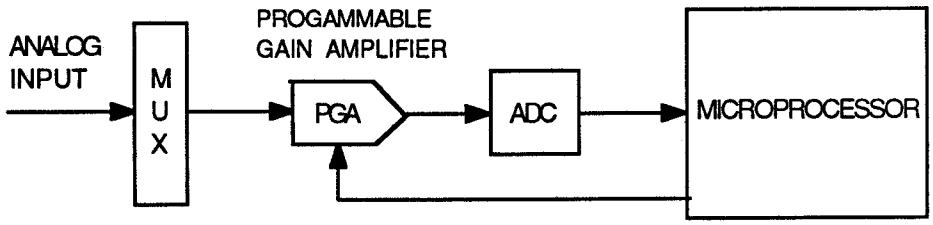

Figure 4.9: Schematic diagram of a programmable gain ADC.

4.6.3. Instrumentation for the Selected Distribution Network

In view of the preceding discussions, load flows for several operating conditions were conducted. Relay currents for faults at different locations in the distribution network were determined. Load currents and fault currents at the relay locations for faults at both ends of each line during maximum and minimum load and generating conditions are listed in Table 4.2. This table shows that the ratio of the fault current to load current in all cases is exceedingly high. To keep the cts from saturating during faults, two set of cts are provided at each relay location [34]. The smaller rating cts are for load current measurements and for overload protection. The higher rating cts are for protection from faults. In this application, 1000/5 A cts experience 10 to 20 kA fault currents and 2000/5 A cts experience 20 to 50 kA fault currents. The details of how cts are selected is given in Appendix A. Cts for metering and overload protection are selected on the basis of maximum load currents that the circuits experience. The selected ct ratios are also listed in Table 4.2.

While programmable gain ADC is a choice for obtaining large dynamic range, it is suitable for use with one ct per relaying location. Since two cts for each relaying location have been selected, two separate ADCs are used. Using separate ADCs also relieves some computational burden from the relaying processor. An auxiliary transformer is used to reduce the current levels before applying it to the current to voltage converter resistor. For selecting the ratings of the auxiliary transformers, a dc-offset factor of 2 was used. The procedure for selecting auxiliary transformers is illustrated in Appendix B.

Figure 4.10 shows the arrangements of cts and ADCs for relay 1-1. Figure 4.10 shows that both input channels are active all the time but relay processes only one set of data depending on the levels of the inputs it receives.

Table 4.2: Load and fault currents, and ratings of cts and auxiliary transformers.

Relay	Operating Conditions	Load Currents (Amps)	Fault Currents (Amps)		Ct Ratings		Phase Fault & O/L Auxiliary Transform. Ratings
			Near-end Faults	Far-end Faults	Measuring & O/L cts	PhaseFault cts	
1 -1	Max. Load & Gen. Level (Line 1-20 Closed)	398	46815	4941	800/5 C50	2000/5 C400	35:1 2:1
	Min. Load & Gen. Level (Line 1-20 Closed)	181	42546	4440			
	Max. Load & Gen. Level (Line 1-20 Open)	646	40648	5703			
	Min. Load & Gen. Level (Line 1-20 Open)	337	36503	5273			
1-4	Max. Load & Gen. Level (Line 1-20 Closed)	404	42642	3875	600/5 C50	2000/5 C400	30:1 2:1
	Min. Load & Gen. Level (Line 1-20 Closed)	192	38804	3692			
	Max. Load & Gen. Level (Line 1-20 Open)	-	-	-			
	Min. Load & Gen. Level (Line 1-20 Open)	-	-	-			
1-6	Max. Load & Gen. Level (Line 1-20 Closed)	522	42490	8741	600/5 C50	2000/5 C400	30:1 2:1
	Min. Load & Gen. Level (Line 1-20 Closed)	223	38940	8670			
	Max. Load & Gen. Level (Line 1-20 Open0)	557	38328	8947			
	Min. Load & Gen. Level (Line 1-20 Open)	298	34605	8638			
2-1	Max. Load & Gen. Level (Line 1-20 Closed)	241	15331	6738	400/5 C50	1000/5 C100	20:1 2:1
	Min. Load & Gen. Level (Line 1-20 Closed)	111	13998	6403			
	Max. Load & Gen. Level (Line 1-20 Open)	362	15246	6764			
	Min. Load & Gen. Level (Line 1-20 Open)	154	13971	6471			
2-2	Max. Load & Gen. Level (Line 1-20 Closed)	81	18574	4806	200/5 C50	1000/5 C100	30:1 2:1
	Min. Load & Gen. Level (Line 1-20 Closed)	34	17369	4669			
	Max. Load & Gen. Level (Line 1-20 Open)	164	18493	4828			
	Min. Load & Gen. Level (Line 1-20 Open)	78	17278	4693			

3-1	Max. Load & Gen. Level (Line 1-20 Closed)	100	16179	3526	300/5 C50	1000/5 C100	25:1
	Min. Load & Gen. Level (Line 1-20 Closed)	48	14784	3407			2:1
	Max. Load & Gen. Level (Line 1-20 Open)	200	16207	3560			
	Min. Load & Gen. Level (Line 1-20 Open)	97	14812	3442			
3-4	Max. Load & Gen. Level (Line 1-20 Closed)	210	14915	4544	300/5 C50	1000/5 C100	20:1
	Min. Load & Gen. Level (Line 1-20 Closed)	103	13540	4357			2:1
	Max. Load & Gen. Level (Line 1-20 Open)	113	14887	4577			
	Min. Load & Gen. Level (Line 1-20 Open)	53	13502	4387			
4-1	Max. Load & Gen. Level (Line 1-20 Closed)	153	14509	1806	300/5 C50	1000/5 C100	20:1
	Min. Load & Gen. Level (Line 1-20 Closed)	75	13240	1739			2:1
	Max. Load & Gen. Level (Line 1-20 Open)	261	14596	3361			
	Min. Load & Gen. Level (Line 1-20 Open)	123	13299	3180			
4-4	Max. Load & Gen. Level (Line 1-20 Closed)	158	15596	3497	200/5 C50	1000/5 C100	25:1
	Min. Load & Gen. Level (Line 1-20 Closed)	76	14360	3375			2:1
	Max. Load & Gen. Level (Line 1-20 Open)	79	14029	3446			
	Min. Load & Gen. Level (Line 1-20 Open)	30	12838	3319			
5-1	Max. Load & Gen. Level (Line 1-20 Closed)	389	16499	2725	400/5 C50	1000/5 C100	25:1
	Min. Load & Gen. Level (Line 1-20 Closed)	167	15380	2265			2:1
	Max. Load & Gen. Level (Line 1-20 Open)	326	11941	4395			
	Min. Load & Gen. Level (Line 1-20 Open)	50	10958	3983			
5-2	Max. Load & Gen. Level (Line 1-20 Closed)	322	13185	1251	800/5 C50	1000/5 C100	20:1
	Min. Load & Gen. Level (Line 1-20 Closed)	157	12314	1109			2:1
	Max. Load & Gen. Level (Line 1-20 Open)	612	14130	3512			
	Min. Load & Gen. Level (Line 1-20 Open)	298	13171	3212			

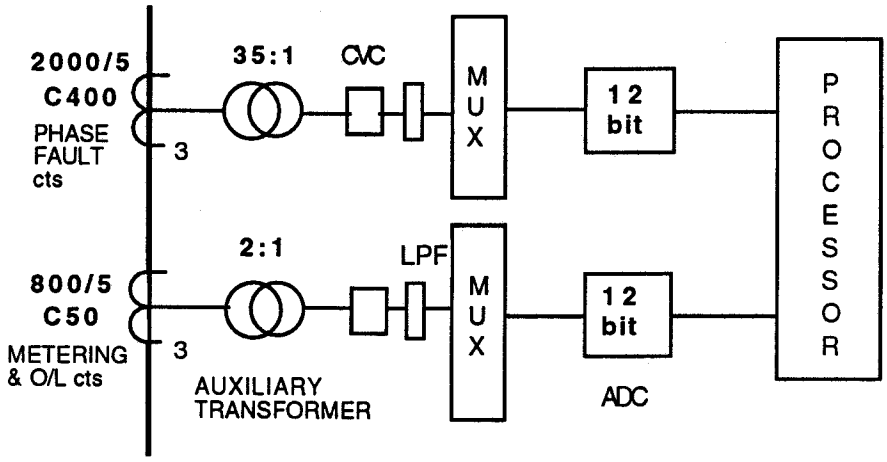

Figure 4.10: Arrangements of cts and ADCs for relay 1-1.

4.7. Summary

In this chapter, an adaptive protection system has been described. Several problems presently encountered have been outlined and their alleviation by using the adaptive approach have been discussed. The selected distribution network and the functioning of an adaptive relaying system have also been described. System studies showed that the selected distribution network experiences large changes of load and fault currents and, therefore, each circuit requires separate equipment for instrumentations and relaying. It is proposed that separate cts be used at each relaying location, one set for overload and the other for fault protection. Also, separate ADCs are proposed for each relay location which ensures sufficient dynamic range during moderate overloads and faults.

5. SOFTWARE FOR DIRECTIONAL OVERCURRENT RELAYS

5.1. Introduction

The objective of an adaptive protection system, stated in Chapter 4, is to change the relay settings as load currents, expected fault currents and system topology change. In this manner, the operating times of all relays will be kept close to a selected minimum level while proper coordination margins are maintained. The development of such an adaptive relaying scheme requires two major software packages, one for the relaying software and the other for calculating relay settings and checking for coordination. Also two application softwares are needed, one for communication between relays and other station computers, and the other for communication between the station control computers and the central control computer.

This chapter describes the software for directional overcurrent relays and its implementation on a TMS320C25 DSP microprocessor.

5.2. Relaying Software

Directional overcurrent relays, in conjunction with instantaneous relays, are considered for protecting the selected distribution network. A relay for the selected application must include softwares for modelling relay characteristics, implementing directional units, estimating line currents and voltages, and formulating the trip decision logic. A presently available model of overcurrent relay characteristics was modified to make it suitable for the work reported in this thesis. An approach that is different than the existing technique, was developed for implementing the directional units. Some modifications were incorporated in the usual decision logic. These software segments are discussed in the following sections.

5.2.1. Designing Current-Time Characteristics

Mathematical equations are used to model the inverse time overcurrent relay characteristics [35]. Chapter 3 reviews the presently available equations to represent their current-time characteristics. These characteristics express the contact closing times as functions of the relay current. Usually, a family of curves is considered for representing the characteristics; each curve corresponds to a time multiplier setting *(TMS)*. Presently available microprocessor based relays store relay characteristics corresponding to several *TMS* values. For the adaptive application, only one characteristic corresponding to *TMS* value of 1 and multiples of pickup current up to 25 is stored in the relaying processor. The relay characteristics corresponding to other *TMS* values are calculated in the on-line mode whenever it becomes necessary to use them.

The following equation, suggested by the International Electrotechnical Commission [15], was selected to model the relay characteristics:

$$t = \frac{k \times TMS}{(I_{mpu})^n - 1}, \tag{5.1}$$

where:

t	is the relay operating time,
k	is a constant,
n	is an index that determines the type of the characteristic,
TMS	is the time multiplier setting and
I_{mpu}	is the multiple of pickup current.

This equation provides inverse, very inverse or extremely inverse characteristics depending on the values assigned to k and n. For the purpose of the studies in this thesis, the very inverse characteristic was selected, for which k and n are 13.5 and 1 respectively.

5.2.1.1. Instantaneous Element

It was decided that in conjunction with each overcurrent relay, an instantaneous overcurrent element be used. The instantaneous protection would provide high speed operation for near-end faults and reduce overall operating times. The use of instantaneous elements is generally recommended when the ratio of near-end fault (maximum and/or minimum) and far-end fault (maximum) is on the order 1.15 to 1.3 or more [13, 36]. The pickup value of an instantaneous unit is defined as

$$I_{IT} = K_i \times I_{FF}, \tag{5.2}$$

where:

I_{IT} is the pickup setting of the instantaneous trip unit,
I_{FF} is the current for a fault at the far-end of the line and
K_i is the ratio of the instantaneous pickup and maximum far-end fault currents.

The operation of an instantaneous element depends on the magnitude of the current in it; it operates almost instantaneously whenever the current exceeds the pickup setting. The usual operating time of an instantaneous element is approximately two time periods of the system frequency. A similar delay was built in the units designed for this project.

5.2.2. Modelling Directional Overcurrent Relay

All line relays in the network are of the directional overcurrent type. As such, directional features were incorporated in the overcurrent relays. Electromechanical directional overcurrent relays develop torque that must be more than a pre-specified value to conclude that the fault is on the line side of the relay. The torque, T, is usually expressed as

$$T = k_1 |V| |I| \cos(\theta - \tau) - k_2, \tag{5.3}$$

where:

V is the voltage phasor (polarizing quantity),
I is the current phasor,
θ is the phase angle between I and V phasors,

τ is the maximum torque angle,

k_1 is the relay constant and

k_2 is the torque offset.

The implementation of Equation 5.3 in a microprocessor is cumbersome because $cos(\theta - \tau)$ is to be estimated at every sampling instant. Singh et al. [18] proposed that the operating criterion be implemented by advancing the polarizing voltage phasor and taking the projection of the current phasor on the modified polarizing voltage phasor. A similar but somewhat different approach was developed in this application. Using well known trigonometric identities, Equation 5.3 was modified to

$$T = k_1(|V||I|cos\theta\, cos\tau + |V||I|sin\theta\, sin\tau) - k_2. \tag{5.4}$$

Since the phasor estimates are in the form of their real and imaginary components, $|V||I|cos\theta$ were replaced by $(V_r I_r + V_i I_i)$; V_r and I_r are the real components of voltage and current phasors, and V_i and I_i are imaginary components of voltage and current phasors. Similarly, $|V||I|sin\theta$ were replaced by $(V_r I_i - V_i I_r)$ and the following equation was obtained:

$$T = [(V_r I_r + V_i I_i)\,(k_1 cos\tau) + (V_r I_i - V_i I_r)\,(k_1 sin\tau)] - k_2. \tag{5.5}$$

The most commonly used connections to develop maximum torque under fault conditions is the 90° connection with a maximum torque angle of 30° or 45°. The 90° connection applies a voltage that lags the unity power factor current by 90°. Since fault currents generally lag the unity power factor phasors by approximately 60°, a maximum torque angle of 30° should produce the most torque. During implementation of Equation 5.5, a relay connection angle of 90° and a maximum torque angle of 30° were used. Corresponding to a selected maximum torque angle, $cos\tau$ and $sin\tau$ are to be calculated in the off-line mode and stored in the microprocessor memory. The factors k_1 and k_2 were selected as 1 and 1/16. The algorithm uses the first part of Equation 5.5 to estimate and then compare with a threshold value of 1/16, selected to compensate for the A/D converter drift errors and estimation errors.

For a three phase fault at the relay location, polarizing voltage collapses to zero and consequently no torque is produced. To prevent such a condition, memory action was incorporated in the design. This technique uses a combination of the pre-fault and the post fault voltages at the relay location. Some aspects of the memory action are further discussed in the section on implementation.

5.3. Estimation of Current and Voltage Phasors by LES

Least Error Squares (LES) algorithm was selected for estimating current and voltage phasors. LES is a curve fitting technique which assumes that the composition of the voltage and current signals are known in advance. Since most of the computations are performed off-line, the on-line computational burden is not excessive. The detailed mathematical formulation of this technique has been described in Chapter 3. The strengths and weaknesses of the algorithm are as follows [37]:

1. It effectively rejects the high frequency components.
2. It attenuates noise.
3. It effectively rejects the decaying dc components.
4. Its transient response is slower than short window techniques but is comparable to the Fourier analysis approach.
5. It might require more multiplications than the Fourier approach.

The selected approach models the voltages and currents by the first two terms of the Taylor series expansion of a decaying dc component, a fundamental frequency component, and the second, third, fourth and fifth harmonics. A data window of 13 samples at a sampling frequency of 720 Hz were chosen as the best trade-off between the speed/size of the window versus the accuracy of its estimates and its ability to suppress noise. This provided a data window of 18.1 *msecs* long with approximately 1.4 *msecs* time to perform the necessary calculations and implement trip logic. The LES filter coefficients were computed in the off-line mode and used in the algorithm; the coefficients are listed in Table 5.1. Quantized voltages and currents in conjunction with these filters were used to estimate real and imaginary components of their phasors.

It can be shown from the filter coefficients, listed in Table 5.1, that the variances of the noise in the voltage and current estimates provided by the cosine and the sine filters is 0.36011 and 0.15217 times the variance of the noise in the inputs. Therefore, both filters will suppress noise quite effectively. Appendix C describes the noise aspects of the filters in detail. Figure 5.1 shows the frequency responses of the LES filters; the response of the sine filter is quite satisfactory and that all harmonics except the sixth are suppressed to zero. The frequency response of the cosine filter is also satisfactory except that its main lobe is offset from the fundamental frequency by about 18.5 Hz.

Table 5.1: The filter coefficients for a 13 point LES filter.

Data Point	Cosine Coefficients	Sine Coefficients
x (-6)	0.3110042	-0.0869565
x (-5)	-0.0833333	-0.1370912
x (-4)	-0.1443376	-0.0905797
x (-3)	-0.1666667	0.0072464
x (-2)	-0.1443376	0.0760870
x (-1)	-0.0833333	0.1515839
x (0)	0.0000000	0.1594203
x (1)	0.0833333	-0.1515839
x (2)	0.1443376	-0.0760870
x (3)	0.1666667	-0.0072464
x (4)	0.1443376	0.0905797
x (5)	0.0833333	0.01370912
x (6)	-0.3110042	0.0869565

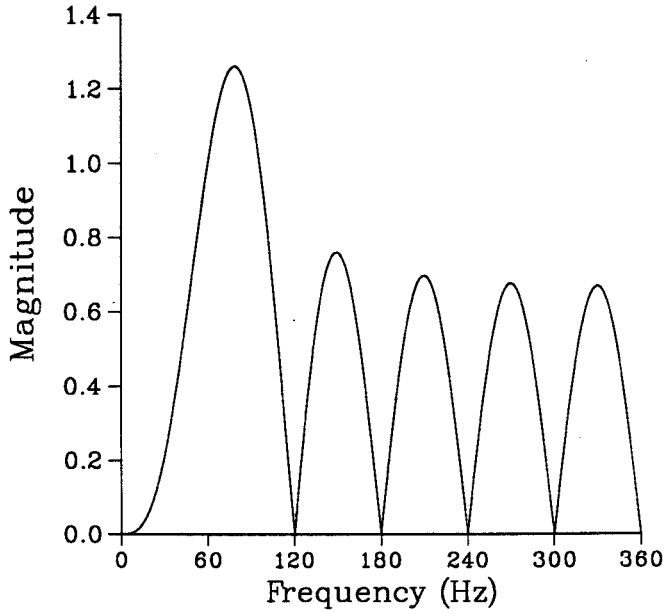

(a)

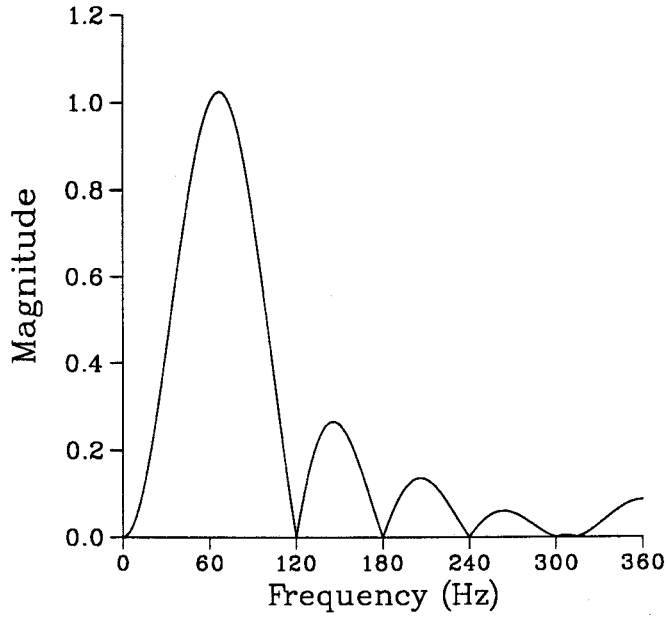

(b)

Figure 5.1: Frequency response of an LES filter: (a) Cosine filter, (b) Sine filter.

5.3.1. Amplitude Estimation

The amplitude of the fundamental frequency component of a current or voltage can be computed from the real and imaginary components of its phasor as follows. The amplitude of a signal can be estimated by

$$I_{ampl} = \sqrt{I_r^2 + I_i^2}. \tag{5.6}$$

The implementation of a square root function is computationally expensive. To reduce the computational burden, a piecewise linear approximation technique was used. The amplitude was expressed as

$$I_{ampl} = Lx + Sy, \tag{5.7}$$

where:

L	represents the larger of two values, $\|I_r\|$ and $\|I_i\|$,
S	represents the smaller of two values, $\|I_r\|$ and $\|I_i\|$ and
x and y	are the coefficients for the region in which the fraction S/L lies.

Table 5.2 shows the coefficients of x and y for a four region approximation.

Table 5.2: Coefficients for piecewise linear interpolation using four regions of approximation.

Region	x	y
0.00 = S/L ≤ 0.25	0.7036	0.0873
0.25 < S/L ≤ 0.50	0.6641	0.2473
0.50 < S/L ≤ 0.75	0.6015	0.3738
0.75 < S/L ≤ 1.00	0.5337	0.4649

5.4. Implementation of the Relaying Software

The overcurrent together with directional and instantaneous algorithms were implemented on TMS320C25 DSP microprocessors. The software was implemented in floating point format. The floating point functions were written in standard ANSI C language [38] and then cross-compiled into TMS assembly language suitable for use on Ariel corporation's [39] DSP-C25 boards. The boards are interfaced to the expansion ports of MS-DOS personal computers which served as hosts to the DSP boards. An interface program, written in Lattice C, was used to upload the program and input data to the DSP-C25 board and to download the outputs to the host computer.

5.4.1. Overcurrent Relay

The time delays, emulating the time-current characteristic, were realized by using the concept of a counter and weights. At every sampling instant, a weight was calculated depending on the magnitude of the current and was added to a cumulative weight stored in the counter. The weighting factor, $w_r(t)$, is zero when the current is less than the pickup value. For higher current multiples, a larger weight was assigned; it could be related as

$$w_r(t) = N_{target}\frac{I(t)^n - 1}{k}, \tag{5.8}$$

where:

$I(t)$	is the current observed at time t in multiples of the pickup current,
$w_r(t)$	is the weight corresponding to $I(t)$ and
N_{target}	is the target number selected for implementing the relay characteristic.

If the current during a fault is constant, the weighting factor at each instant will be the same. However, if the current changes with time, the operating time of relay must be calculated taking changes into consideration. It was achieved by integrating a function that depends on the observed current [18]. The description of the procedure used in the software follows.

Ideally, the integration of Equation 5.8 would start after the inception of a fault when the current exceeds the pickup value. When the integration exceeds the target number, a trip command is issued. This is mathematically expressed as

$$\int_0^t w_r(t) > N_{target}. \tag{5.9}$$

If the estimated current falls below the pickup value, a resetting process is undertaken. Using the rectangular rule for integration and the fact that the currents are sampled at intervals of ΔT, Equation 5.9 can be written for k^{th} sample as

$$\sum_{k=0}^{M} w_r(k)\,\Delta T > N_{target}. \tag{5.10}$$

Alternatively, this equation can be written as

$$\sum_{k=0}^{M} W_r(k) > N_{target}, \tag{5.11}$$

where:

$W_r(k) = 0$ when the current is less than the pickup current and

$W_r(k) = \frac{N_{target}\,\Delta T}{i(k)}$ when the current is greater than the pickup value.

The relay operating time can be expressed as $M\Delta T$, but M is unknown. It is determined by calculating the value of $W_r(k)$ and upon evaluating Equation 5.11.

During a fault, when the directional element determines that the fault is in the tripping direction, weights corresponding to multiples of pickup currents are determined and added to a trip counter. If the current is less than the pickup value or the torque of the directional unit is less than the threshold, resetting of the trip counter is initiated. When the summation reaches the target number, a trip command is issued.

5.4.1.1. Target Number

A target number is required to be selected for implementing the relaying algorithm, discussed in the preceding section. In this project, a floating point format was used for processing data. Unlike the integer format, the floating point format does not introduce truncation errors. A target number of 1 was selected for the work reported in this thesis.

5.4.1.2. Lookup Table

The weighting factor W_r, defined in Equation 5.11, can be calculated using w_r obtained by substituting the fault current in Equation 5.8 and then multiplying the result by ΔT. On-line calculations of the weighting factors would require excessive computations to be performed in one sampling interval.

A more computationally efficient method is to have a look-up table of the multiples of pickup current and their corresponding weights. The weights were calculated off-line for a time multiplier setting of one, multiples of pickup current up to 25 and the current-time characteristic. These weights were then stored in a look-up table. Whenever *TMS* other than one will be required, the target number will be multiplied with the selected *TMS*. For currents that were not listed in the lookup table, the following linear interpolation to determine their weights was programmed:

$$W_r(k) = W_1 + \frac{(W_2 - W_1)(I_k - I_1)}{I_2 - I_1}, \tag{5.12}$$

where:

- I_k is the estimated current in multiples of pickup,
- $W_r(k)$ is the weight corresponding to I_k,
- I_1 and I_2 are the currents, in multiples of pickup, that are listed in the table and are lesser and greater than the estimated current,
- W_1 is the weight corresponding to the current I_1 and
- W_2 is the weight corresponding to the current I_2.

For currents greater than 25 multiples of pickup value, the software uses the weight corresponding to 25 multiples of pickup current. Figure 5.2 shows the weighting curves for IEC current-time characteristics up to current multiples of 25. Since the characteristic curve is linear, there will be insignificant error during linear interpolation.

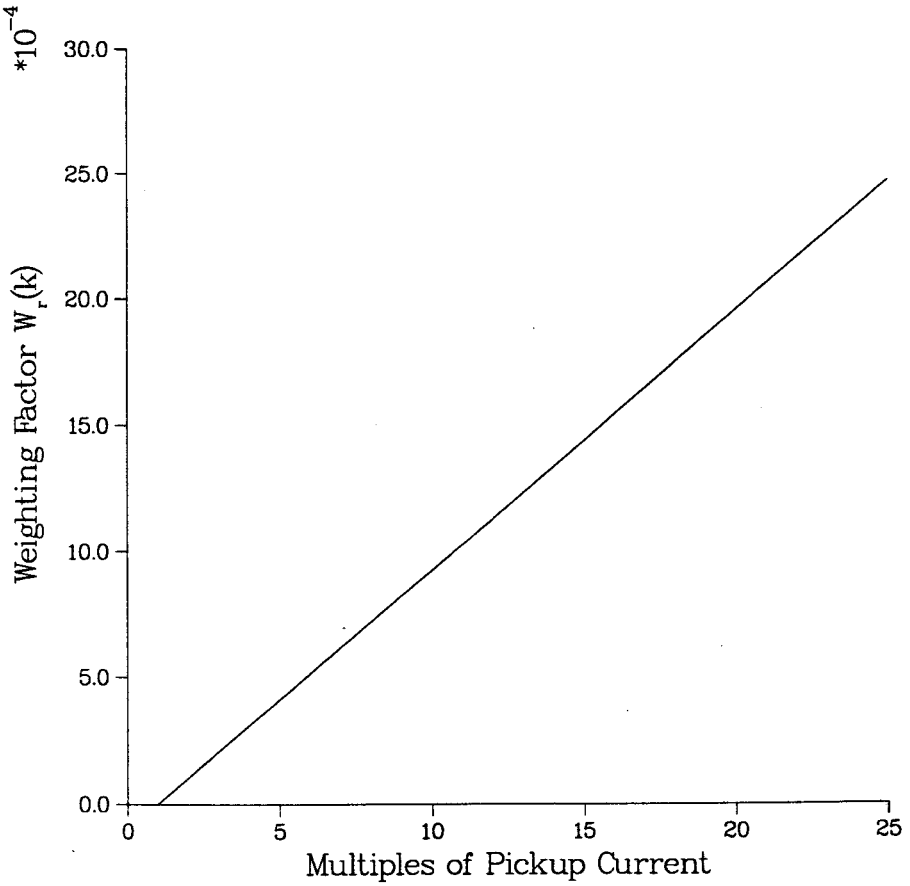

Figure 5.2: Calculated weighting factors for IEC current-time characteristic.

5.4.1.3. Resetting

Resetting should take place as soon as currents in a protected circuit reduce to levels below the pickup setting. While electromechanical overcurrent relays reset gradually due to the force of a restraining spring, solid state relays reset either gradually or without any time delay. The microprocessor based relays can have a variety of resetting characteristics because they are software controlled. Three types of setting characteristics, instantaneous, linear and exponential were provided in the design. The instantaneous reset characteristic sets the trip counter sum $W_r(k)$ to zero. The linear reset characteristic gradually resets the relay with time. It modifies $W_r(k)$ using equation

$$\sum W_r(k+1) = \{\sum W_r(k)\} - L, \qquad (5.13)$$

where:

L is a number that determines the rate of resetting.

The third characteristic resets $\sum W_r(k)$ exponentially with time. This was achieved from the following equation:

$$\sum W_r(k+1) = E \sum W_r(k), \tag{5.14}$$

where:

E is a fractional number which controls the rate of resetting.

5.4.2. Instantaneous Element

Each instantaneous unit was implemented by using its weighting factor. At any instance when the estimated current is greater than its instantaneous pickup setting, a weight was added to its trip counter. A current-time integration of a straight line characteristic was implemented.

5.4.3. Memory Action

During a near-end three phase fault, the voltage at the relay location would be close to zero. This makes it difficult for the directional element to produce the required torque. To overcome this problem memory action was implemented using pre-fault voltages. To begin with, the relay checks the phase voltages against a threshold to see if they have collapsed. If all three have collapsed, all acquired samples are discarded and the values of 13 samples, taken earlier, are used. The process of discarding new samples and replacing them with the pre-fault values continues until appropriate decisions are made.

5.5. Overall Implementation and Tripping Logic

Figure 5.3 describes a simplified flowchart illustrating the overall implementation scheme and the tripping logic of the designed relay. At the time of commissioning the relay, the directional overcurrent algorithm goes through a process of initialization when the relay settings are defined and the data windows are set up. In all, six 13-point data windows are used, one for each phase voltage and current. These windows are updated by a new data point at each sampling interval. Using these data windows, the real and imaginary components of the phase voltages and currents are estimated.

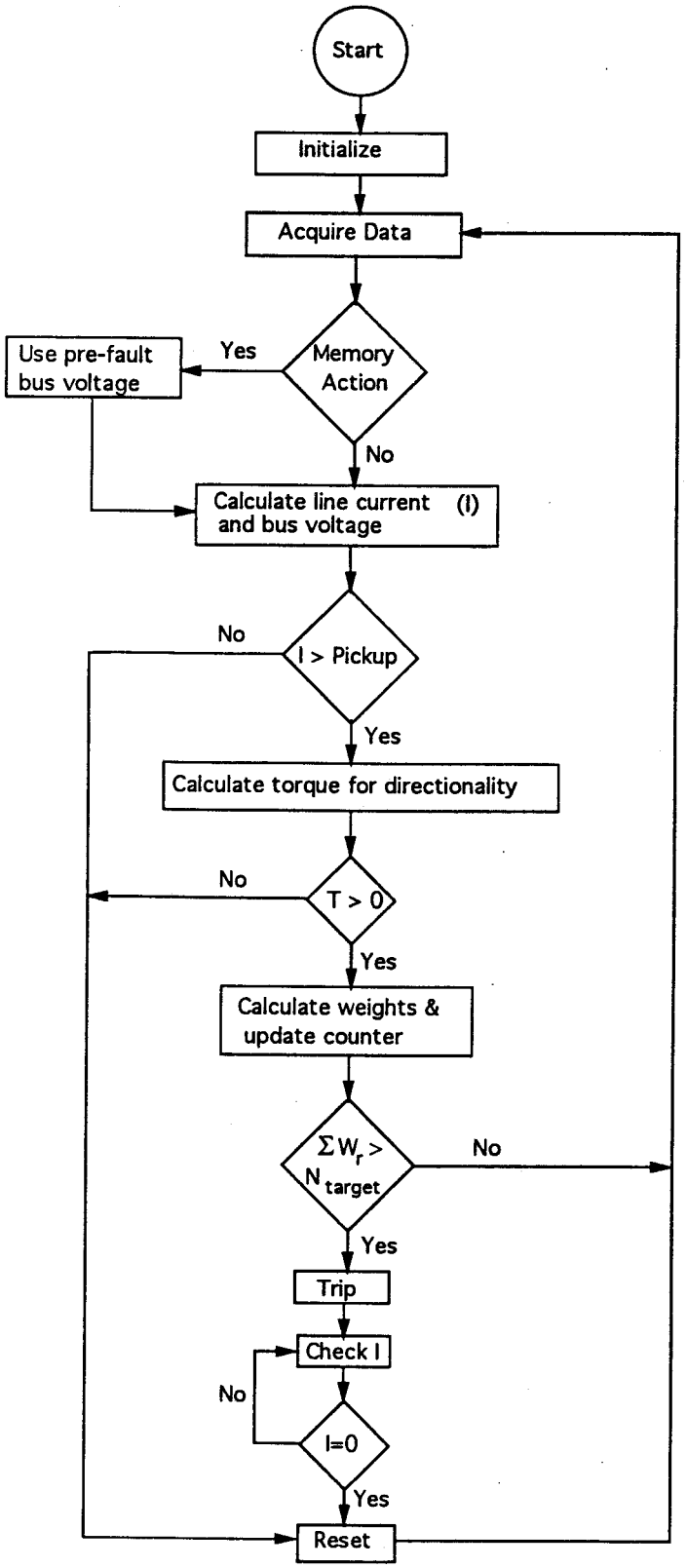

Figure 5.3: Illustration of overall implementation and tripping logic.

At each sampling instant, the relay first checks if all three phase voltages have reduced to values less than the setting of the memory action; if they have, memory action is invoked. The estimated lines currents are then compared against the pickup settings for the overcurrent units; this process acts as a fault detecting element. If currents in all lines are less than the overcurrent pickup setting, its trip counter is reset. If one of the estimated currents exceeds the pickup value, the relay estimates the phase voltages and proceeds to evaluate the torque to determine directionality. The directionality is checked at each sampling interval. This ensures that the directional element does not perform calculations unnecessarily. New data are acquired and the check is performed again.

If the difference between an estimated torque and torque offset is greater than zero the relay decides that the fault is on the line side of the relay. Once the directional flag is 'on', the overcurrent unit is allowed to increment its trip counter using appropriate weights. The overcurrent unit then determines if the tripping criterion has been met. If it has, a trip signal is generated. After issuing the trip signal, the line current is checked and if the current is less than a set value resetting of the relay is then begun.

5.6. Testing

The operation of the designed inverse time overcurrent relay was tested using a fundamental frequency current of constant magnitude. The errors introduced by A/D conversion and by the estimation procedure were neglected. The operating time was emulated from the number of sampling intervals required to generate a trip signal. The results are listed in Table 5.3. This table shows that compared to the theoretical values, computed using Equation 5.1, the relay effectively emulates the IEC current-time characteristic and the errors are within 1%.

5.7. Summary

This chapter has discussed the adaptive relaying software and its implementation on TMS320C25 DSP microprocessors. The modifications to the presently available methods of modelling overcurrent relay characteristic necessary for this project have been outlined. It is proposed that only one characteristic be stored and other

Table 5.3: The performance of an inverse-time overcurrent relay set at TMS=1.0.

Current Multiples	IEC Time (sec) (Theoretical)	Emulated Time (sec) (Experimental)	Percent Difference
1.5	27.000	27.001389	0.005144
2.0	13.500	13.501389	0.010288
2.5	9.000	9.001389	0.015433
3.0	6.750	6.751389	0.020578
3.5	5.400	5.401389	0.025722
4.0	4.500	4.501389	0.030867
4.5	3.857	3.858333	0.036078
5.0	3.375	3.376389	0.041156
5.5	3.000	3.001389	0.046300
6.0	2.700	2.701389	0.051444
7.0	2.250	2.251389	0.061733
8.0	1.928	2.077778	0.072044
9.0	1.687	1.688889	0.082336
10.0	1.500	1.501389	0.092600
12.5	1.174	1.175000	0.085179
15.0	0.964	0.965278	0.144408
17.5	0.818	0.819444	0.169804
20.0	0.710	0.711111	0.195634

characteristics be initiated in the on-line mode when they are needed. An algorithm for implementing directional elements has been developed. Some considerations in sampling rate, selection of data window and phasor estimation are discussed. The test results show that the implemented IEC characteristics matches the theoretical values.

6. SOFTWARE FOR SYSTEM ANALYSIS AND RELAY COORDINATION

6.1. Introduction

The design and implementation of relaying software for an adaptive protection system have been presented in the previous chapter. Another software package is needed for changing the settings of relays in the on-line mode and ensure that proper coordination among all relays is maintained during all operating conditions.

This chapter describes the development of a software for determining in an on-line mode relay settings and for checking their coordination. The software which consists of four software modules resides in a central control computer, remote from the relays. The functions performed by these modules are to detect the network topology, estimate the state of the power system, calculate fault current levels, and determine properly coordinated relay settings. The topology detection algorithm, discussed in this chapter, was developed considering the on-line status of breakers and isolators. For state estimation, the fast-decoupled load flow technique was used. The mathematical development of this technique is briefly outlined. The fault analysis algorithm was developed using the Thevenin's theorem. The algorithm and its mathematical development are described. The relay setting and coordination algorithm which was designed using an optimization technique is also presented.

In case the central control computer is unable to send the new settings to the relays when an operating state had changed, relays would change their settings locally. A method for relays to do this and avoid unnecessary trippings was developed. This chapter discusses the scenarios if the central computer is unable to send the information due to failure of communication service.

6.2. Network Topology Detection

The topology of the system must be detected for load flow studies and for fault analysis. Several topology detection techniques [40, 41] have been reported in the past. Sasson et al. [40] presented a scheme for on-line topology monitoring for transmission lines. They used the concept of flow measurement status that has similarities with that of breaker status. The measurement status was analysed to detect whether the opening of a breaker stops the line flow because in some arrangements a single breaker cannot be associated with a single line. Couch and Morrison [41] suggested a technique that uses the concepts of feeder connection vector and status vector. The feeder connection vector provides a description of the substation's internal configuration. This information from each substation is then processed at a higher level computer to generate overall network configuration information and to provide each substation with a concise description of the system external to the substation. The feeder status vector provides information concerning whether each feeder is live or earthed.

In the network considered in this thesis, each line is controlled by dedicated circuit breakers. As such, the status of breakers and isolators adjoining them, is used for identifying the system topology. The following software segments were developed for this purpose.

I. Off-Line Data Table: In this segment of the topology detection software, a data table, Table 6.1, containing identification of each circuit, parameters of the line/transformer and identification of the circuit breaker and isolators controlling the line is prepared and stored in the computer in an off-line mode. The circuit is defined as line or transformer electrically connected to a circuit breaker. Each circuit breaker and isolator in the system is assigned an identification number.

II. On-Line Data Acquisition: Another table, Table 6.2, which contains information concerning the real-time status of circuit breakers and isolators is prepared and updated in an on-line mode. The status of a closed circuit breaker/isolator is designated by '1' and an open circuit breaker is designated by '0'. The status of the breakers/isolators are continuously monitored so that any changes can be included in the Table 6.2.

Table 6.1: Identification of circuits and switches.

Circuit No.	Breaker/Isolator No.	Line/Transformer Parameter
1	CB 1	$r_1 + jx_1$
2	CB 2	$r_2 + jx_2$
3	CB 3	$r_3 + jx_3$
.	.	.
.	.	.
.	.	.

Table 6.2: Status of circuit breakers and isolators.

Circuit No.	Breaker/Isolator No.	Line/Transformer Parameter
1	CB 1	1
2	CB 2	1
3	CB 3	0
.	.	.
.	.	.
.	.	.

III. Final Configuration Table: Table 6.3 is then prepared from Tables 6.1 and 6.2 by extracting the lines whose controlling circuit breakers and isolators are closed. This table contains a list of all lines in operation.

Table 6.3: Final configuration table.

Circuit No.	Breaker/Isolator No.	Line/Transformer Parameter
1	CB 1	$r_1 + jx_1$
2	CB 2	$r_2 + jx_2$
.	.	.
.	.	.

6.3. A State Estimation Technique

Pre-fault currents in various branches of the network are required for estimating the pickup currents of relays. Also, the pre-fault voltages at system buses are needed for fault analysis. The fast-decoupled load flow technique [42] is used for estimating the system state.

Decoupled load flow methods recognize that the voltage magnitudes do not affect substantially with MW flows in lines and voltage phase angles do not affect the Mvar flows. Except for this assumption, decoupled and Newton-Raphson algorithms use the same mathematical technique.

The active and reactive powers flowing into any bus p of an n bus system can be written as

$$P_p = |V_p| \sum_{q=1}^{n} |V_q|(G_{pq}cos\delta_{pq}+B_{pq}sin\delta_{pq}), \tag{6.1}$$

$$Q_p = |V_p| \sum_{q=1}^{n} |V_q|(G_{pq}sin\delta_{pq}-B_{pq}cos\delta_{pq}), \tag{6.2}$$

where:

$G_{pq}+jB_{pq}$	is the $(p,q)^{th}$ element of the bus admittance matrix,
δ_{pq}	is the phase angles of voltages at buses p and q,
V_p	is the voltage at bus p and
V_q	is the voltage at bus q.

A similar pair of non-linear equations can be obtained for each bus. Equations 6.1 and 6.2 indicate that P_p and Q_q are functions of the phase angles and magnitudes of the bus voltages. An iterative solution of the equations is initiated by estimating an initial solution vector $[\delta^0 \ |V^0|]^T$ and expanding each function in the neighbourhood of this estimate using the Taylor series as illustrated in Appendix D.

Now, the mismatches of active and reactive powers can be defined as

$$\Delta P_p = P_p(scheduled) - P_p(calculated), \tag{6.3}$$

$$\Delta Q_p = Q_p(scheduled) - Q_p(calculated). \tag{6.4}$$

Using the above definitions and taking first two terms of Taylor series, the following set of equations can be obtained:

$$\begin{bmatrix} \Delta P \\ -- \\ \Delta Q \end{bmatrix} = \begin{bmatrix} J_1 & | & J_2 \\ - & - & - \\ J_3 & | & J_4 \end{bmatrix} \begin{bmatrix} \Delta\delta \\ --- \\ \Delta V/|V| \end{bmatrix} \tag{6.5}$$

where:

J_1, J_2, J_3 and J_4	are the submatrices of the Jacobian matrix.
$\Delta\delta$	is the vector increments in phase angles and
ΔV	is the vector of increments in the voltage magnitudes.

The first step in decoupling is to neglect the submatrices J_2 and J_3 in Equation 6.5. The elements of the submatrices J_1 and J_4 are determined by taking the partial derivatives of Equations 6.1 and 6.2 with respect to δ and $|V|$, which are provided in Appendix D.

In practical power systems, the following assumptions may be made:

1. $\cos\delta_{pq} \approx 1$; $G_{pq}\sin\delta_{pq} << B_{pq}$ *and* $Q_p << B_{pp}|V_p|^2$.
2. Omit the representation of those network elements that predominantly affect Mvar flows, such as shunt reactances and off-nominal transformer taps.
3. Neglect the angle shifting effects of phase shifters.

Incorporating the above modifications, the simplified equations are

$$[\Delta P/|V|] = [B'][\Delta\delta], \tag{6.6}$$

$$[\Delta Q/|V|] = [B''][\Delta V]. \tag{6.7}$$

In the iterative process, Equations 6.6 and 6.7 were solved until $[\Delta P/|V|]$, $[\Delta V/|V|]$ were within the specified tolerances.

6.4. Fault Analysis

Fault currents for faults at critical locations are required for determining relay settings. Using the Thevenin's equivalent approach [43], a fault analysis program was developed. The solution steps are described in this section.

Figure 6.1 is a power network with n buses with fault at bus k. The first step is to

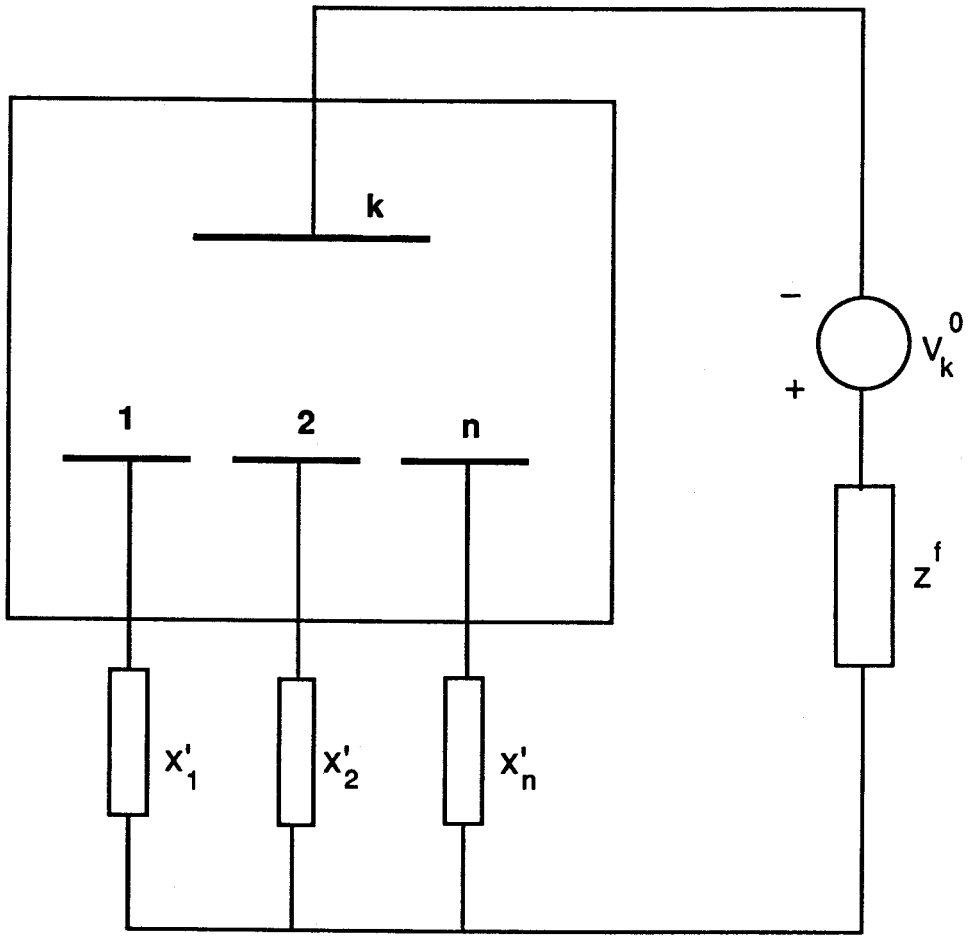

Figure 6.1: A network model of an n-bus system with fault at bus k.

obtain pre-fault voltages at all buses and currents in all lines by conducting load flow study. Thevenin's theorem is then applied to obtain the postfault bus voltages by superposition of the pre-fault bus voltages and the changes in the bus voltages caused by the equivalent emf connected to the faulted bus. This can be expressed in the following vector equation:

$$[v_b^f] = [v_b^0] + [\Delta v_b], \tag{6.8}$$

where:

$[v_b^f]$ is the bus voltage vector at postfault,
$[v_b^0]$ is the bus voltage vector at pre-fault and
$[\Delta v_b]$ is the change in bus voltage vector.

For a fault at k^{th} bus of an n bus system, the passive Thevenin network be excited with $-V_k^0$ in series with Z^f as shown in Figure 6.1. Therefore, changes in bus voltages for this network can be written as

$$[\Delta v_b] = [Z_{nk}]\,[j]^f, \tag{6.9}$$

where:

$[Z_{nk}]$ is the bus impedance matrix of the passive Thevenin network and
$[j]^f$ is bus current injection vector.

The network is injected with current $-I^f$ only at the k^{th} bus, hence Equation 6.8 can be re-written as

$$[v_b^f] = [v_b^0] - [Z_{nk}]\,I^f. \tag{6.10}$$

Now the postfault voltage at the fault bus satisfies the relation $V_k^f = Z^f I^f$, the fault current at the faulted bus can be expressed as

$$I^f = \frac{V_k^0}{Z^f + Z_{kk}}. \tag{6.11}$$

Since the fault current at faulted bus is known, bus voltages are determined using Equations 6.12 and 6.13 as follows:

$$V_i^f = V_i^0 - \frac{Z_{ik}}{Zf + Z_{kk}} V_k^0, \quad i=1,2,.....,n \quad i \neq k, \tag{6.12}$$

$$V_k^f = \frac{Zf}{Zf + Z_{kk}} V_k^0. \tag{6.13}$$

After obtaining the post fault bus voltages, post fault currents are calculated using the following equation:

$$I_{pq}^f = \frac{V_p^f - V_q^f}{Z_{pq}}, \tag{6.14}$$

where:

V_p^f and V_q^f	are the voltages at bus p and q respectively and
Z_{pq}	is the impedance of the line between buses p and q.

Equations 6.12, 6.13 and 6.14 were used to determine the bus voltages and fault currents at different branches.

6.5. Relay Settings and Coordination Technique

The key issue in selecting the relay settings is to achieve the minimum possible relay operating times while maintaining coordination among all relays. Usually, the coordination of relays involves several iterations before a satisfactory solution is achieved. Traditionally, a trial and error procedure is employed for setting relays in multiloop networks. In the past few years several mathematical techniques have been reported [44]. Knable [45] proposed a technique to break all the loops, at the so called break points, and locate the starting relays from where coordination starts. Since loop circuits are normally protected by directional relays located at both ends, the loops formed in both clockwise and anticlockwise directions are taken into consideration in the determination of break points. Dwarakanath and Nowitz [46] later dealt with this problem and suggested a systematic method in determining the relative sequence setting

of the relays in a multiloop network using simple linear graph theory results; enumerating in the form of a directional loop matrix. A minimal set of break points spanning all the loops of the system graph is obtained from this matrix. Reference [19] further extended the graph theoretic concepts and proposed systematic algorithms for determining a relative sequence matrix and a corresponding set of sequential pairs which minimizes the number of iterations. Jenkins et al. [47] proposed a functional dependency concept to the topological analysis of the protection scheme. All the constraints on the relay settings are expressed through a set of functional dependencies. Relay coordination is systematically carried out through the identification of a break point set (BPS) and a relative sequence matrix. The choice of the initial settings of the BPS relays is used to select the settings of the remaining relays of the protection scheme.

Both the graph theoretic approach and functional dependency approach provide a solution which is the best of the alternative settings considered, but does not provide an optimal solution. A parametric optimization approach is reported recently by Urdanneta et al. [48]. They optimize the time multiplier settings (TMS) using Simplex method. Optimal values of pickup currents for selected TMS are then determined using generalized reduced gradient technique.

6.6. Proposed Relay Settings and Coordination Algorithm

The proposed relay coordination algorithm was developed using an optimization technique. The pickup currents were determined by the system requirements. As a result, Equation 5.1 that models the relay characteristics became linear. The linear programming approach [49, 50] was then used to determine feasible settings which were optimal with respect to a linear objective function. The method can determine a plan which maximizes or minimizes linear functions over feasible plans that satisfy specified restrictions in the form of a system of linear inequalities. In this case, operating times of primary relays for near-end faults were minimized while the operation of backup relays formed the constraints. The optimum values of time multiplier settings were obtained. The Simplex method which is a computational procedure for solving linear programming problems was used.

6.6.1. The Algorithm

The relay coordination algorithm is developed based on the two-phase Simplex method. The theory of Simplex method has been described in Appendix E. In two-phase Simplex method, Phase I finds a feasible solution and Phase II finds the optimal values. In Phase I, it is moved from the origin to an initial extreme point of the feasible region. If it cannot find an initial extreme point, it is because the feasible region is empty. In Phase II, pivoting is done from the initial extreme point to an optimal extreme point. If it cannot find an optimal extreme point, it is because the problem has an unbounded optimal solution.

The linear programming model can be written in general form as follows:

Objective: Minimize

$$z = \sum_{j=1}^{n} c_j x_j. \tag{6.15}$$

Subject to

$$\sum_{j=1}^{n} a_{ij} x_j \geq b_i \ (i=1, 2,...m), \qquad x_j \geq 0, \tag{6.16}$$

where:

c_j	are the coefficients of the objective function,
x_j	are the decision variables,
a_{ij}	are the constraint coefficients and
b_i	are the values of the constraints.

To begin with, the inequalities of the constraints are replaced by equalities upon introducing the suitable non-negative variables. In the above form of inequalities, illustrated in Equation 6.16, non-negative *surplus variables*, $x_{s1}, x_{s2},.....,x_{sm}$ were introduced.

The algorithm then finds whether a feasible solution to the original problem exists.

This is accomplished by introducing a second set of variables called 'artificial variables' in Equation 6.16. Let $x_{t1}, x_{t2}, \ldots\ldots\ldots, x_{tm}$ be the non-negative artificial variables then Equation 6.16 can be written in canonical form as follows:

$$a_{11}x_1 + a_{12}x_2 + \ldots\ldots\ldots + a_{1n}x_n - x_{s1} + x_{t1} = b_1$$

$$a_{21}x_1 + a_{22}x_2 + \ldots\ldots\ldots + a_{2n}x_n - x_{s2} + x_{t2} = b_2$$

$$\ldots\ldots\ldots\ldots\ldots\ldots\ldots\ldots\ldots\ldots\ldots\ldots\ldots\ldots$$

$$a_{m1}x_1 + a_{m2}x_2 + \ldots\ldots\ldots + a_{mn}x_n - x_{sm} + x_{tm} = b_m$$

The feasible solution to the original problem is obtained when all the above artificial variables are zero. Since artificial variables are all non-negative, they are all zero only when their sum is zero.

The attempt is made to eliminated the artificial variables by minimizing w, such that $w = x_{t1} + x_{t2} + \ldots\ldots\ldots + x_{tm}$. During the process of minimization of w, the original objective function z is also updated. The process by which w is minimized is called Phase I and it is performed in table format; generally known as tableau. The initial tableaus of Phase I are shown in Tables 6.3 and 6.4 where artificial variables are in the basis.

The following procedure is followed to minimize the w function.

Step 1 If $\overline{w}_j \leq 0$ for $j = 1,2,\ldots,n+2m$ then stop; feasible solution is obtained. Here $\overline{w}_j$ is the current coefficient of column j in the w row. If it is not, then continue because there exists some $\overline{w}_j > 0$.

Step 2 Select the column to pivot in, i.e. the variable to introduce into the basis as

$$\overline{c}_l = \max_j \{\overline{w}_j\}$$

Such that $\overline{w}_j > 0$.

Table 6.4: Tableau for initial arrangement of the problem.

Basis	Current Values	x_1	x_2	.....	x_n	x_{s1}	x_{s2}	.....	x_{sm}	x_{t1}	x_{t2}	.....	x_{tm}
x_{t1}	b_1	a_{11}	a_{12}	....	a_{1n}	-1				1			
x_{t2}	b_2	a_{21}	a_{22}	.....	a_{2n}		-1				1		
.	.												
.	.												
.	.												
.	.												
x_{tm}	b_m	a_{m1}	a_{m2}	....	a_{mn}				-1				1
z	0	$-c_1$	$-c_2$	....	$-c_n$								
w	0	0	0	....	0					-1	-1	....	-1

Table 6.5: Starting tableau of Phase I Simplex method.

Basis	Current Values	x_1	x_2	.....	x_n	x_{s1}	x_{s2}	.....	x_{sm}	x_{t1}	x_{t2}	.....	x_{tm}
x_{t1}	b_1	a_{11}	a_{12}	....	a_{1n}	-1				1			
x_{t2}	b_2	a_{21}	a_{22}	.....	a_{2n}		-1				1		
.	.												
.	.												
.	.												
.	.												
x_{tm}	b_m	a_{m1}	a_{m2}	....	a_{mn}				-1				1
z	0	$-c_1$	$-c_2$	....	$-c_n$								
w	Σb_m	Σa_{m1}	Σa_{m2}	....	Σa_{mn}	-1	-1	....	-1	0	0	....	0

Note: In w row, 0 appears in the last three columns; w row of the previous table is also part of the summation.

Step 3 Choose the row r to pivot in (i.e. the variable to drop from the basis) by the ratio test:

$$\frac{\bar{b}_r}{\bar{a}_{rl}} = \min_i \{\frac{\bar{b}_i}{\bar{a}_{il}}\}, \quad \bar{a}_{il} > 0.$$

Where $\bar{b}_i$ and $\bar{a}_{il}$ are the current values of row i and current coefficient of column l in row i respectively.

Step 4 Replace the basic variables in row r with variables l as follows:

$$\bar{b}_r^{new} = \frac{\bar{b}_r}{\bar{a}_{rl}},$$

$$\bar{b}_i^{new} = \bar{b}_i - \frac{\bar{b}_r}{\bar{a}_{rl}} \geq 0, \quad i \neq r.$$

Step 5 Go to Step 1.

At the end of Phase I if current value of w reduces to zero, current values of all artificial variables become zero. A feasible solution to the original problem is thus obtained. At this stage all artificial variables become non-basic as shown in Table 6.6. If w cannot reduces to zero, no feasible solution exists to the original problem. One or more artificial variables at this stage will still be in the basis with positive values. This is further discussed in Appendix E. In such case, at the end of Phase I, infeasible constraints corresponding to these positive artificial variables are withdrawn from the original problem. Phase I is again conducted to obtain the feasible solution. Phase II of the Simplex method then starts and the objective function z of the original problem is minimized by dropping the artificial variables. The procedure of minimizing the object function z is similar to minimizing the w function which has also been discussed in Appendix E.

Table 6.6: Final tableau of Phase I Simplex method.

Basis	Current Values	x_1	x_2	.....	x_n	x_{s1}	x_{s2}	.....	x_{sm}	x_{t1}	x_{t2}	.....	x_{tm}
x_g	b_g	a_{g1}	a_{g2}	.....	a_{gn}	a_{gs1}	a_{gs2}	.....	a_{gsm}	a_{gt1}	a_{gt2}	.....	a_{gtm}
x_h	b_h	a_{h1}	a_{h2}	.....	a_{hn}	a_{hs1}	a_{hs2}	.....	a_{hsm}	a_{ht1}	a_{ht2}	.....	a_{htm}
.	.												
.	.												
.	.												
.	.												
x_k	b_k	a_{k1}	a_{k2}	.....	a_{km}	a_{ks1}	a_{ks2}	.....	a_{ksm}	a_{kt1}	a_{rk}	.....	a_{ktm}
z	b'	c'_1	c'_2	.....	c'_n	c'_{s1}	c'_{s2}	.....	c'_{sm}	c'_{t1}	c'_{t2}	.....	c'_{tm}
w	0	w_1	w_2	.....	w_n	w_{s1}	w_{s2}	.....	w_{sm}	w_{t1}	w_{t2}	.....	w_{tm}

Note: $w_1, w_2, \ldots\ldots, w_{s1}, w_{s2}, \ldots\ldots\ldots w_{t1}, w_{t2}, \ldots\ldots\ldots$ in w row are either 0 or less than 0.

In connection with relay coordination, the operating times for the near-end faults of primary protection were minimized, and the operating times of the back-up relays formed the inequality constrains. The objective function in this case is as follows:

Minimize:

$$z = t_{1-1,1-1} + t_{1-4,1-4} + t_{1-6,1-6} + t_{2-1,2-1} + t_{2-2,2-2} + t_{3-1,3-1} + t_{3-4,3-4} + t_{4-1,4-1} + t_{4-4,4-4} + t_{5-1,5-1} + t_{5-2,5-2}. \quad (6.17)$$

In the above equation, $t_{1-1,1-1}$ is the operating time of relay 1-1 for a fault at location FL 1-1; a near-end fault. The relay 1-1 is equipped with the circuit breaker CB 1-1. Similarly, operating times of other relays for the near-end faults, such as $t_{1-4,1-4}$ etc., were also the parts of the objective function as illustrated in Equation 6.17.

The constraints were formulated based on the operating times of the back-up relays as follows.

$$t_{2-1,1} \geq t_{1-1,1-1} + 0.2,$$

$$t_{3-4,1} \geq t_{2-1,1} + 0.2,$$

$$t_{4-4,1} \geq t_{3-4,1} + 0.2,$$

$$t_{5-2,1} \geq t_{4-4,1} + 0.2,$$

. .
. .
. .
. .
. .

$$t_{1-1,1-1} \geq 0.05,$$

. .
. .
. .
. .

where:

$t_{2-1,1}$ is the operating time of back-up relay 2-1 for a fault at a location FL 1-1,

0.2 sec is the relay coordination time interval and
0.05 sec is the minimum operating time of overcurrent relay.

Similarly $t_{3-4,1}$ etc., are the operating times of the back-up relays 3-4 and so on for a fault location FL 1-1. All such operating times of the back-up relays for other fault locations as marked in Figure 4.3 were considered in formulating the constraints.

6.7. Adaptive System Failure

In adaptive protection, relay settings are monitored at regular time intervals. The relay settings are changed when the operating conditions of the power network changes. This section first describes the scenarios if relays fail to update their settings due to failure of the communication system. A technique is then presented to describe how relays can update their settings locally maintaining slim coordination margins.

6.7.1. Scenario-I: Relays fail to update during increased load.

In adaptive protection, pickup current settings are changed as load current changes. Therefore, if load currents increase, the relay pickup settings must be increased to avoid unnecessary trippings. However, only by increasing the pickup current settings, desired relay coordination may not be achieved. As the relay pickup increases, multiple of pickup current (I_{mpu}) during fault reduces. As a result, if the time multiplier setting (*TMS*) is kept unchanged, the relay operating time will increase. Hence, if a relay that has failed to update its setting might not trip before the back-up relay trips. Therefore, *TMS* values must also be changed along with the change of the pickup value to obtain the desired relay operating time to maintain coordination.

6.7.2. Scenario-II: Relays fail to update when load has reduced

Similarly when load reduces, the pickup value should be reduced to maintain sensitivity of the relays. But again, relay coordination cannot be achieved by only reducing the pickup setting. The reduced pickup setting increases the multiple of pickup current during fault. Therefore, if the relay that has failed to update its setting could operate as a back-up relay before the operation of primary relays. Therefore, in addition to changes of the relay pickup setting, TMS must also be changed.

6.7.3. Proposed Method for Local Relay Settings

From the preceding discussion, it is apparent that relays should have some facilities to change their settings locally if the communication system fails to function. A proposed technique for changing the relay settings locally is discussed in this section.

Each relay continuously monitors the operating conditions of the element it is protecting. Therefore, the information regarding the local load flows is available to the relays. So, relays can locally change their pickup settings according to the change of the load currents. The method used for changing the *TMS* value within the relaying processor is described in this section.

Recall Equation 5.1; the relay operating time is defined as

$$t = \frac{k \times TMS}{(I_{mpu})^n - 1}. \tag{6.18}$$

The relay settings are optimized (minimized) for the near-end faults when I_{mpu} are high. Hence, Equation 6.18 can be approximated to

$$t \approx \frac{k \times TMS}{(I_{mpu})^n}. \tag{6.19}$$

Replacing I_{mpu} by fault and pickup current, the following equation is obtained:

$$t \approx \frac{k \times TMS \times (I_{pickup})^n}{(I_F)^n}. \tag{6.20}$$

For two different operating conditions of the network, the above equation can be written as

$$\frac{t_1}{t_2} \approx \frac{TMS_1}{TMS_2} \times \frac{(I_{pickup1})^n}{(I_{pickup2})^n} \times \frac{(I_{F2})^n}{(I_{F1})^n}. \tag{6.21}$$

A further approximation can be made by assuming that fault current level remains unchanged. This assumption is reasonable because changes in generation levels are likely to be small. By ignoring the effect of generation level changes, Equation 6.21 can, therefore, be approximated as

$$\frac{t_1}{t_2} \approx \frac{TMS_1}{TMS_2} \times \frac{(I_{pickup1})^n}{(I_{pickup2})^n}. \tag{6.22}$$

For two different power system operating conditions, relay operating times for near-end faults should be fairly constant which is generally very small. So, the ratio t_1/t_2 should approximately 1. Also, n is chosen as 1 for the work of this thesis. Hence, from Equation 6.22,

$$TMS_1 \times I_{pickup1} \approx TMS_2 \times I_{pickup2}. \tag{6.23}$$

Thus, the revised TMS value can be computed from Equation 6.23 by the relaying processor. Later, in the chapter on system studies, it is reported how the TMS values differ if they are estimated locally from those estimated by the central computer when adaptive approach is in service.

6.8. Summary

This chapter discusses the development of a software for on-line relay coordination and setting. The software consists of four modules; mathematical development of each module is described. The topology detection module is developed based on the status of the circuit breakers and isolators. For state estimation, the fast decoupled load flow technique was used. The mathematical bases for this technique is discussed. The fault analysis module has been developed using the Thevenin's approach. The procedure for developing the algorithm is described. Finally the relay coordination and setting algorithm is described. This technique has been developed based on the optimization technique. The development of the algorithm using the two-phase Simplex method is then described. A technique is also proposed for changing relay settings locally in case central computing system cannot provide the settings due to failure of the communication system.

7. DESIGN AND IMPLEMENTATION OF AN ADAPTIVE PROTECTION SYSTEM

7.1. Introduction

Two major software packages that are developed for implementing an adaptive distribution protection system have been described in the previous two chapters. The first package is the relaying software and the second package is the relay coordination software.

This chapter describes the development of a prototype system for an adaptive distribution protection using the software packages developed in Chapter 5 and 6, and using two communication packages. The chapter first describes the prototype system that was designed in the Power System Research Laboratory at the University of Saskatchewan. The hardware used to build the system are then outlined. This is followed by a description of the development of the two communication softwares. Finally, the implementation of the coordination software is outlined and testing of the programs is presented.

7.2. The Designed Prototype

The block diagram of the designed control and relaying scheme of the prototype system is shown in Figure 7.1. The implemented scheme includes Taylor substation (substation 2) of the the selected distribution network. This substation has five relays which were implemented on five TMS320C25 DSP boards. Each board is placed in a dedicated MS-DOS personal computer (pc). These pcs are also interfaced with the Network Interface Cards [51] for communicating with a substation controller. One pc was used for the substation controller which also functions as a 'File Server' for the local area network (LAN). This pc is also interfaced with a Network Interface Card and

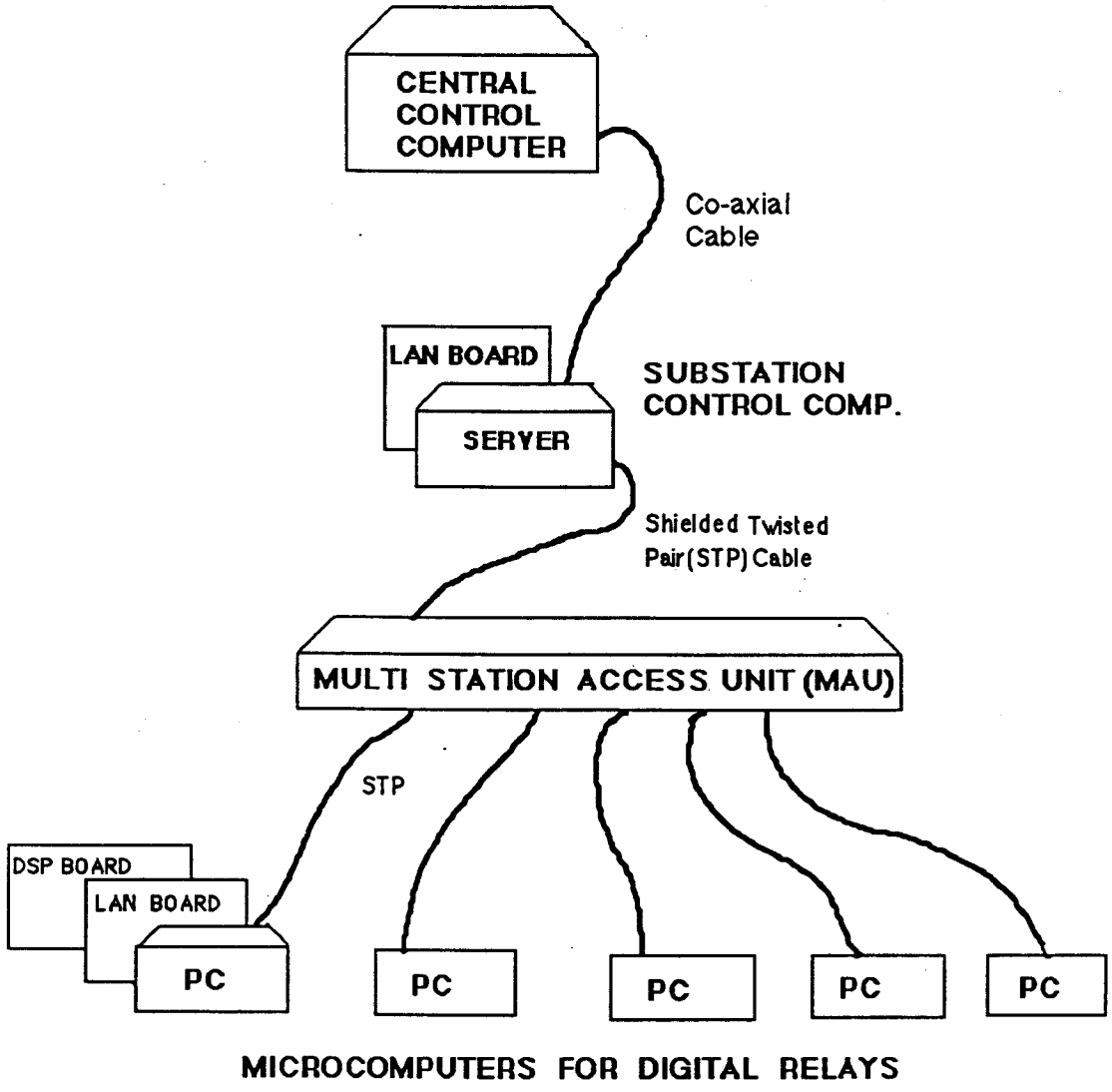

Figure 7.1: A prototype for the adaptive protection scheme.

connected to the five relaying pc's via a 'Multi-station Access Unit (MAU)' [52]. Another pc was used for the central control computer where the coordination software resides. This pc is equipped with a serial communication adapter, 'Digiboard' [53] that has eight RS 232 channels. In this project, one channel was used to connect the pc of the central computer to the pc of substation 2 control computer. The asynchronous communication using RS-232 standard was employed for communicating between the station control computer and with the central control computer.

7.3. Hardware

The performance of a microprocessor based system is largely dependent upon the selection of the hardware. The hardware were selected keeping in mind that they can be used in a power system environment. During selection, modular-design of hardware was also emphasised so that any module can be replaced if necessary. The details of hardware are discussed in the following sections.

7.3.1. MS-DOS Personal Computer

Altogether, seven pcs were used, five for relaying purpose, one for substation controller and one for central control computer. Among the five pcs, two are Commodore PC 40-III series and the main board of the other three pcs are manufactured by American Megatrends Inc. The commodore pcs are 286 machines and the remaining three pcs are 386 SX machines. The expansion ports of these pcs are interfaced with the digital signal processor (DSP) boards and these pcs act as host computers. The host computer controls the operation of the DSP board and provides access to its program development system.

The pc for the station control computer is a 386DX machine and its main board is manufactured by American Megatrends Inc. The pc, used as a central computer, is a Commodore PC 40-III series 286 machine.

7.3.2. DSP Board

The DSP board has a TMS320C25, 40MHz microprocessor. The memory section of the board consists of 64K words of zero wait-state program/data RAM. The board has a double buffered bidirectional serial I/O. This is typically used to communicate with serial devices, such as serial A/D converters and DACs and other serial systems. The maximum speed of the serial port is 5 MHz. The board also has a 16 bit host I/O port and a 16 bit memory mapped programmable timer. The timer register is a down counter continuously clocked by the main CPU clock. A timer interrupt is generated whenever the timer decrements to zero. The timer is then reloaded with the value contained in the period register and the process continues. The timer is generally used for controlling the rate of sampling data and for measuring the computation time. When the timer is not being used, the period register can also be used as a general storage register.

7.3.3. Local Area Network

A typical substation will have several relays, equipped with the breakers. In adaptive protection, information is required to be exchanged between the relays and with the station control computer for which a communication link is needed. Two options were initially evaluated, asynchronous serial communication using RS 232 standard and using a local area network. While asynchronous serial communication is simple when connected with one or two devices, its control logic becomes complex if several computers are required to be communicated. Also, the communication scheme becomes expensive because of additional requirement of the serial communication adapters to support several RS 232 ports. Moreover, the communication system within the substation must support the integrated control and protection operations for which a larger volume and faster data rate are important. Considering all these requirements, a local area network was considered as a communication link within the substation [54, 55].

During selecting the LAN, options for Ethernet (IEEE 802.3) and Token Passing (IEEE 802.4 & 802.5) were evaluated. In consideration with on-line application for adaptive protection, Token Ring (IEEE 802.5) configuration was finally preferred [56].

7.3.4. Network Interface Board

Network interface board, conforming to IEEE 802.5, consists of a Texas Instruments TMS380C16 Token Ring COMMprocessor, a bus master DMA (Direct Memory access) and 128K DRAM on-board buffer memory. The processor has pipe-lined architecture which process multiple frames of data simultaneously. A data frame can be transferred from memory, while another frame is being built into a packet, while yet another is being transmitted on the network. A bus master interface takes control of the pcs I/O bus and transfers data independently of the central processing unit. The bus master DMA is faster than host DMA used in many other LAN boards. In host DMA techniques, data are moved in two steps; firstly from I/O adapter to the host DMA controller and secondly from the DMA controller to main memory. Using a bus master DMA, data are moved in one step, directly from adapter to main memory. Bus mastering is twice as efficient as standard DMA without the potential problems of shared memory [57].

7.3.4.1. Multi-station Access Unit

Although the physical configuration of Token Ring looks like a star topology, it is actually connected in a ring. The multi-station access unit (MAU), shown in Figure 7.2, is a central hub which connects pcs in a ring network. The MAU is also called concentrators or wiring centres. Transmissions are routed through the MAU to the network devices. If a cable breaks or a network card malfunctions, MAU helps to isolate the device.

In this project, Proteon's Series 70 Intelligent Wire Center was used as an MAU. The wire center is intelligent and active (dc power required). It allows eight pcs to be connected in the network. Several such MAUs can be connected to form a main trunk ring. It supports up to 16 Mbps token ring networks over unshielded twisted pair, shielded twisted pair (STP), and fiber optics. In this project, STP cable was used for connecting the station control computer to the relaying pcs via an MAU.

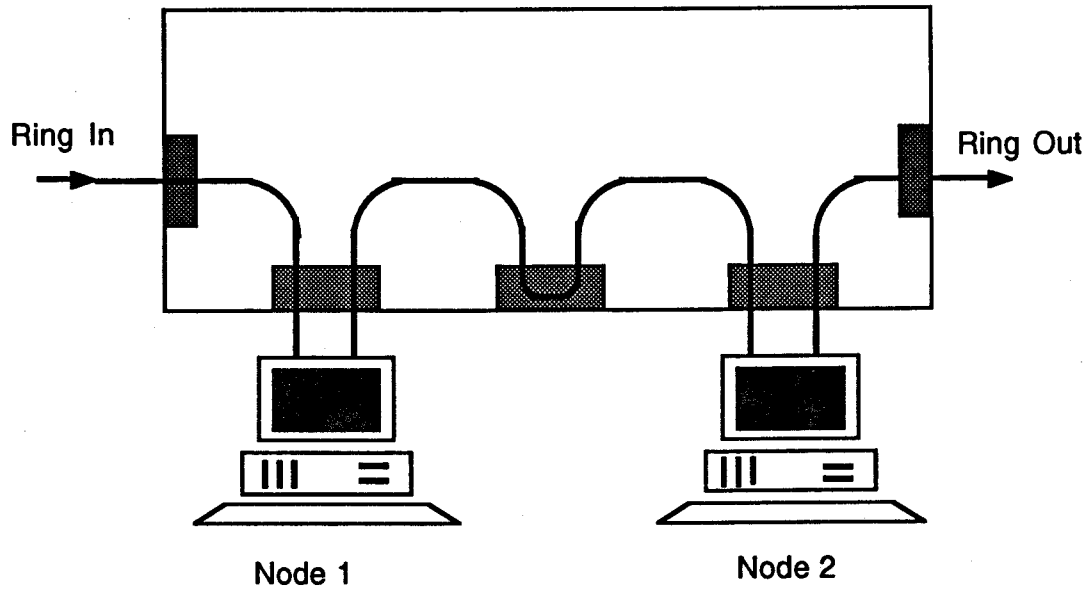

Figure 7.2: Multi-station access unit.

7.3.5. Digiboard

It is an intelligent 16 bit high-speed multichannel serial communication adapter. The board's 8 MHz 80186 microprocessor and associated on-board real-time operating system allow the intelligent Digiboard to act as a front-end processor. This relieves the host computer of much of the processing burden associated with multichannel communications. The digiboard also has a 64 k of dual-ported RAM for data buffering. The dual ported RAM allows to access both the Digiboard and the host computer's processor. The RAM provides communication and control between the host computer and the Digiboard. Hence, it improves the total system speed by allowing the same data buffer to be written to by one processor and read by the other without the need for additional memory transfer. Each Digiboard supports up to eight serial channels, all the channels support full handshaking (CTS, RTS, DSR, DTR) and full modem control (RI, DCD).

7.3.6. RS 232 Link

In adaptive application, several substation controllers will communicate with a remote central control computer. Two possibilities were evaluated for this communication; either using wide/metropolitan area network or by asynchronous serial communication using telephone lines. Considering the volume of data flow between the remote central control computer and station control computer, and economic viability a RS 232 link using modem was preferred.

7.3.6.1. Null Modem Cable

The null modem cable is generally used for connecting two devices within a short distance. In this project, a null modem cable was used to connect the central computer with one of the channels of the Digiboard. The pin connections of this cable is shown in Figure 7.3. A DB-25 connector was used at one end of the cable to connect the substation computer and a RJ-45 connector was used at the other end for connecting with the Digiboard. The Digiboard is connected with the central computer.

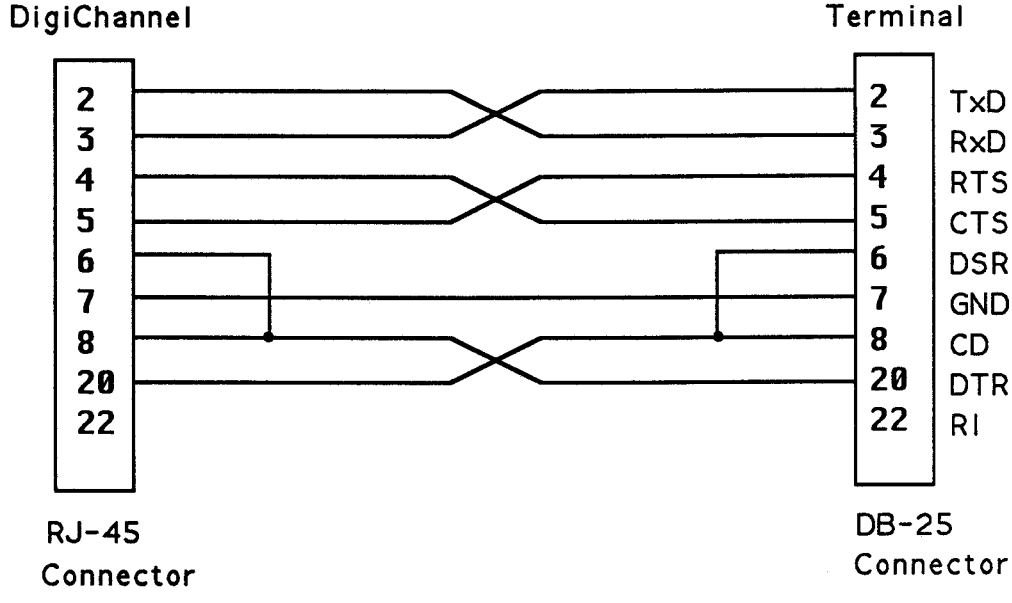

Figure 7.3: Pin connections in a null modem cable.

7.4. Software

The softwares for adaptive protection system were developed in modular structure so that it would be easier for modification and debugging the programs. A man-machine interface has been included in each module to change the program if necessary and for testing the software. This section first describes the development of the two application softwares for communication purpose. Implementation and testing of different software modules are then discussed.

7.4.1. Communication Application Software

Two application softwares were needed for information exchange, one for the relaying pc to communicate with the station computer and vice versa, and another for the central control computer to communicate with the station computer and vice versa. The development of these application software are discussed in this section.

7.4.1.1. Software for Communication Between the Relaying pc and the Station Computer

The application software was developed using a commercially available (Btrieve) Record Management Software [58]. The developed software has two segments, one segment resides in the station computer whereas the other segment resides in each relaying pc. The software that resides in the substation control computer manages the records in a table format. The table contains all the information concerning the relays, such as the relay designation, relay pickup, *TMS* values, bus voltage, line currents and status of the controlling breakers and isolators. The other segment of the software that resides in the relaying pc also manages records in a table format but only information pertinent to its relay is stored. The software was written in C and was compiled using Turbo C compiler.

During development of this software, Btrieve's 'UPDATE' routine was used for updating the data. The steps that were followed in developing the program are illustrated below.

1. Operation code for UPDATE is 3, which was first set.

2. Pass the position block for the file containing the record.
3. Store the updated record in the data buffer.
4. Set the data buffer length to the length of the updated record.
5. Set the key number used for retrieving the record in the key number parameter.

The details of position block, data buffer and key are included in Appendix F.

7.4.1.2. Software for Communication Between the Station Control Computer and the Central Computer

The application software was developed based on file transfer protocol, available in Greenleaf's asynchronous communication software [59]. Greenleaf CommLib supports five different families of file transfer protocols which are listed below.

- XMODEM
- YMODEM
- ZMODEM
- Kermit
- ASCII

In this project ZMODEM file transfer protocol was used because of the following reasons.

1. It is faster than the other protocols.
2. In the absence of network delay it allows rapid error recovery.
3. File transfers begin immediately with no delay.
4. All transaction are protected by 16 or 32 bit CRC.
5. It uses entire file as a window to simplify buffer management.
6. It retains file attributes for transferred files.

The application software was written in C and was compiled using Microsoft C compiler. The steps that were followed during implementation are listed below.

1. The substation control computer was used as a master and it either transmits or receives file from the central control computer.

2. During transmission of the file to the central computer channel '0' of Digiboard was opened; channels are numbered from 0 to 7.
3. Greenleaf's level 2 file transfer routine 'ZModemSend' was used to transmit the file. This ZModem file transfer is performed using 16 bit CRC checksum error calculation method.
4. During receiving the file, ZModemReceive routine was used.

7.4.2. Relaying Software

The implementation of relaying software has been discussed along with its development in Chapter 5. This software was written in ANSI standard C and was cross compiled with TMS compiler. The interface program was written in Lattice-C programming language. The Lattice-C program runs on the host pc and provides a user-interface with the microcomputer board.

7.4.3. Coordination Software

The coordination software was written in FORTRAN and was compiled with Microsoft FORTRAN. This software was developed in four modules which are listed below.

1. Topology detection module.
2. State estimation module.
3. Fault analysis module.
4. Coordination module.

The structure of the software is shown in Figure 7.4. Each module executes sequentially, i.e. after executing one module the next module starts to execute. The implementation of each module is described in this section.

7.4.3.1. Topology detection module

Figure 7.5 shows a flow chart illustrating the implementation of the topology detection module. The module first accepts a set of data concerning the circuit numbers and their parameters.

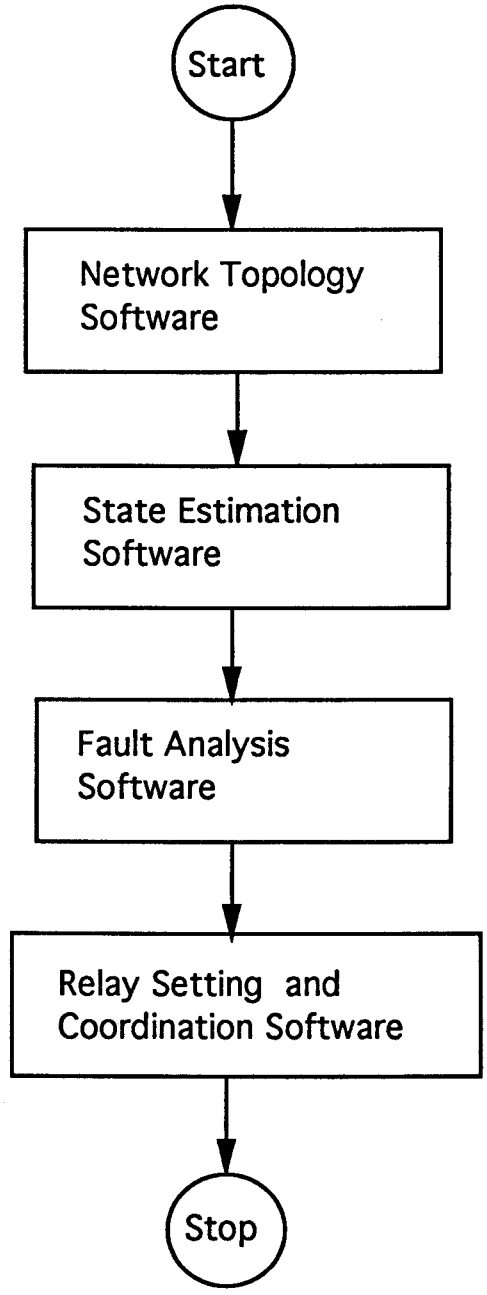

Figure 7.4: Structure of the coordination software.

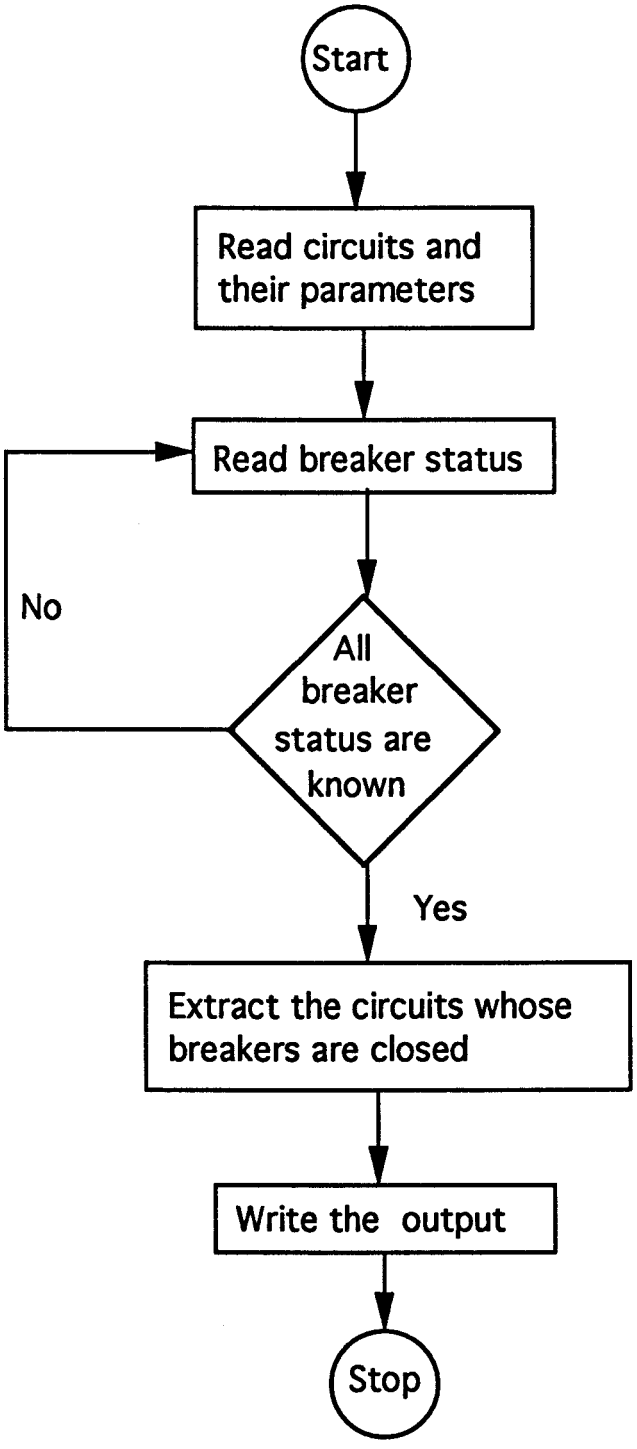

Figure 7.5: Implementation of the topology detection module.

It then accepts another set of data representing the status of breakers. These data were generated by simulating the breaker status; a number '1' was assigned for a closed breaker and a number '0' was assigned for an opened breaker. The module then starts checking each breaker status. On completing the checking of all breaker status, it generates a file that provides a list of the circuits in operation.

7.4.3.2. State estimation module

Figure 7.6 illustrates the implementation of state estimation module. The software first accepts the file generated by the topology detection software module. It then reads the data concerning real and reactive power at all load buses and generated power at generator buses. The slack bus is specified along with its voltage magnitude and phase angle. The other bus voltages are assumed.

The software then proceeds to estimate Y_{bus} matrix and calculates [B'] and [B''] matrices. The iteration counters at this point are initialized. It calculates the mismatch of real power and then compares with the specified tolerance limit. It also checks the mismatch of reactive power and compares with the specified tolerance. When both of them are within the tolerance limit, i.e. convergence is obtained, the program calculates the line flows and bus voltages. A tolerance limit of 0.0005 was considered for convergence. A maximum iteration count of 500 was specified and if the convergence is not achieved after that, the program terminates to check the software and the input files.

7.4.3.3. Fault analysis module

Figure 7.7 shows the implementation scheme of the fault analysis module. This module accepts the output file obtained from the state estimation module concerning pre-fault currents and voltages. It then accepts the source impedances at generator buses and load impedances at load buses. The Y_{bus} matrix is first formulated. This Y_{bus} matrix is, however, different than the Y_{bus} matrix formulated in state estimation module. The Z_{bus} matrix is then determined by inverting the Y_{bus} matrix. The software then estimates the post fault bus voltages and post-fault line currents using Equations 6.11 through 6.14 as described in Section 6.4.

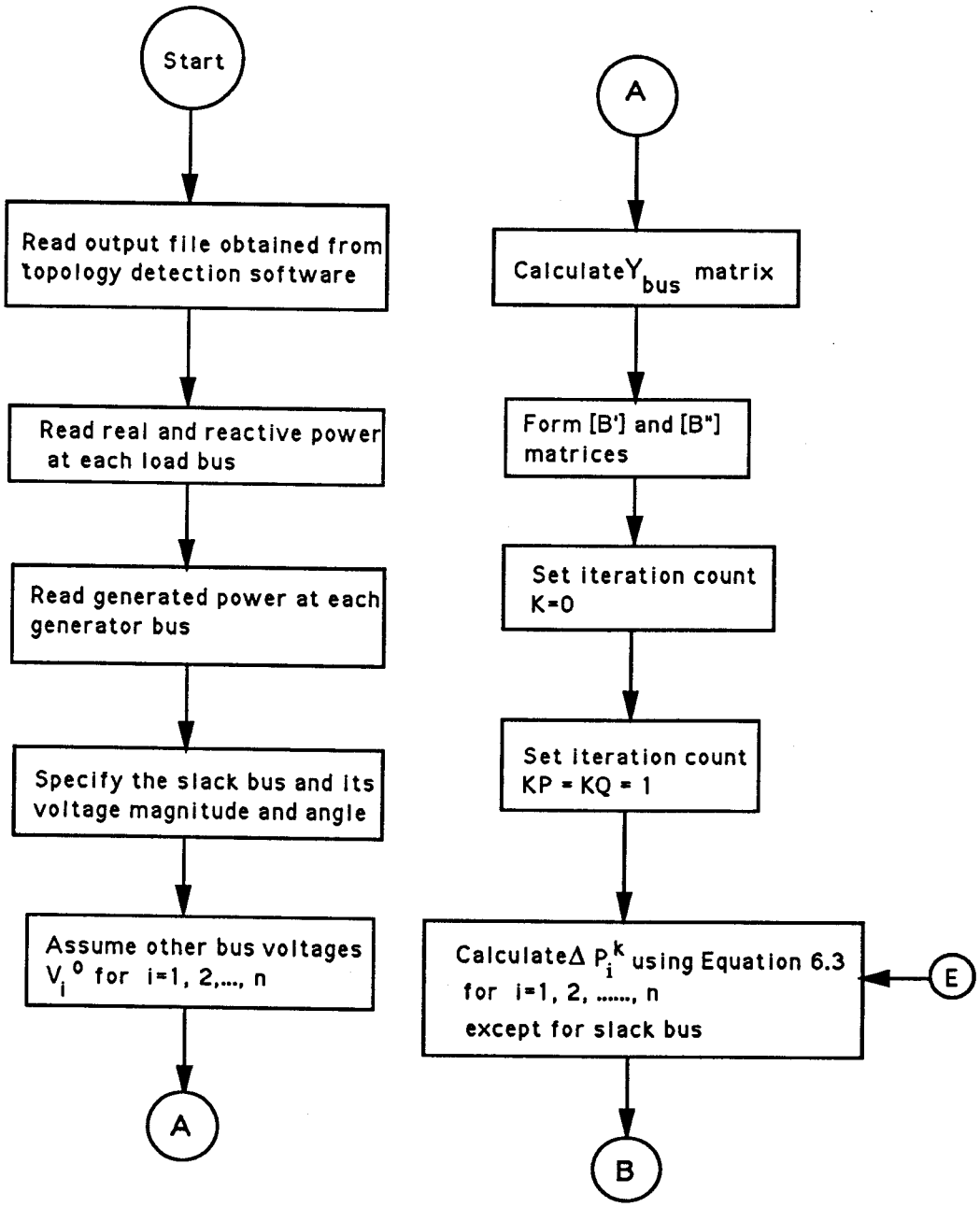

Figure 7.6: Implementation of the state estimation module.

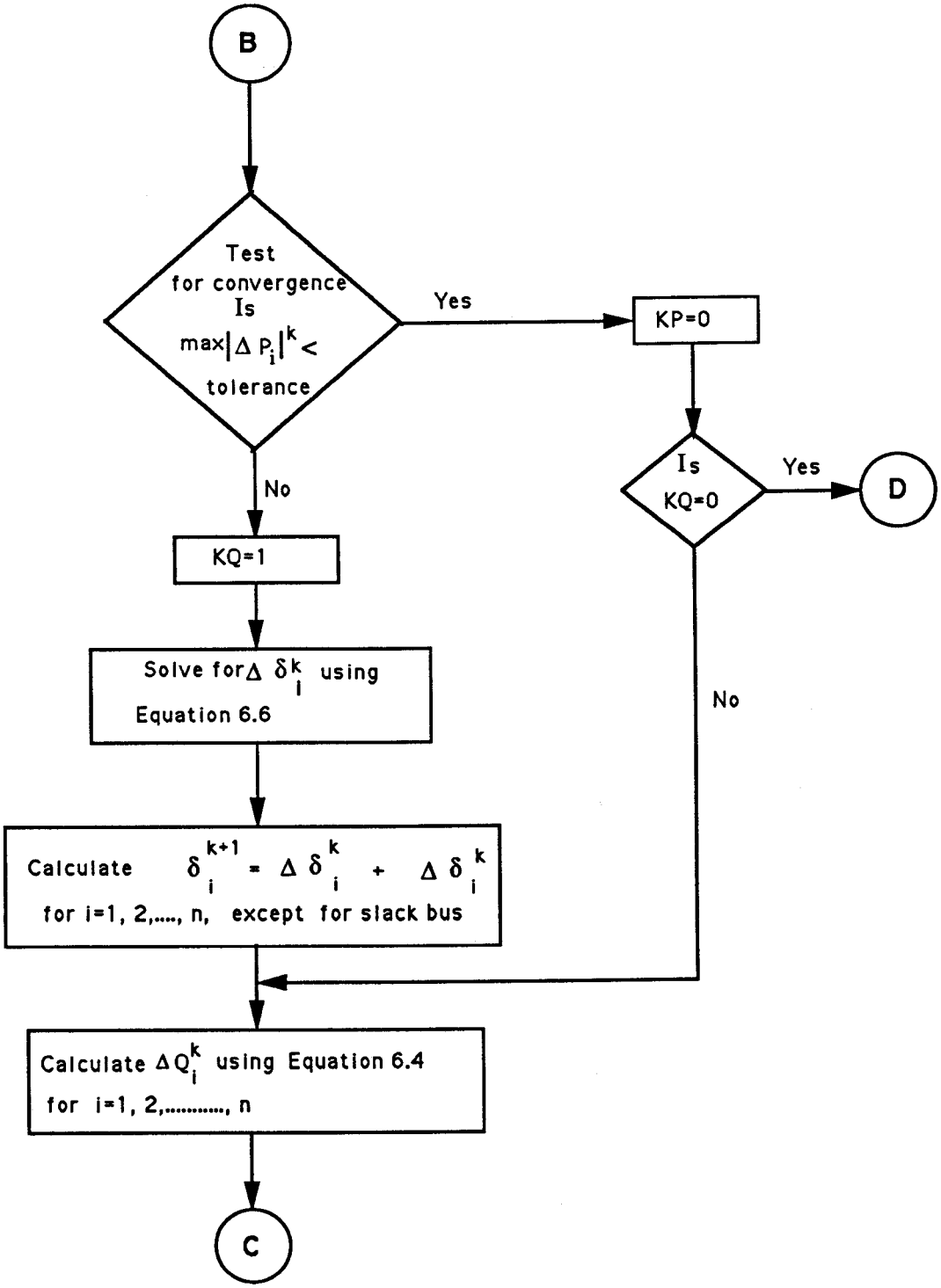

Figure 7.6 continued.

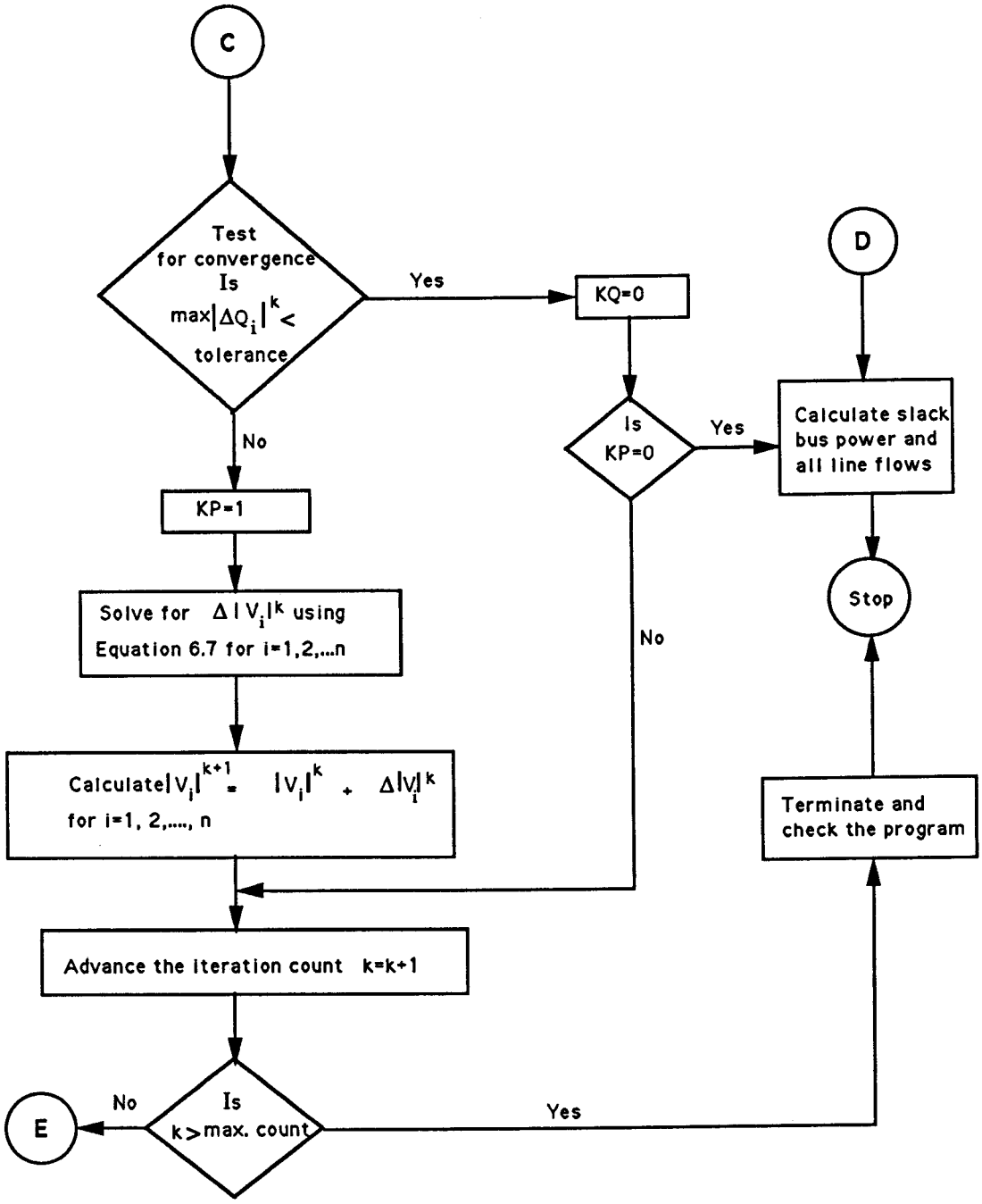

Figure 7.6 continued.

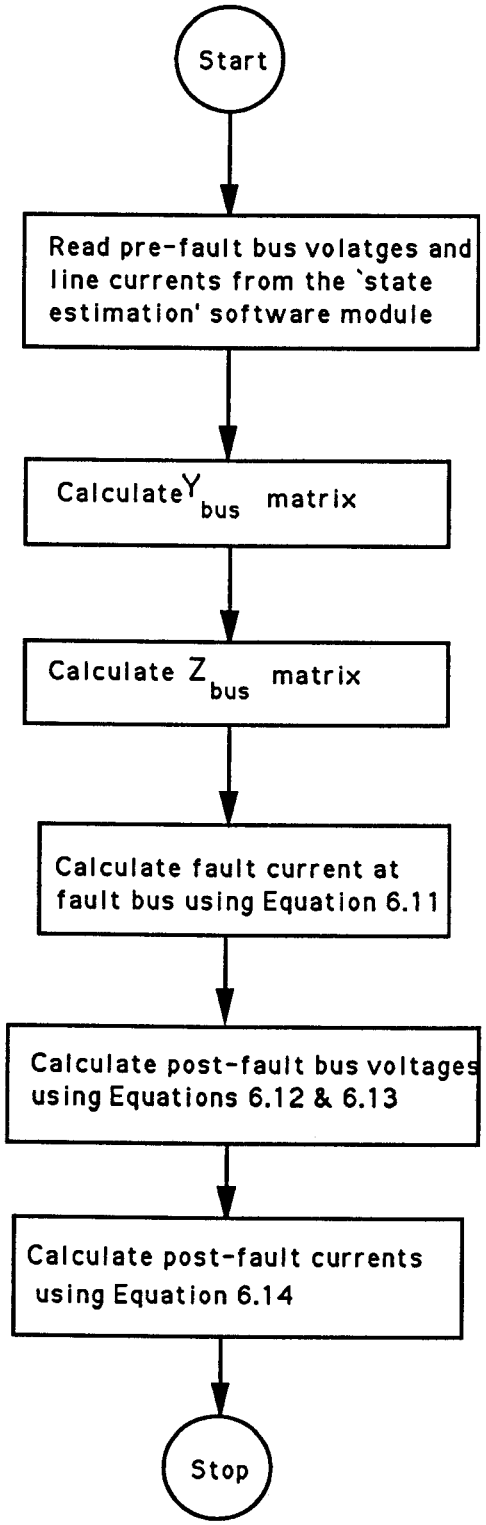

Figure 7.7: Implementation of the fault analysis module.

7.4.3.4. Relay Coordination Module

The relay coordination software consists of two segments. The first segment of the software calculates the secondary pickup settings of the overload, overcurrent and instantaneous relays. The pickup settings are estimated based on the system conditions and on the choice of users. From the fault currents, it estimates the operating times of overcurrent relays for near-end faults which form the objective function as described in Section 6.6.1. Upon calculating the coefficients of the objective function, it determines the constraints considering the coordination time between operating times of primary and back up relays. The segment calculates the *w* function and formulates the canonical form after incorporating the surplus and artificial variables in the constraints as described in Section 6.6.1. Figure 7.8 illustrates the implementation for this segment of the software.

The second segment of the software starts by optimizing the *w* function. After optimizing *w* function and upon completion of Phase I successfully, the Phase II starts to optimize the *z* function as discussed in the Section 6.6.1. The result of the second segment provides the optimized *TMS* values for all the relays. Figure 7.9 illustrates the flow diagram for this segment of the software.

7.5. Testing

All the developed software were tested in the laboratory for their intended performance. During testing, all the data were simulated and stored in files. Four extreme operating conditions of the distribution system were considered during the testing. However, test results for only one condition, i.e. maximum load and generating condition with line 1-20 open has been reported in this section. The test results for other conditions are illustrated in Appendix G.

7.5.1. Relaying Software

The testing of this software has been discussed along with its development and implementation in Chapter 5. It was demonstrated in that chapter that the relays emulate the current time characteristic as desired and the test results are within 1% of the actual values.

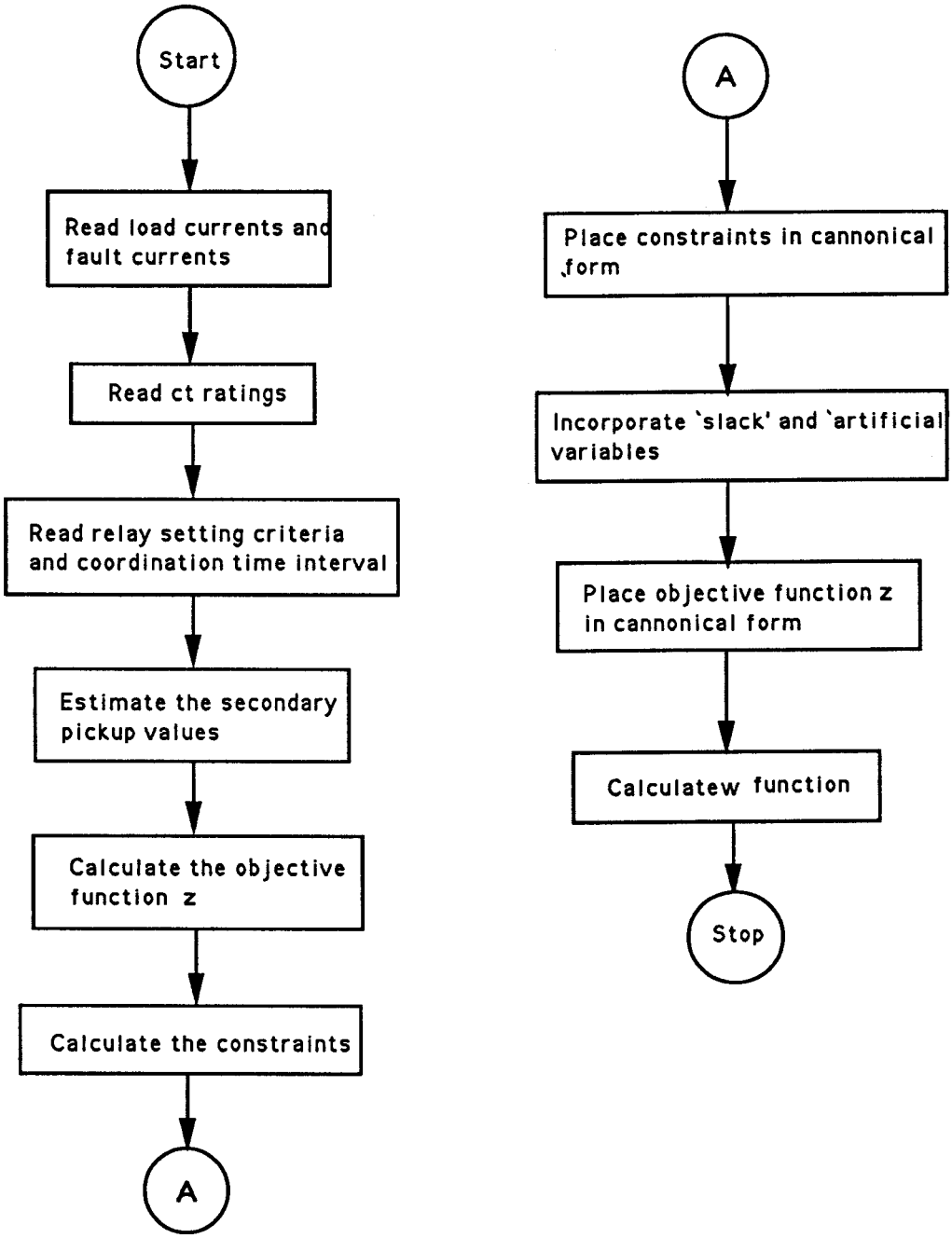

Figure 7.8: Implementation of the first segment of the relay coordination module.

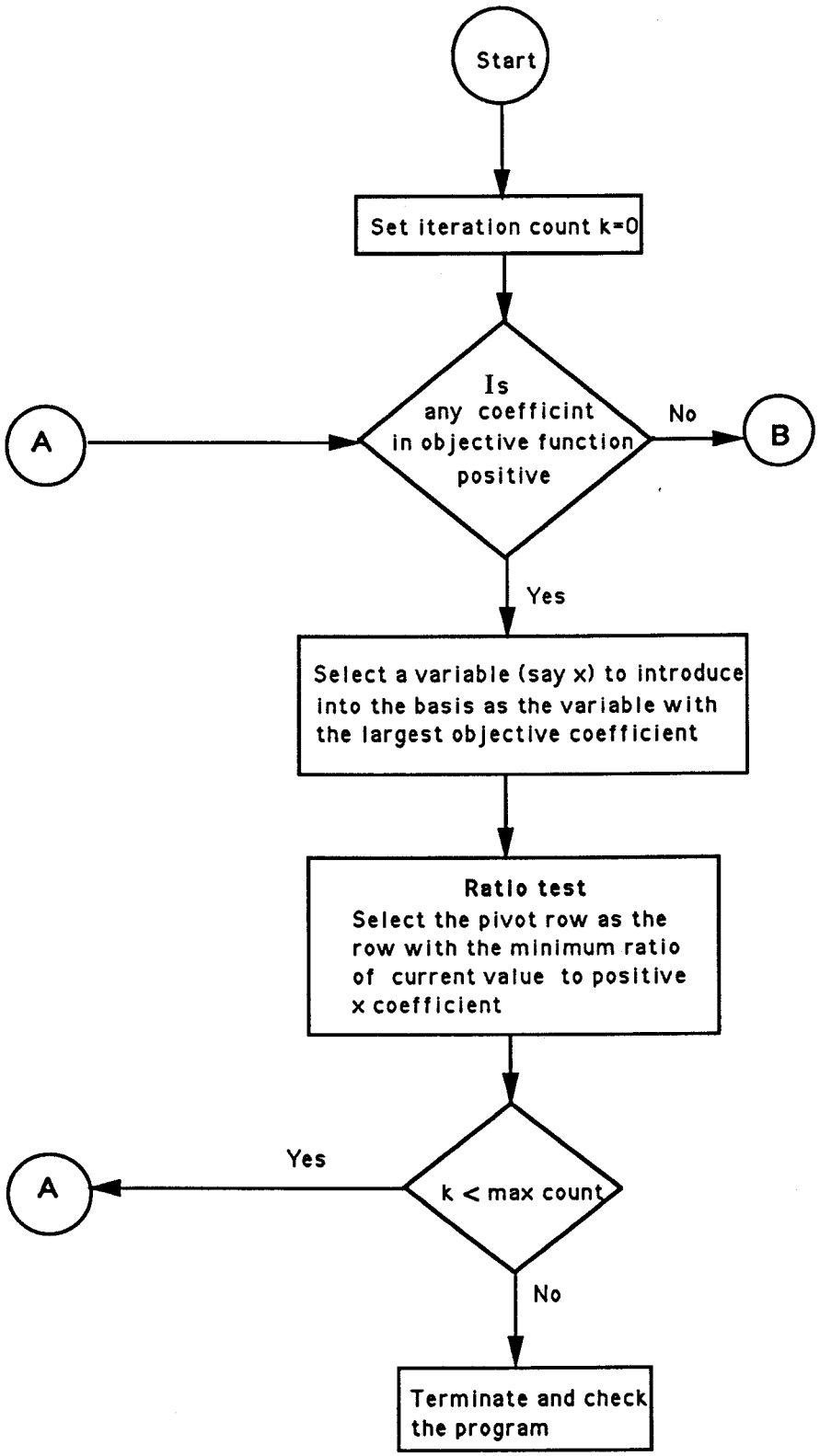

Figure 7.9: Implementation of the optimization segment of the relay coordination module.

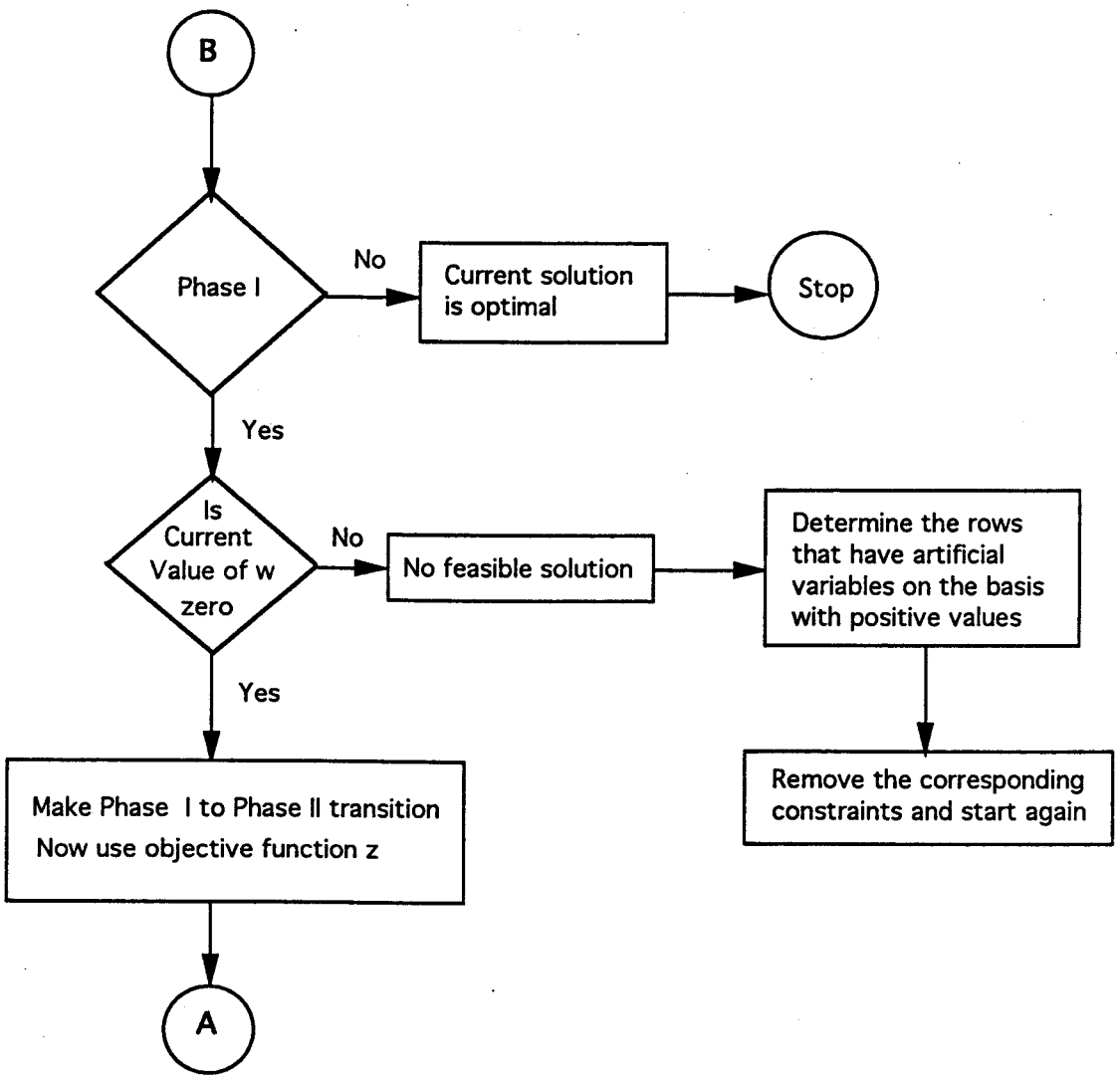

Figure 7.9 continued.

7.5.2. Coordination Software

The four modules of the coordination software were tested individually. The topology module was tested using two input files, one file contains information concerning line parameters and other file contains breaker/isolator status. The first input file was prepared from the system data, available from the electrical department of the 'City of Saskatoon' distribution system. This input file is shown in Table 7.1. The second input file, Table 7.2, contains status of all the breakers. This file was obtained by simulating breaker 1-4 as open and other breakers as closed. After executing the program, the topology detection module provides the lines that are in operation. The output of this program is illustrated in Table 7.3. The output shows that the program gives the desired result. The execution time of this program was 0.31 sec.

The state estimation module was tested using the output file produced by the topology detection module and with the help of another input file, shown in Table 7.4. This input file contains the active and reactive powers supplied to each load bus and generated power at each generating bus under maximum load and generating condition. After executing the program, the output file shown in Table 7.5, provided the pre-fault voltages and currents. It can be examined from the table that the bus voltages are those that are expected from a load flow study. The line flows are, therefore, the desired results. The program converged after 46 iterations and execution time of this software was 1.21 sec.

The fault analysis program was tested using the output file obtained from the state estimation module and using another input file, Table 7.6, containing source and load impedances under maximum generating and load condition. The faults were conducted at critical locations as shown in Figure 4.3. The output of this program provided fault currents at all branches of the network which is shown in Table 7.7. Considering the given source impedances at generating buses, it can be analysed that the fault currents obtained from the program are in order. The execution time of this software was 3.73 sec when currents at all the branches were calculated considering faults at the critical locations.

Table 7.1: Circuit identification and circuit parameter inputs for the topology detection module.

Circuit No.	Breaker No.	From	To	Line Parameter *p.u*
1	CB 1-6	1	6	0.723+j0.270
2	CB 1-1	1	28	0.386+j1.048
3	CB 1-4	1	20	0.585+j0.817
4	CB 2-1	2	8	1.218+j0.861
5	CB 2-2	2	9	1.047+j3.333
6	CB 3-1	3	12	0.555+j1.734
7	CB 3-4	3	11	0.591+j1.841
8	CB 4-1	4	16	0.688+j1.842
9	CB 4-4	4	15	1.042+j3.248
10	CB 5-1	5	21	0.427+j1.065
11	CB 5-2	5	22	0.536+j1.241
12	-	6	7	0.683+j1.064
13	-	7	8	0.243+j0.374
14	-	9	10	0.209+j0.653
15	-	10	11	0.077+j0.240
16	-	12	13	0.663+j2.160
17	-	13	14	0.357+j1.163
18	-	14	15	0.149+j0.463
19	-	16	17	1.024+j3.180
20	-	17	18	0.400+j0.616

Table 7.1.

21	-	18	19	0.165+j0.498
22	-	19	20	0.165+j0.498
23	-	20	21	0.804+j1.759
24	-	22	23	0.251+j0.407
25	-	23	24	0.337+j0.653
26	-	24	25	0.110+j0.171
27	-	25	26	0.173+j0.266
28	-	26	27	0.521+j0.801
29	-	27	28	0.464+j1.402

Table 7.2: Circuit breaker and isolating switch inputs for the topology detection module.

Circuit No.	Breaker No.	From	To	Breaker/Isolator Status
1	CB 1-6	1	6	1
2	CB 1-1	1	28	1
3	CB 1-4	1	14	0
4	CB 2-1	2	8	1
5	CB 2-2	2	9	1
6	CB 3-1	3	12	1
7	CB 3-4	3	11	1
8	CB 4-1	4	16	1
9	CB 4-4	4	15	1
10	CB 5-1	5	21	1
11	CB 5-2	5	22	1

Table 7.3: Output file from the topology detection module showing the circuits that are in operation.

Circuit No.	Breaker No.	From	To	Line Parameter *p.u*
1	CB 1-6	1	6	0.723+j0.270
2	CB 1-1	1	28	0.386+j1.048
4	CB 2-1	2	8	1.218+j0.861
5	CB 2-2	2	9	1.047+j3.333
6	CB 3-1	3	12	0.555+j1.734
7	CB 3-4	3	11	0.591+j1.841
8	CB 4-1	4	16	0.688+j1.842
9	CB 4-4	4	15	1.042+j3.248
10	CB 5-1	5	21	0.427+j1.065
11	CB 5-2	5	22	0.536+j1.241
12	-	6	7	0.683+j1.064
13	-	7	8	0.243+j0.374
14	-	9	10	0.209+j0.653
15	-	10	11	0.077+j0.240
16	-	12	13	0.663+j2.160
17	-	13	14	0.357+j1.163
18	-	14	15	0.149+j0.463
19	-	16	17	1.024+j3.180
20	-	17	18	0.400+j0.616

Table 7.3 continued.

21	-	18	19	0.165+j0.498
22	-	19	20	0.165+j0.498
23	-	20	21	0.804+j1.759
24	-	22	23	0.251+j0.407
25	-	23	24	0.337+j0.653
26	-	24	25	0.110+j0.171
27	-	25	26	0.173+j0.266
28	-	26	27	0.521+j0.801
29	-	27	28	0.464+j1.402

Table 7.4: Input file to state estimation module concerning load and generated power at different buses.

Bus	Load		Generation	Voltage	Phase
No.	P	Q	P	Magnitude	Angle
	p.u	*p.u.*	*p.u*	*p.u*	*rad.*
1	0	0	0	1.02	0
2	1.35	0.653	1.768	1.02	0
3	1.102	0.534	1.862	1.02	0
4	1.373	0.665	2.075	1.02	0
5	0.0	0.0.0	1.626	1.02	0
6	0.0	-0.24	0.0	1.00	0
7	1.093	0.529	0.0	1.00	0
8	0.135	-0.0546	0.0	1.00	0
9	0.63	0.305	0.0	1.00	0
10	0.0	-0.12	0.0	1.00	0
11	0.0315	0.0152	0.0	1.00	0
12	0.018	0.0872	0.0	1.00	0
13	0.081	0.392	0.0	1.00	0
14	0.521	0.2524	0.0	1.00	0
15	0.0	-0.12	0.0	1.00	0
16	0.18	0.0872	0.0	1.00	0
17	0.27	0.1307	0.0	1.00	0
18	0.6367	0.3084	0.0	1.00	0

Table 7.4 continued.

19	0.0	-0.12	0.0	1.00	0
20	0.1035	0.0501	0.0	1.00	0
21	0.8704	0.2415	0.0	1.00	0
22	0.278	0.1349	0.0	1.00	0
23	0.45	0.0984	0.0	1.00	0
24	0.028	0.0135	0.0	1.00	0
25	0.162	0.0784	0.0	1.00	0
26	0.09	0.0436	0.0	1.00	0
27	0.3303	0.3997	0.0	1.00	0
28	0.39	0.19	0.0	1.00	0

Table 7.5: Output file from the state estimation module.

Bus No.	Generated P *p.u*	Voltage Magnitude *p.u*	Phase Angle *rad.*	From	To	Line Flow P	Q
1	-0.43965	1.02000	0.00000	1	6	1.259	-0.653
2	1.64332	1.02000	-0.03721	1	28	1.628	0.213
3	0.70218	1.02000	-0.04470	2	8	0.007	0.920
4	1.14484	1.02000	-0.06564	2	9	0.411	0.070
5	1.24918	1.02000	-0.05726	3	12	0.507	0.030
6	-	1.01284	-0.00786	3	11	0.253	0.138
7	-	1.00896	-0.02361	4	16	0.585	0.317
8	-	1.01220	-0.02641	4	15	0.117	0.163
9	-	1.01358	-0.04975	5	21	1.495	0.430
10	-	1.01559	-0.04883	5	22	0.131	0.819
11	-	1.01604	-0.04841	6	7	1.244	-0.418
12	-	1.01676	-0.05301	7	8	0.140	-0.964
13	-	1.01327	-0.06312	9	10	-0.221	-0.241
14	-	1.01216	-0.06780	10	11	-0.221	-0.122
15	-	1.01362	-0.06769	12	13	0.487	0.017
16	-	1.01037	-0.07398	13	14	0.405	-0.027
17	-	0.99936	-0.08438	14	15	-0.117	-0.281
18	-	0.99832	-0.08485	16	17	0.402	0.222

Table 7.5 continued.

19	-	1.00027	-0.08269	17	18	0.130	0.085
20	-	1.00164	-0.08034	18	19	-0.507	-0.224
21	-	1.00935	-0.07095	19	20	-0.508	-0.105
22	-	1.00935	-0.05458	20	21	-0.612	-0.157
23	-	1.00700	-0.05231	22	23	-0.151	0.676
24	-	1.00530	-0.04651	23	24	-0.602	0.576
25	-	1.00504	-0.04483	24	25	-0.632	0.558
26	-	1.00515	-0.04192	25	26	-0.795	0.478
27	-	1.00634	-0.03267	26	27	-0.886	0.432
28	-	1.01177	-0.01574	27	28	-1.222	0.025

Table 7.6: Input file to the fault analysis module.

Bus No	Source Impedance *p.u*	Load Impedance *p.u.*
1	0.000264+j0.01171	2.7608+j1.3369
2	0.0+j0.03729	1.35+j0.653
3	0.0+j0.03483	1.102+0.5336
4	0.0+j0.03627	1.373+0.665
5	0.0+0.04688	0.0+j0.0
6	0.0+j0.0	0.0-j0.24
7	0.0+j0.0	1.093+j0.529
8	0.0+j0.0	0.135-j0.0547
9	0.0+j0.0	0.63+j0.3051
10	0.0+j0.0	0.0-j0.12
11	0.0+j0.0	0.0315+j0.0152
12	0.0+j0.0	0.018+j0.0087
13	0.0+j0.0	0.081+j0.0392
14	0.0+j0.0	0.521+j0.2524
15	0.0+j0.0	0.0-j0.12
16	0.0+j0.0	0.18+j0.0872
17	0.0+j0.0	0.27+j0.1307
18	0.0+j0.0	0.6367+j0.3084
19	0.0+j0.0	0.0-j0.12
20	0.0+j0.0	0.1035+j0.0501

Table 7.6 continued.

21	0.0+j0.0	0.8704+j0.2415
22	0.0+j0.0	0.278+j0.1349
23	0.0+j0.0	0.45+j0.0984
24	0.0+j0.0	0.028+j0.0135
25	0.0+j0.0	0.162+j0.0784
26	0.0+j0.0	0.09+j0.0436
27	0.0+j0.0	0.3303+j0.3997
28	0.0+j0.0	0.39+j0.19

Table 7.7: Output of the fault analysis module.

Relay Location	Fault Location	Fault Current *Amps*
1-1	2-1/2-2	-616
1-1	3-1/3-4	403
1-1	4-1/4-4	1487
1-1	5-1/5-2	5703
1-1	1-1	40648
1-6	2-1/2-1	8948
1-6	3-1/3-4	2505
1-6	4-1/4-4	630
1-6	5-1/5-2	-480
1-6	1-6	38328
2-1	1-1/1-6	6764
2-1	3-1/3-4	-2020
2-1	4-1/4-4	101
2-1	5-1/5-2	978
2-1	2-1	15246
2-2	1-1/1-6	-1808
2-2	3-1/3-4	4828
2-2	4-1/4-4	1059
2-2	5-1/5-2	-118
2-2	2-2	18493

Table 7.7 continued.

3-1	1-1/1-6	-162
3-1	2-1/2-2	-900
3-1	4-1/4-4	3560
3-1	5-1/5-2	799
3-1	3-1	16207
3-4	1-1/1-6	1971
3-4	2-1/2-2	4577
3-4	4-1/4-4	-894
3-4	5-1/5-2	117
3-4	3-4	14887
4-1	1-1/1-6	1245
4-1	2-1/2-2	209
4-1	3-1/3-4	-490
4-1	5-1/5-2	3361
4-1	4-1	14596
4-4	1-1/1-6	251
4-4	2-1/2-2	1063
4-4	3-1/3-4	3446
4-4	5-1/5-2	-640
4-4	4-4	14030
5-1	1-1/1-6	4395
5-1	2-1/2-2	1127
5-1	3-1/3-4	246

Table 7.7 continued.

5-1	4-1/4-4	-863
5-1	5-1	11941
5-2	1-1/1-6	-649
5-2	2-1/2-2	485
5-2	3-1/3-4	1113
5-2	4-1/4-4	3512
5-2	5-2	14130

The optimization program was tested using the output file created by the state estimation and fault analysis programs. The coefficients of the constraints, objective function z and coefficients of the w functions are shown in Table 7.8. The optimization program was then used to obtain the optimized *TMS* values. The software successfully converged in Phase I after 31 iterations. In Phase II, the optimized *TMS* values were obtained after 2 iterations and total execution time including Phase I and Phase II was 0.93 sec. These *TMS* values were then used to analyze the system under four extreme operating conditions. It is examined in the next chapter that these are the desired output.

7.5.3. Communication Software

The testing of communication software was performed by sending files from relaying pc to the station controller's pc and from the station controller's pc to the central control computer. It was then checked whether the information received by the pcs are uncorrupted. It was examined that under the laboratory environment correct information was received by the pcs.

Tables 7.9 and 7.10 show the nature of information that were exchanged between the different pcs.

7.6. Summary

This chapter has described a prototype system for an adaptive protection of a distribution network. The different hardware used to design the system are described. Two application software, developed for communication purpose, are also described. The application software that was developed for communication between the relays and the station control computer was written in C programming language and compiled with Turbo C. The other application software was also written in C programming language and was compiled with Microsoft C. The compilation requirement came from the type of commercial software used to design the application software. The implementation of the coordination software and testing of each module of the software have been described. The software modules provided the intended performance.

Table 7.8: Inputs to the optimization module.

	Current value	t_{11}	t_{16}	t_{21}	t_{22}	t_{34}	t_{31}	t_{44}	t_{41}	t_{52}	t_{51}
Coefficients of the constraints	0.2	-0.59		1.68							
	0.2			-1.68		5.91					
	0.2								12.57		-3.00
	0.2								2.93		-0.97
	0.2						58.74		-2.93		
	0.2	-5.73		44.50							
	0.2			-0.70		2.04					
	0.2					-2.04		17.50			
	0.2		-2.94								32.99
	0.2		-0.59								3.00
	0.2					-0.57		2.85			
	0.2		23.87		-2.48						
	0.2		2.94		-0.57						
	0.2							-0.60		7.46	
	0.2				32.78		-3.02				
	0.2				2.48		-0.56				
	0.2	5.73								-1.31	
	0.2						3.02		-0.58		
	0.05	0.59									
	0.05		0.59								
	0.05			0.70							
	0.05				0.57						
	0.05						0.56				
	0.05					0.57					
	0.05								0.58		
	0.05							0.60			
	0.05										0.97
	0.05									1.31	
z-row	0.0	-0.59	-0.59	-0.70	-0.57	-0.57	-0.56	-0.60	-0.58	-1.31	-0.97
w-row	4.1	0.00	23.87	44.50	32.78	5.91	58.74	20.35	12.57	7.46	32.99

Note: Row 1 corresponds to fault location at F 1-1.

Table 7.9: Information transmitted from a relay to the central computer via substation control computer.

Relay Designation	Secondary Pickup Current			TMS Value	Bus Voltage (kv)	Line Current (Amps)	Breaker Status
	O/L	O/C	Inst.				
R 2-2	6.0	4.0	30.0	0.080	13.8+j0.0	140-j50	1

Table 7.10: Information received by the relay from the central control computer via substation control computer.

Relay Designation	Secondary Pickup Current			TMS Value
	O/L	O/C	Inst.	
R 2-2	6.5	4.5	31	0.100

8. SYSTEM STUDIES

8.1. Introduction

The testing of the relay coordination software is reported in the previous chapter. This chapter uses the test results and analyzes the relay settings. The chapter also demonstrates the benefits that can be obtained from the adaptive protection. Several operating conditions of the selected distribution system were considered in the studies.

The relay setting criteria used for selecting the secondary pickup/tap settings for the overload, phase fault overcurrent and instantaneous overcurrent relays under the different operating conditions are outlined. The estimated time multiplier settings for all the relays are reported. The chapter then describes the comparisons of relay operating characteristics, relay operating times and coordination margins for overcurrent relays under the adaptive and conventional (non-adaptive) protection system. A comparison of the percentage of line protected by the instantaneous overcurrent relays has also been presented. These studies were carried out by considering that the adaptive approach was functioning properly.

The selected values of time multiplier settings when the adaptive approach fails to function, are also presented.

8.2. Operating Conditions

The following four operating conditions of the distribution system were considered in conducting the studies.

1. Maximum system load and maximum system generation with line 1-20 closed (MXLG-1).

2. Minimum system load and minimum system generation with line 1-20 closed (MNLG-1),
3. Maximum system load and maximum system generation with line 1-20 open (MXLG-2) and
4. Minimum system load and minimum system generation with line 1-20 open (MNLG-2).

8.3. Relay Settings

In each operating condition, the state estimator calculated the pre-fault currents in the lines and voltages at the substation buses as discussed in Sections 6.3 and 7.4.3.2. Using these pre-fault currents, the secondary pickup currents of the overload and the phase fault overcurrent relays were determined. The fault analysis program was then used to calculate the currents for faults on each line at critical locations as discussed in Sections 6.4 and 7.4.3.3. Three phase symmetrical faults at the near and far-ends of the relays were simulated. The location of near-end fault for relay 1-1 is marked as F 1-1, and the far-end fault is marked as F 5-1 which are shown in Figure 4.3. The near and far-end faults for other relays are also shown in Figure 4.3. The relay setting criteria for each protection are discussed in the following section.

8.3.1. Overload Pickup Settings

The secondary pickup or tap setting of an overcurrent relay is calculated using the relation, Secondary Pickup value = % Setting $\times$ Secondary Load Current/100. The range of settings have been selected between 150% to 200% of the maximum load current. With the decrease in load, pickup settings are also reduced to obtain lower relay operating times during overloads. While selecting the pickup settings for the overload, it has been verified that the settings do not affect the coordination between the backup overload relays and primary phase fault relays. This is usually accomplished because overload relays would experience fault currents up to three times of ct primary ratings after which overcurrent relays would take over. Also, the ct ratios for overload and phase fault relays are separate.

In the case of the non-adaptive approach, however, relay settings are selected based on 200 % of the maximum load current and remain unchanged to avoid any unnecessary tripping.

8.3.2. Overcurrent Pickup Settings

The pickup settings of the phase fault overcurrent relays have been determined considering both the load and fault currents. With the decrease in load current, the pick up setting is also reduced but it must be more than the maximum line current. In this application, load current is first estimated and then compared with the maximum load current. A margin of 20% is then added for any contingency. It is then checked whether the fault currents are within the 25 multiples of pickup current; a common feature of the overcurrent relays. During checking such criteria the relation, Multiples of pickup current = Fault current/(Secondary pickup setting $\times$ ct ratio) is used.

In the case of the non-adaptive approach, a similar criterion has been used but based on the scenario that provides best possible coordination.

8.3.3. Instantaneous Tap Settings

The tap settings of the instantaneous relays are selected at 1.3 times of the far-end fault currents. Since the fault currents change with the change of source impedance due to change of system generation and circuit topology, the settings for instantaneous relays also change.

In the case of the non-adaptive approach, the instantaneous tap settings are kept fixed considering the maximum setting value to avoid undesirable operation of the instantaneous units.

8.3.4. Time Multiplier Settings

After selecting the secondary pickup settings and calculating the fault currents, the coordination software was used to minimize the operating time for the near-end faults to determine the optimum time multiplier settings (*TMS*). In selection of the *TMS* values, coordination among all the relays were also maintained. The detailed procedure in determining the optimized *TMS* values are described in Sections 6.6.1 and 7.4.3.4. Both the overload and overcurrent relays use the same time multiplier settings.

In the case of the non-adaptive approach, the *TMS* values are selected considering the best possible coordination that can be achieved in all operating states. Generally, the maximum load and maximum generating condition satisfies this criterion.

8.4. Results

Table 8.1 shows the percentage settings that are used for the overcurrent protections during adaptive and non-adaptive approaches. Table 8.2 shows the calculated pickup and time multiplier settings of overload, overcurrent and instantaneous overcurrent relays. The table also includes the load currents, fault currents and ct ratios for a comprehensive understanding of the relay settings which are provided in columns 7 to 10 of the table. It can be examined from the table that the pick up settings of the overload relays change as the system operating state changes. This is due to the fact that at different operating conditions the load currents change. The pickup settings of the phase-fault overcurrent relays also change with the change in system conditions but not in all the cases because of the criteria depicted under Section 8.3.2. The instantaneous relay settings are based on the far-end fault currents. As such, it can be seen from the table that the instantaneous tap settings also change with the change in system conditions. The table shows that the instantaneous tap settings for relays 4-1, 5-1 and 5-2 change significantly because of the large variations of the fault currents at different operating states. Table 8.2 also illustrates that the *TMS* values change at different operating conditions. These *TMS* values are the optimum settings which are selected from the optimization technique. Moreover, these *TMS* values also provide optimum coordination time interval among the relays. In the case of the non-adaptive approach, the pickup settings are selected based on the highest value for all the conditions. This would avoid any undesirable relay operation.

Figures 8.1 through 8.11 show the relay operating characteristics that are used during adaptive and non-adaptive approaches. It can be seen that the operating characteristic changes as the system conditions change. The adaptive protection will choose the characteristic corresponding to the operating state in concern. However, the non-adaptive approach will choose one particular characteristic for all operating states and this characteristic would be selected based on the worst case scenario to maintain the

coordination. In the case of relay 1-1, the operating characteristic would be 1-1′, 2-2′, 3-3′ and 4-4′ for the operating conditions MXLG-1, MNLG-1, MXLG-2 and MNLG-2 respectively. But if the conventional non-adaptive approach is used, the relay characteristic 1-5-5′-3′ would be in place for all operating states. This characteristic is obtained from the combination of the relay characteristics at conditions MXLG-1 and MXLG-2. The overcurrent portion of the characteristic is based on the condition MXLG-1 and instantaneous portion is based on MXLG-2 because they provide the maximum setting values. Figures 8.1 through 8.11 also illustrate that in most of the cases the relay characteristics corresponding to maximum load and generating condition are suitable during non-adaptive approach.

Table 8.3 shows the operating times of the relays in primary and backup protection for the condition MNLG-2 during adaptive approach. The relay operating times for other conditions are shown in Appendix G. Table 8.4 shows the relay operating times for the condition MNLG-2 during non-adaptive approach. Although, coordination during non-adaptive case is also achieved, the relay operating times are long compare to adaptive approach.

Figures 8.12 and 8.13 show the comparisons of the relay operating times in the primary protection when the adaptive and non-adaptive approaches are used during minimum load and generating conditions. These figures show that the relay operating times are less when the adaptive approach is used. This is mainly because of the lower pickup settings that has been used during minimum load and generating condition.

Figure 8.14(a) illustrates a case when the overload relay, 5-2, can not operate for a far-end fault under the non-adaptive approach. This is due to the fact that during the non-adaptive application, pickup setting is not revised while the source impedance changes due to changes of load, generation level and circuit configuration. However, using the adaptive approach, the pickup setting is reduced and consequently the relay operates for the same fault. This has been demonstrated in Figure 8.14.(b).

Figure 8.15(a) shows a case when coordination has not been achieved using

non-adaptive approach. As mentioned earlier, the pickup settings for the non-adaptive approach are selected based on maximum load and generating condition to avoid tripping during normal operation. Also to maintain the relay coordination, higher time multiplier settings are chosen. Even with higher pickup and time multiplier settings, adequate selectivity has not been achieved with several trials. This results in slim timing margin between relay 4-1 and 5-1 for a fault at 1-1. The problem is, however, alleviated by the use of the adaptive approach which is shown in Figure 8.15(b).

Figure 8.16 shows the percentage of the line protected by the instantaneous relays when the adaptive and non-adaptive approaches were used at minimum load and generating condition, and line 1-20 open. The figure shows that the coverage of the line during minimum operating state is less in non-adaptive approach compare to adaptive approach.

8.5. Results during the failure of Adaptive System

The procedure, proposed in Section 6.7, for determining the time multiplier settings has been used to determine the *TMS* values locally. The estimates of *TMS* values are based on change of loads from the minimum values to their maximum values and when line 1-20 is open; a worst case scenario. Figure 8.17 shows that the local estimates are close to those estimated by the adaptive approach. These values could be used for a short period.

8.6. Summary

The chapter has described the system studies under four operating conditions. Results have been provided both for the adaptive and non-adaptive approaches. It is examined that the adaptive approach provides lower relay operating times compare to the non-adaptive approach at all four conditions. It is also demonstrated that the relay coordination margins are appropriate when the adaptive approach was used. One case has been presented that shows a non-operating condition of a relay under the non-adaptive approach. The alleviation of the problem using an adaptive approach is demonstrated.

Table 8.1: The selected values of the overcurrent settings.

Relay	Operat. Cond.	Load Current (A)	Maximum Load /Normal Load	% Pickup to be set		% Pickup selected for Adaptive approach
				Non-adaptive	Adaptive	
1 -1	MXLG-1	398	162%	324%	> 162%	200%
	MNLG-1	181	357%	714%	> 357%	425%
	MXLG-2	646	100%	200%	200%	200%
	MNLG-2	337	192%	384%	> 192%	225%
1-4	MXLG-1	404	100%	200%	200%	200%
	MNLG-1	192	210%	420%	> 210%	250%
	MXLG-2	-	-	-	-	-
	MNLG-2	-	-	-	-	-
1-6	MXLG-1	522	107%	214%	> 107%	200%
	MNLG-1	223	250%	500%	> 250%	300%
	MXLG-2	557	100%	200%	200%	200%
	MNLG-2	298	187%	374%	> 187%	225%
2-1	MXLG-1	241	150%	300%	> 150%	200%
	MNLG-1	111	326%	652%	> 326%	400%
	MXLG-2	362	100%	200%	200%	200%
	MNLG-2	154	235%	470%	> 235%	300%
2-2	MXLG-1	81	202%	404%	> 202%	250%
	MNLG-1	34	482%	964%	> 482%	600%
	MXLG-2	164	100%	200%	200%	200%
	MNLG-2	78	210%	420%	> 210%	250%

Table 8.1 continued.

3-1	MXLG-1	100	200%	400%	> 200%	250%
	MNLG-1	48	417%	834%	> 417%	500%
	MXLG-2	200	100%	200%	200%	200%
	MNLG-2	97	206%	412%	> 206%	250%
3-4	MXLG-1	210	100%	200%	200%	200%
	MNLG-1	103	204%	408%	> 204%	250%
	MXLG-2	113	186%	372%	> 186%	200%
	MNLG-2	53	396%	792%	> 396%	475%
4-1	MXLG-1	153	170%	340%	> 170%	200%
	MNLG-1	75	348%	696%	> 348%	425%
	MXLG-2	261	100%	200%	200%	200%
	MNLG-2	123	124%	248%	> 124%	250%
4-4	MXLG-1	158	100%	200%	200%	200%
	MNLG-1	76	208%	416%	> 208%	250%
	MXLG-2	79	200%	400%	> 200%	250%
	MNLG-2	30	527%	1054%	> 527%	650%
5-1	MXLG-1	389	100%	200%	200%	200%
	MNLG-1	167	233%	466%	> 233%	300%
	MXLG-2	326	119%	238%	> 119%	200%
	MNLG-2	50	778%	1556%	> 778%	950%
5-2	MXLG-1	322	190%	380%	> 190%	225%
	MNLG-1	157	390%	780%	> 390%	500%
	MXLG-2	612	100%	200%	200%	200%
	MNLG-2	298	205%	410%	> 205%	250%

Table 8.2: Loads, fault currents and settings of the relays.

Relay	Operat. Cond.	Load Curr. (A)	Fault Currents (Amps)		Phase Fault & O/L cts	Secondary Pickup/ Tap Settings			TMS for O/C & O/L
			Near-end Faults	Far-end Faults		O/L Relay	O/C Relay	Inst. Relay	
1 -1	MXLG-1	398	46815	4941	2000/5 & 800/5	7.00	4.75	16.0	0.088
	MNLG-1	181	42546	4440		6.00	4.50	14.5	0.084
	MXLG-2	646	40648	5703		8.00	4.25	18.5	0.085
	MNLG-2	337	36503	5273		7.00	3.75	17.0	0.086
1-4	MXLG-1	404	42642	3875	2000/5 & 600/5	6.75	5.00	13.0	0.084
	MNLG-1	192	38804	3692		6.00	4.50	12.0	0.086
	MXLG-2	-	-	-		-	-	-	-
	MNLG-2	-	-	-		-	-	-	-
1-6	MXLG-1	522	42490	8741	2000/5 & 600/5	9.25	4.50	28.5	0.089
	MNLG-1	223	38940	8670		8.25	4.00	28.0	0.086
	MXLG-2	557	38328	8947		9.25	4.00	29.0	0.088
	MNLG-2	298	34605	8638		8.25	3.50	28.0	0.100
2-1	MXLG-1	241	15331	6738	1000/5 & 400/5	9.00	3.75	44.0	0.148
	MNLG-1	111	13998	6403		6.75	3.75	42.0	0.140
	MXLG-2	362	15246	6764		9.00	3.75	44.0	0.149
	MNLG-2	154	13971	6471		8.00	3.75	42.0	0.141
2-2	MXLG-1	81	18574	4806	1000/5 & 200/5	7.25	3.75	31.0	0.088
	MNLG-1	34	17369	4669		6.25	3.50	30.0	0.088
	MXLG-2	164	18493	4828		8.25	3.75	31.5	0.100
	MNLG-2	78	17278	4693		7.25	3.50	30.5	0.106
3-1	MXLG-1	100	16179	3526	1000/5 & 300/5	6.00	3.25	23.0	0.108
	MNLG-1	48	14784	3407		5.00	3.00	22.0	0.088
	MXLG-2	200	16207	3560		6.75	3.25	23.0	0.089
	MNLG-2	97	14812	3442		6.00	3.00	22.5	0.090
3-4	MXLG-1	210	14915	4544	1000/5 & 300/5	7.00	3.00	29.5	0.147
	MNLG-1	103	13540	4357		6.25	2.75	28.5	0.157
	MXLG-2	113	14887	4577		6.25	3.00	30.0	0.149
	MNLG-2	53	13502	4387		5.25	2.75	28.5	0.159
4-1	MXLG-1	153	14509	1806	1000/5 & 300/5	7.75	3.00	12.0	0.221
	MNLG-1	75	13240	1739		6.50	2.75	11.5	0.267
	MXLG-2	261	14596	3361		8.75	3.00	22.0	0.096
	MNLG-2	123	13299	3180		7.75	2.75	21.0	0.100
4-4	MXLG-1	158	15596	3497	1000/5 & 200/5	8.00	3.25	23.0	0.092
	MNLG-1	76	14360	3375		7.00	3.00	22.0	0.100
	MXLG-2	79	14029	3446		7.00	3.00	22.5	0.100
	MNLG-2	30	12838	3319		6.00	2.75	21.5	0.108
5-1	MXLG-1	389	16499	2725	1000/5 & 400/5	9.75	4.00	18.0	0.073
	MNLG-1	167	15380	2265		8.50	4.00	15.0	0.068
	MXLG-2	326	11941	4395		9.75	4.00	29.0	0.084
	MNLG-2	50	10958	3983		7.50	4.00	26.0	0.076
5-2	MXLG-1	322	13185	1251	1000/5 & 800/5	6.75	6.25	8.0	0.035
	MNLG-1	157	12314	1109		5.75	6.25	7.5	0.033
	MXLG-2	612	14130	3512		7.75	6.25	23.0	0.038
	MNLG-2	298	13171	3212		6.75	6.25	21.0	0.037

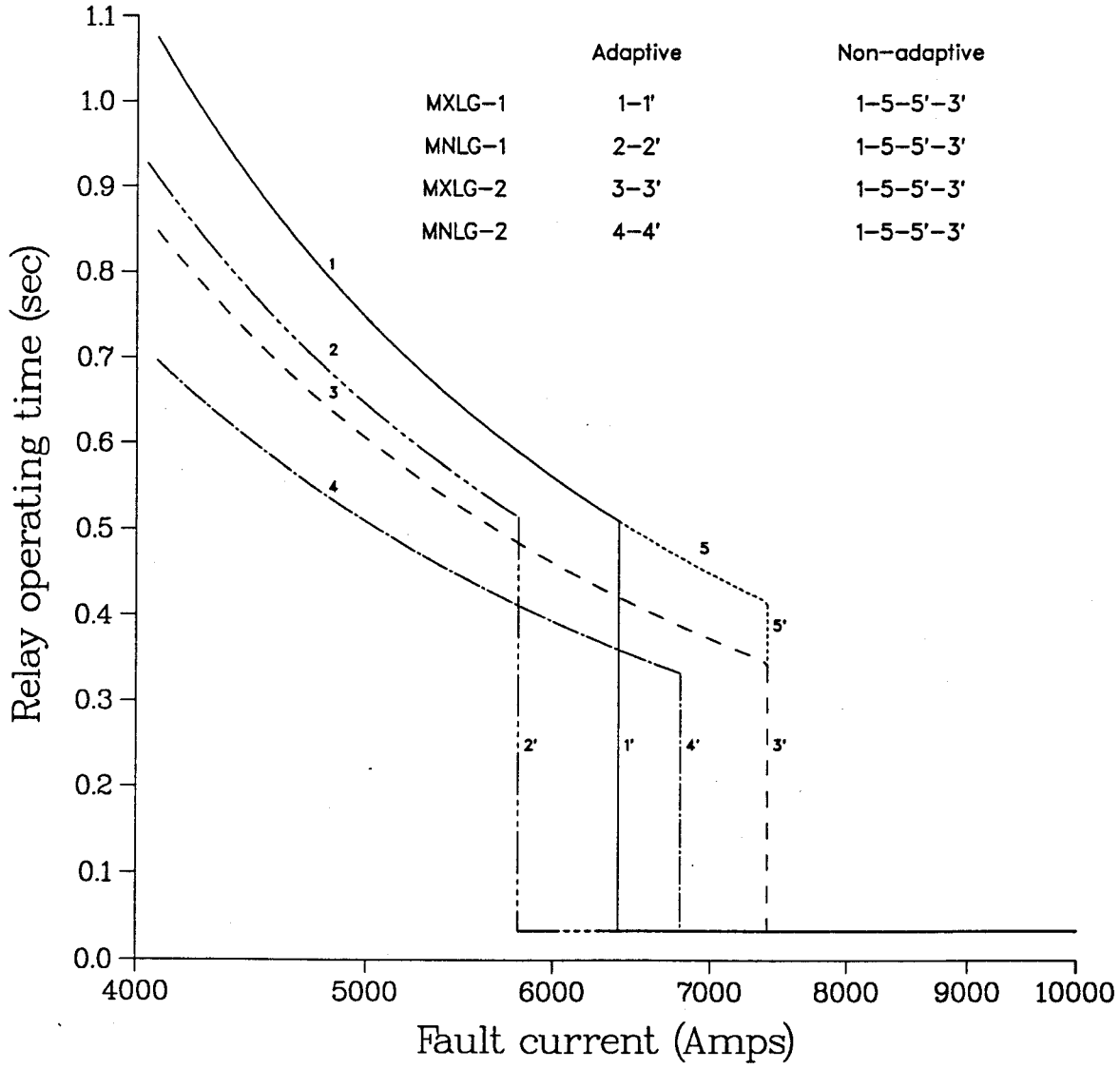

Figure 8.1: Operating characteristics of relay 1-1 with and without adaptive settings.

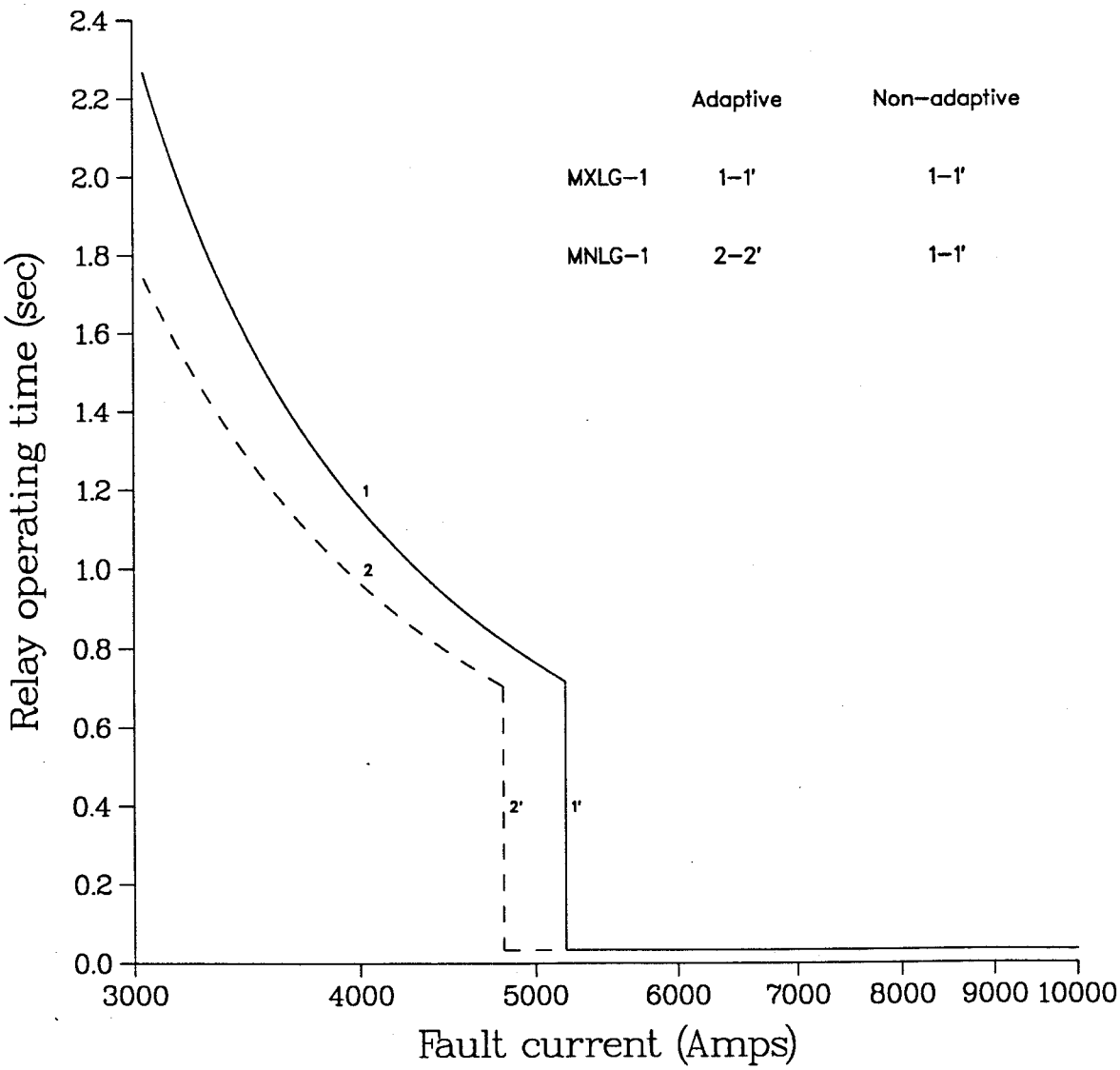

Figure 8.2: Operating characteristics of relay 1-4 with and without adaptive settings.

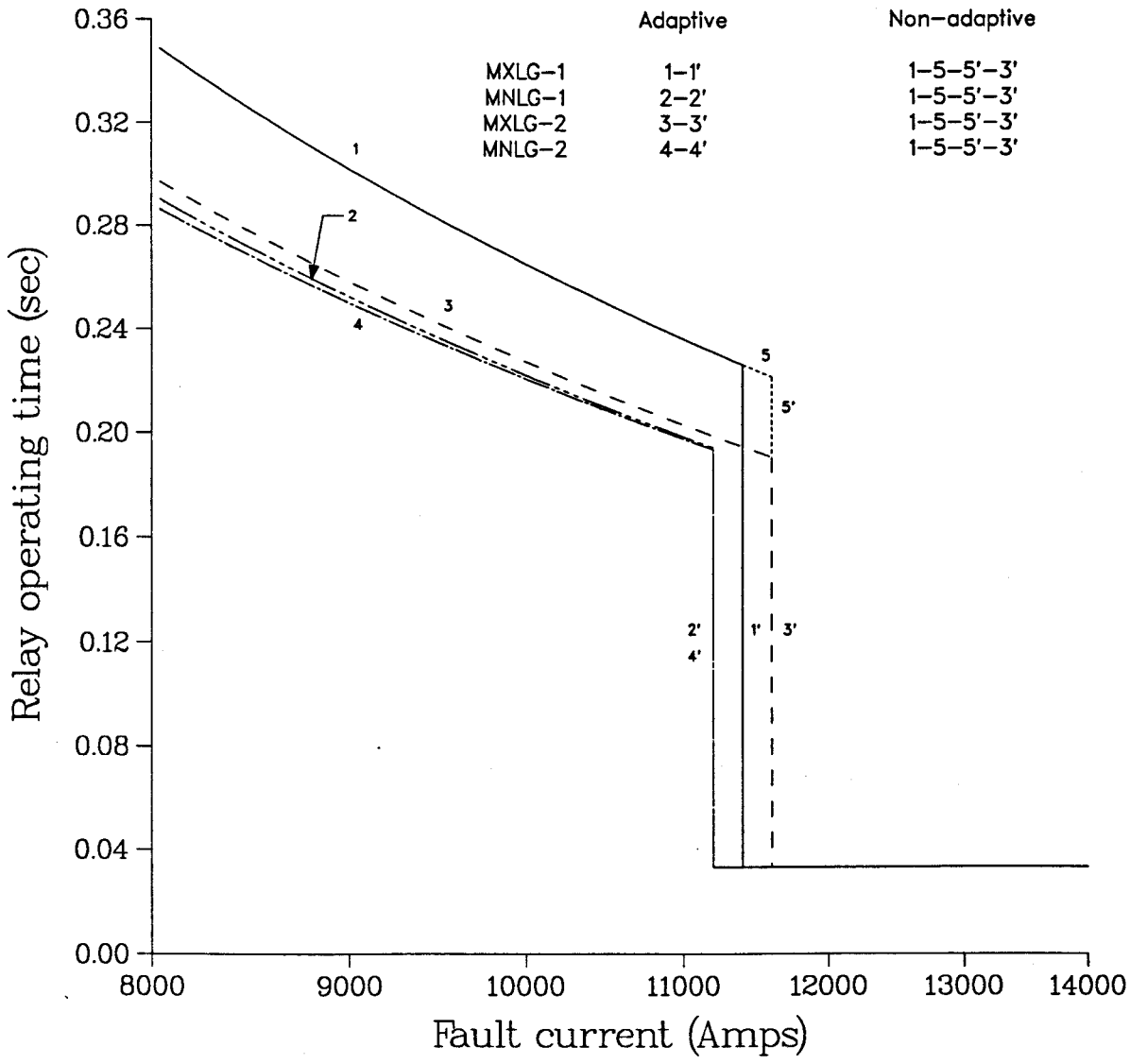

Figure 8.3: Operating characteristics of relay 1-6 with and without adaptive settings.

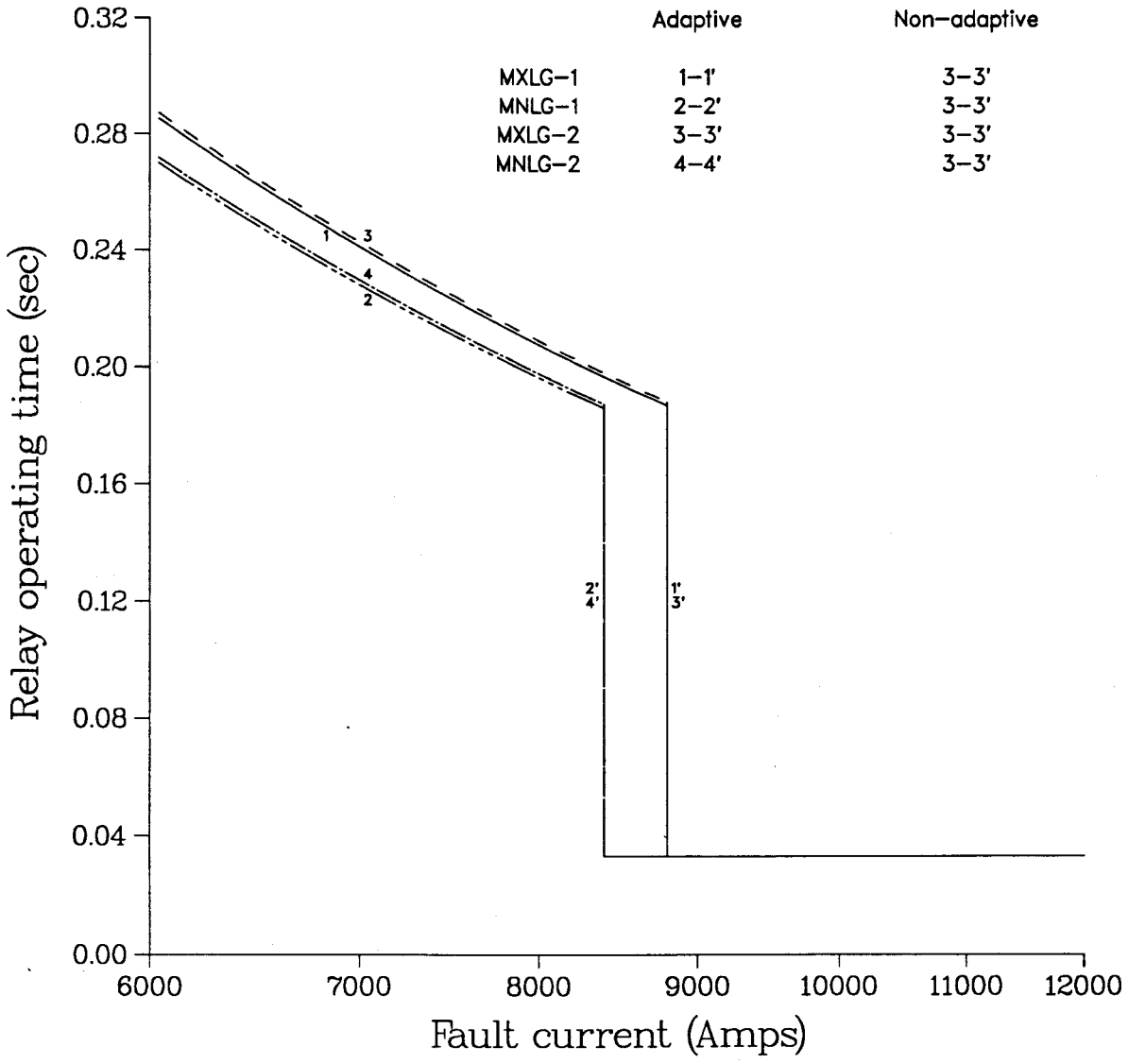

Figure 8.4: Operating characteristics of relay 2-1 with and without adaptive settings.

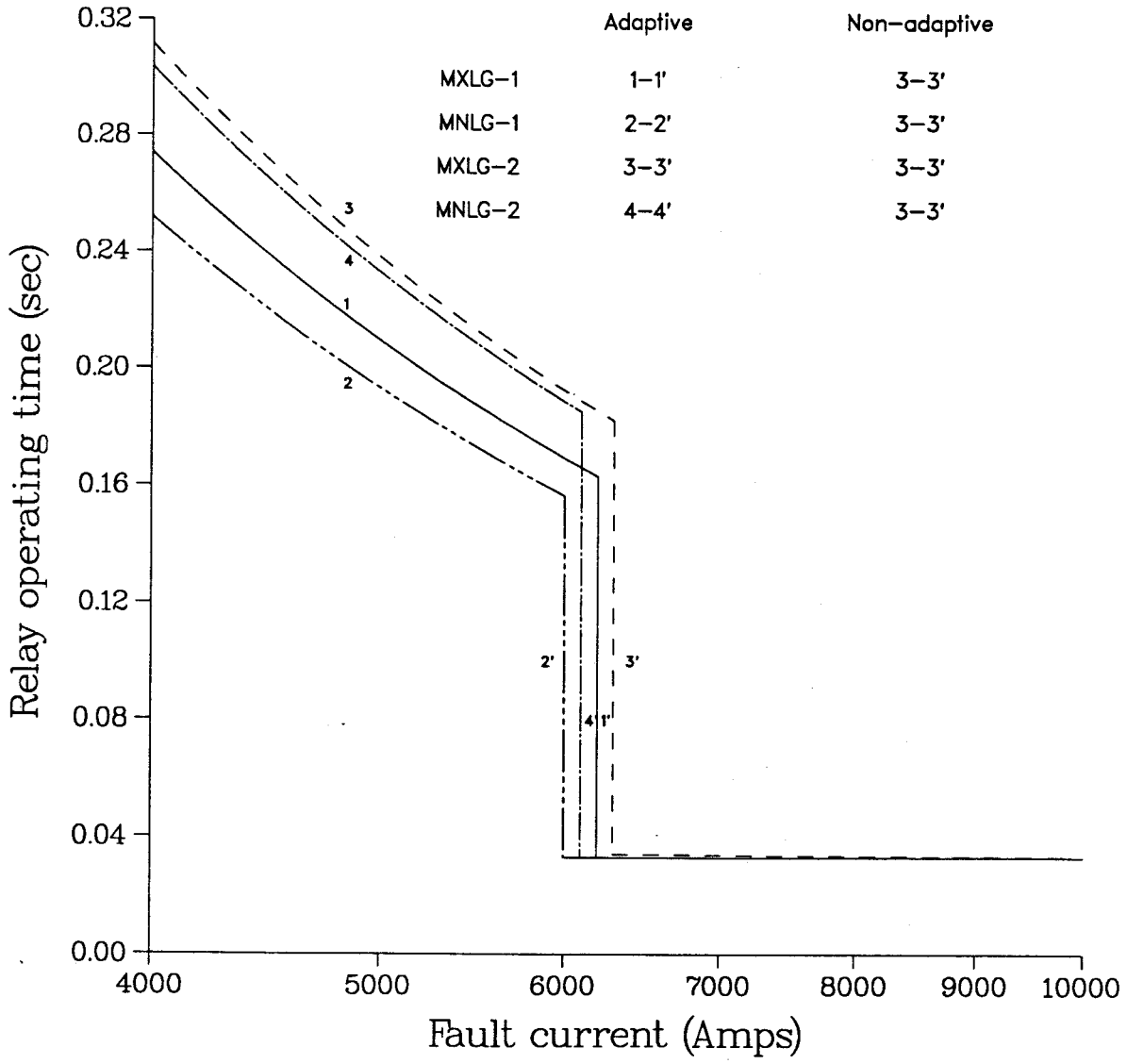

Figure 8.5: Operating characteristics of relay 2-2 with and without adaptive settings.

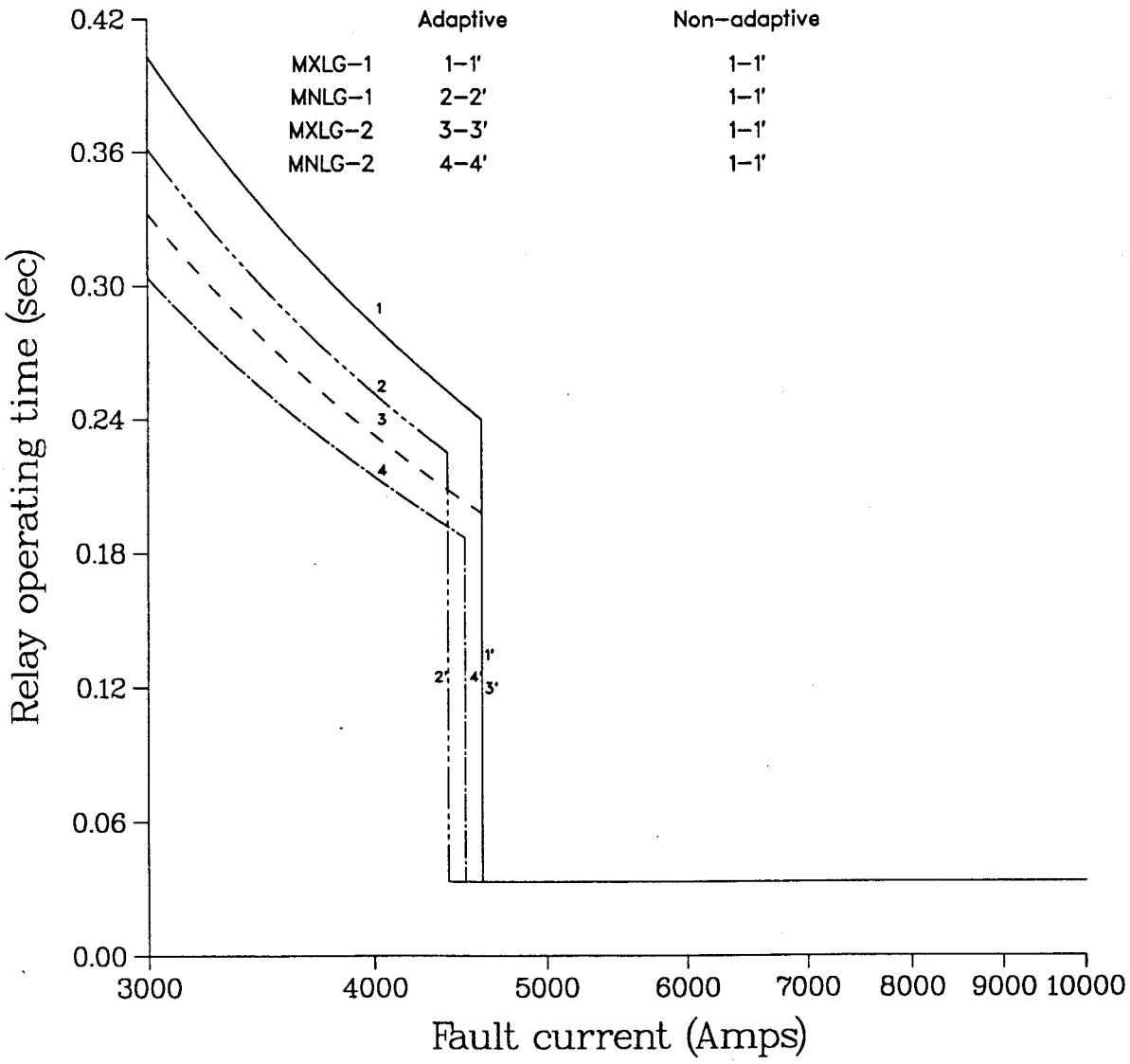

Figure 8.6: Operating characteristics of relay 3-1 with and without adaptive settings.

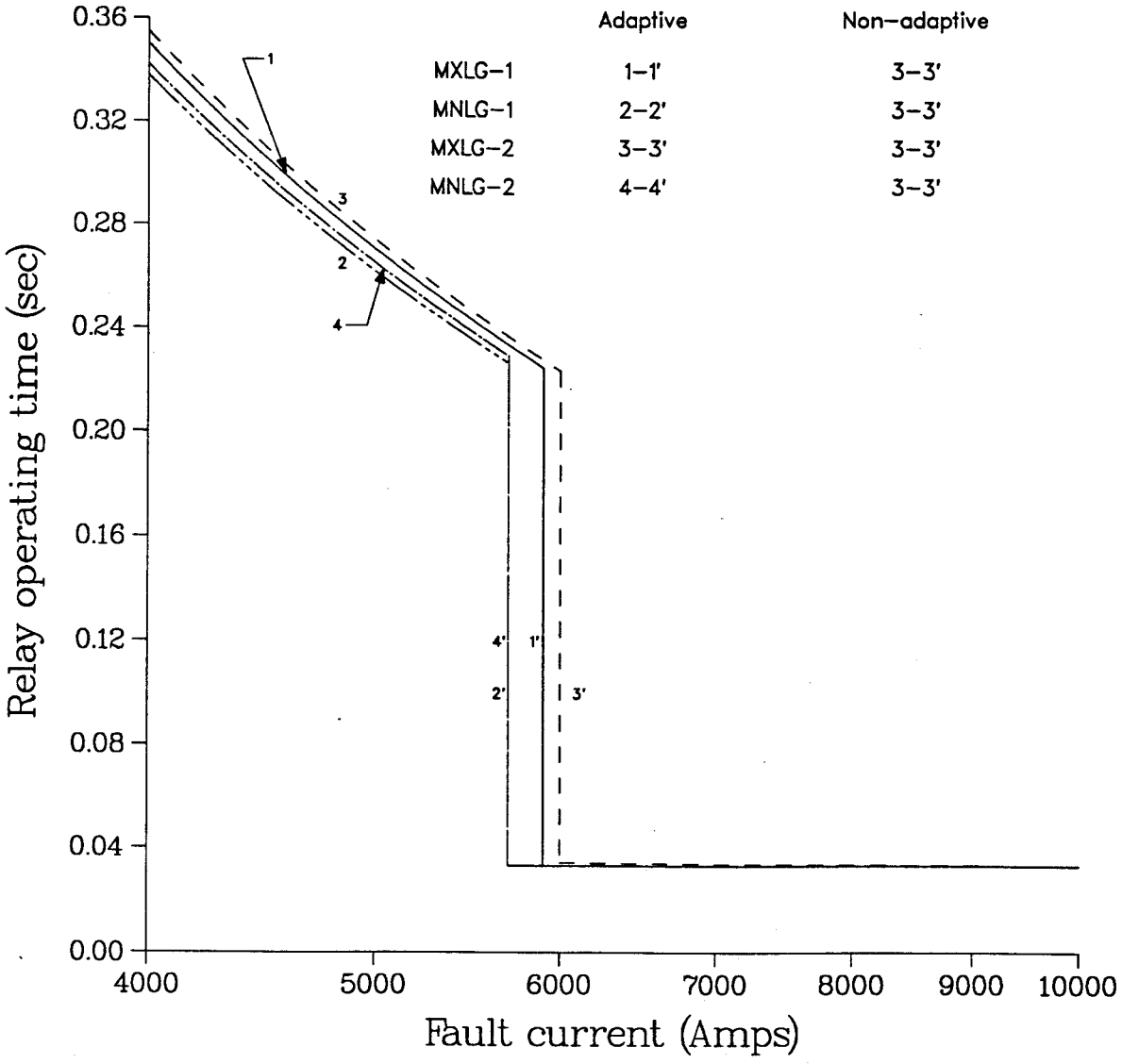

Figure 8.7: Operating characteristics of relay 3-4 with and without adaptive settings.

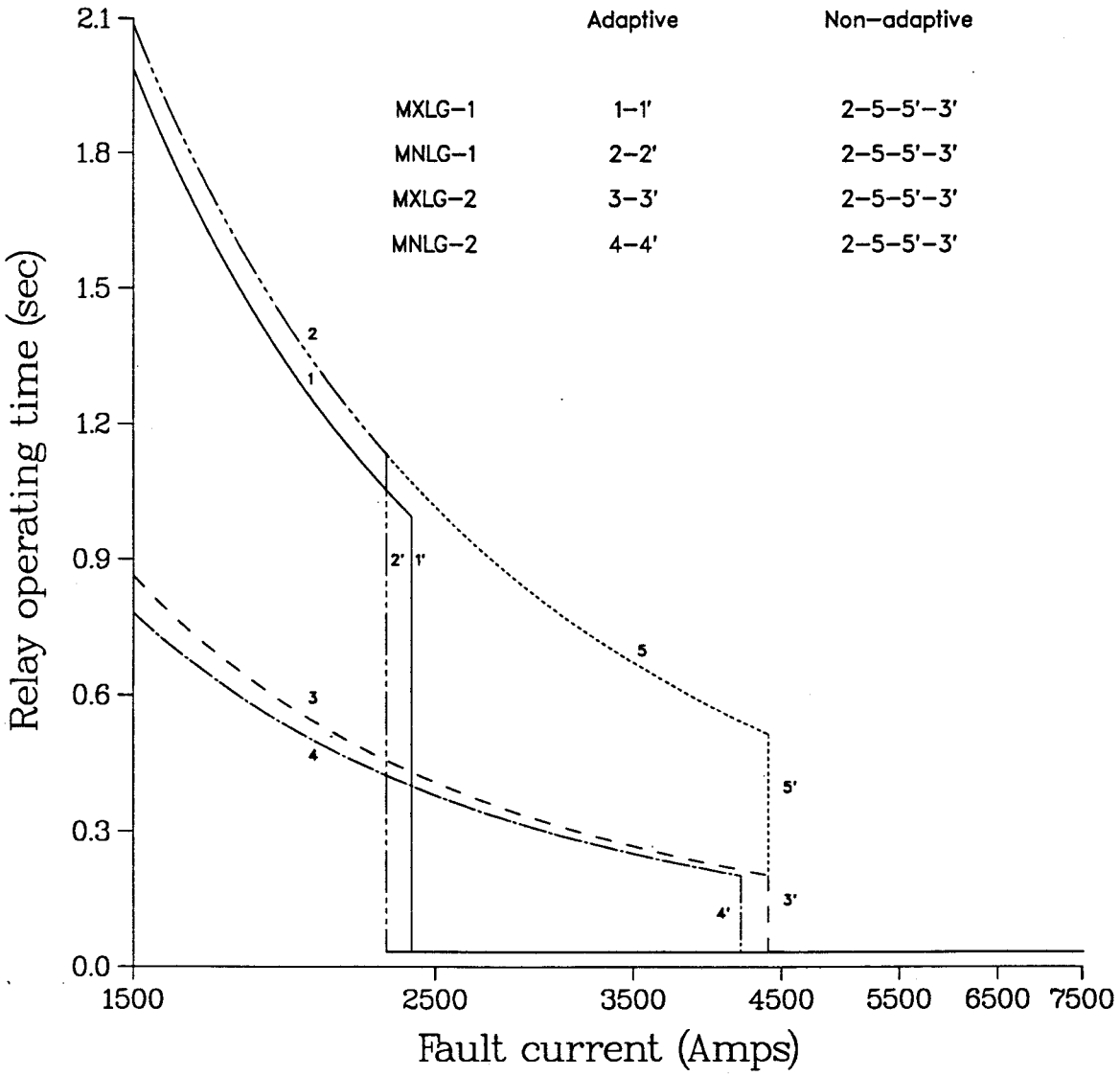

Figure 8.8: Operating characteristics of relay 4-1 with and without adaptive settings.

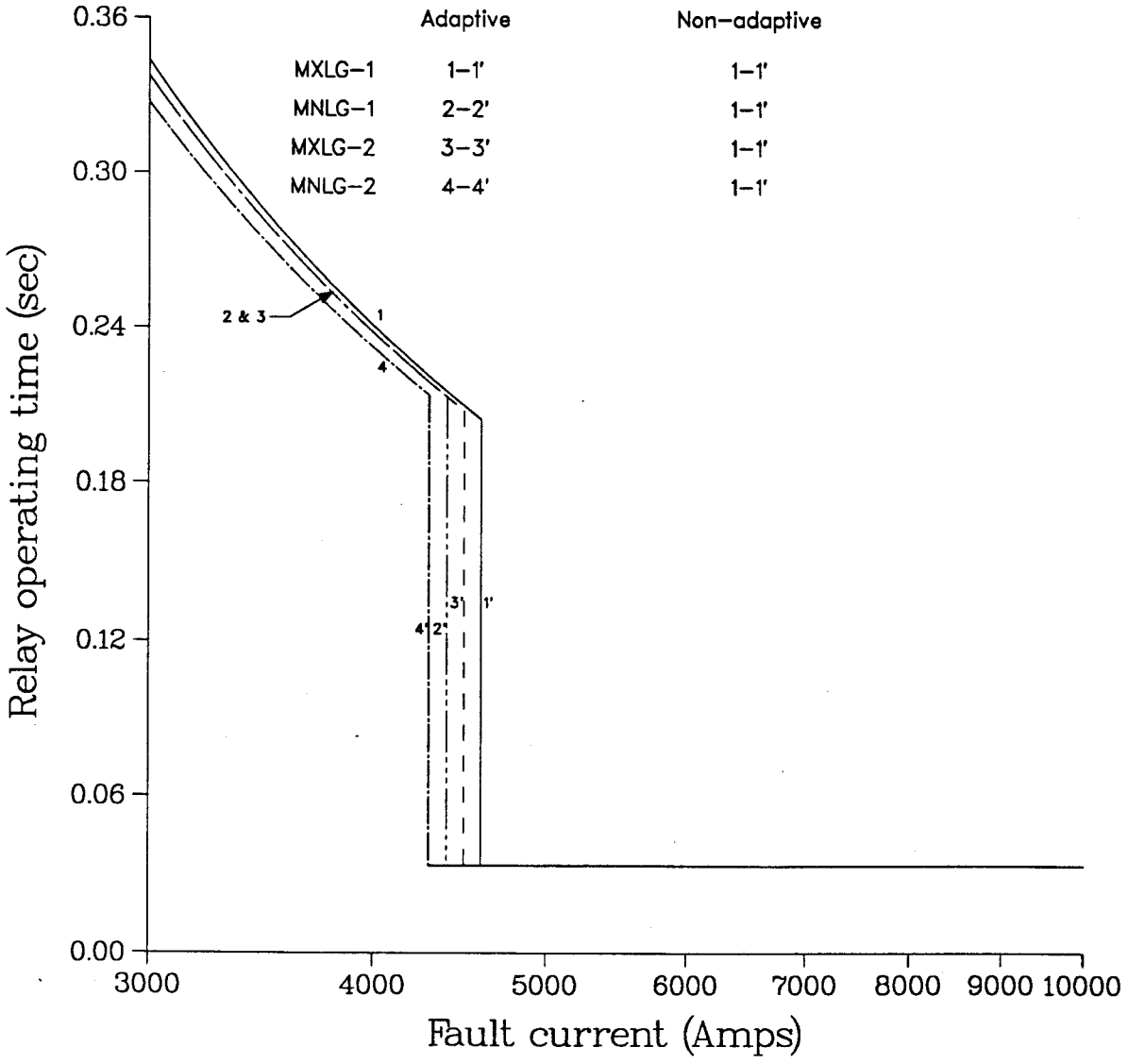

Figure 8.9: Operating characteristics of relay 4-4 with and without adaptive settings.

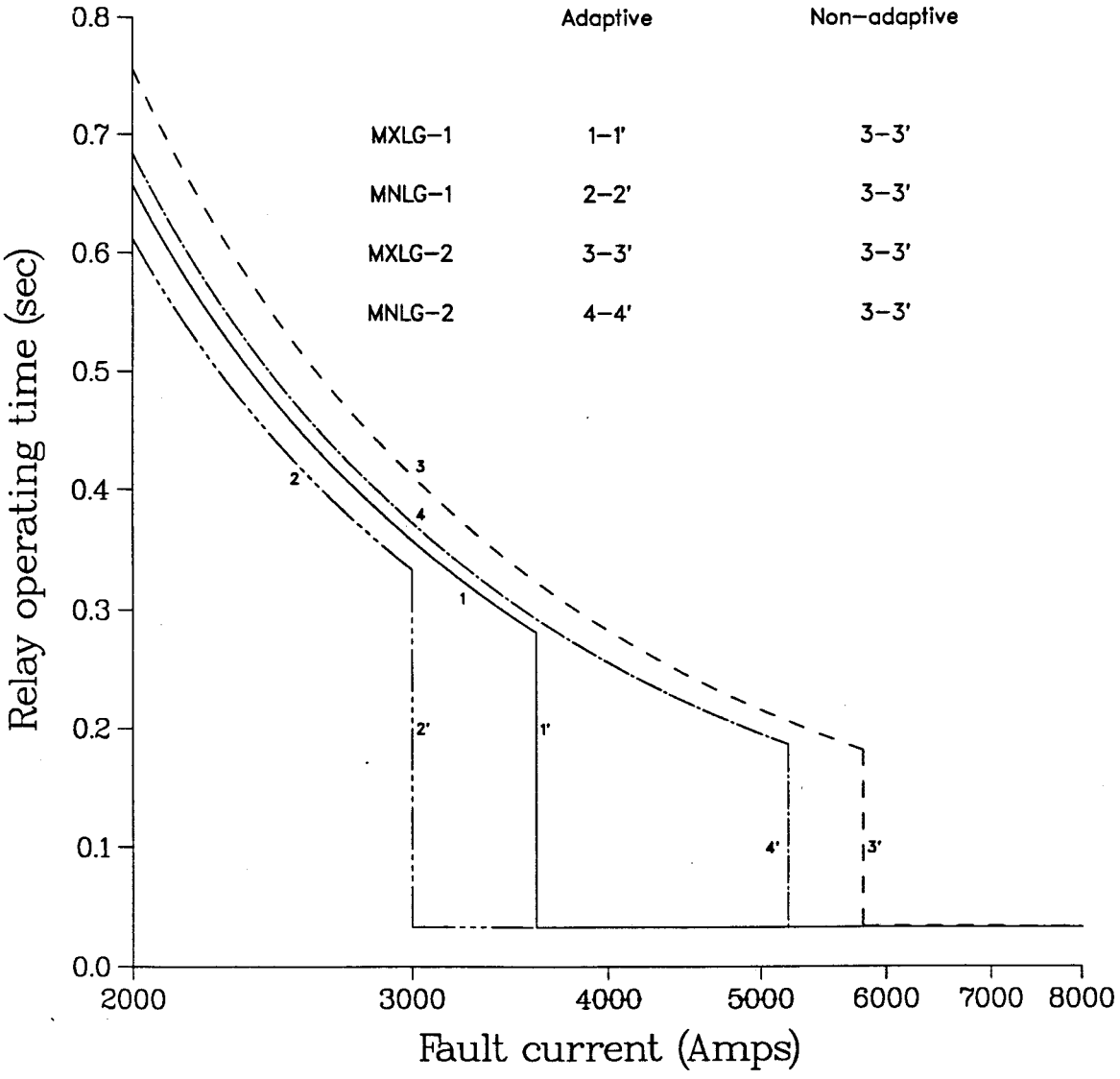

Figure 8.10: Operating characteristics of relay 5-1 with and without adaptive settings.

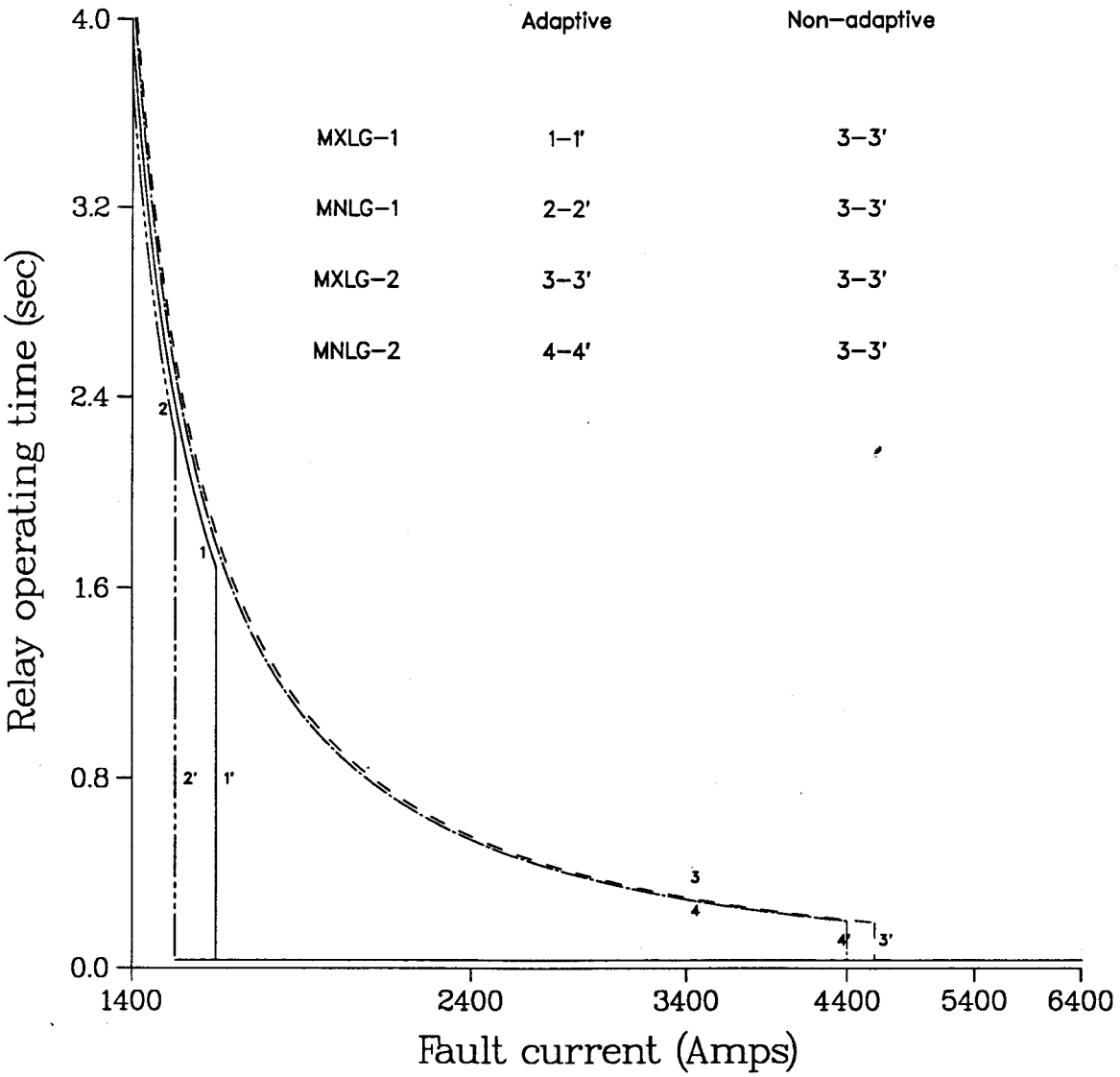

Figure 8.11: Operating characteristics of relay 5-2 with and without adaptive settings.

Table 8.3: Operating times of adaptive relays for primary and backup protection during MNLG-2.

Fault Locat.	Relay Location	Primary Protection			Backup Protection		
		Relay	Type of Prot.	Relay Operat. Time(s.)	Relay	Type of Prot.	Relay Operat. Time (s)
1-1	Near-end	1-1	Inst.	0.033	2-1	O/C	0.250
	Far-end	5-1	O/C	0.257	4-1	O/C	1.301
5-1	Near-end	5-1	Inst.	0.033	4-1	O/C	0.280
	Far-end	1-1	O/C	0.484	2-1	O/L	4.810
1-6	Near-end	1-6	Inst.	0.033	5-1	O/C	0.257
	Far-end	2-1	O/C	0.250	3-4	O/C	0.843
2-1	Near-end	2-1	Inst.	0.033	3-4	O/C	0.308
	Far-end	1-6	O/C	0.261	5-1	O/C	2.762
2-2	Near-end	2-2	Inst.	0.033	1-6	O/C	0.261
	Far-end	3-4	O/C	0.308	4-4	O/C	1.614
3-4	Near-end	3-4	Inst.	0.033	4-4	O/C	0.291
	Far-end	2-2	O/C	0.252	1-6	O/C	1.900
3-1	Near-end	3-1	Inst.	0.033	2-2	O/C	0.252
	Far-end	4-4	O/C	0.291	5-2		-
4-4	Near-end	4-4	Inst.	0.033	5-2	O/C	0.304
	Far-end	3-1	O/C	0.258	2-2	O/C	2.824
4-1	Near-end	4-1	Inst.	0.033	3-1	O/C	0.258
	Far-end	5-2	O/C	0.304	1-1	O/L	16.460
5-2	Near-end	5-2	Inst.	0.033	1-1	O/C	0.464
	Far-end	4-1	O/C	0.280	3-1	O/L	1.051

Table 8.4: Operating times of conventional (non-adaptive) relays for primary and backup protection during MNLG-2.

Fault Locat.	Relay Location	Primary Protection			Backup Protection		
		Relay	Type of Prot.	Relay Operat. Time(s.)	Relay	Type of Prot.	Relay Operat. Time (s)
1-1	Near-end	1-1	Inst.	0.033	2-1	O/C	0.264
	Far-end	5-1	O/C	0.285	4-1	O/C	4.185
5-1	Near-end	5-1	Inst.	0.033	4-1	O/C	0.838
	Far-end	1-1	O/C	0.669	2-1	O/L	10.516
1-6	Near-end	1-6	Inst.	0.033	5-1	O/C	0.285
	Far-end	2-1	O/C	0.264	3-4	O/C	0.892
2-1	Near-end	2-1	Inst.	0.033	3-4	O/C	0.319
	Far-end	1-6	O/C	0.316	5-1	O/C	7.858
2-2	Near-end	2-2	Inst.	0.033	1-6	O/C	0.316
	Far-end	3-4	O/C	0.319	4-4	O/C	2.021
3-4	Near-end	3-4	Inst.	0.033	4-4	O/C	0.302
	Far-end	2-2	O/C	0.257	1-6	O/C	3.647
3-1	Near-end	3-1	Inst.	0.033	2-2	O/C	0.257
	Far-end	4-4	O/C	0.302	5-2		-
4-4	Near-end	4-4	Inst.	0.033	5-2	O/C	0.327
	Far-end	3-1	O/C	0.339	2-2	O/C	3.312
4-1	Near-end	4-1	Inst.	0.033	3-1	O/C	0.339
	Far-end	5-2	O/C	0.327	1-1	O/L	-
5-2	Near-end	5-2	Inst.	0.033	1-1	O/C	0.669
	Far-end	4-1	O/C	0.838	3-1	O/L	4.531

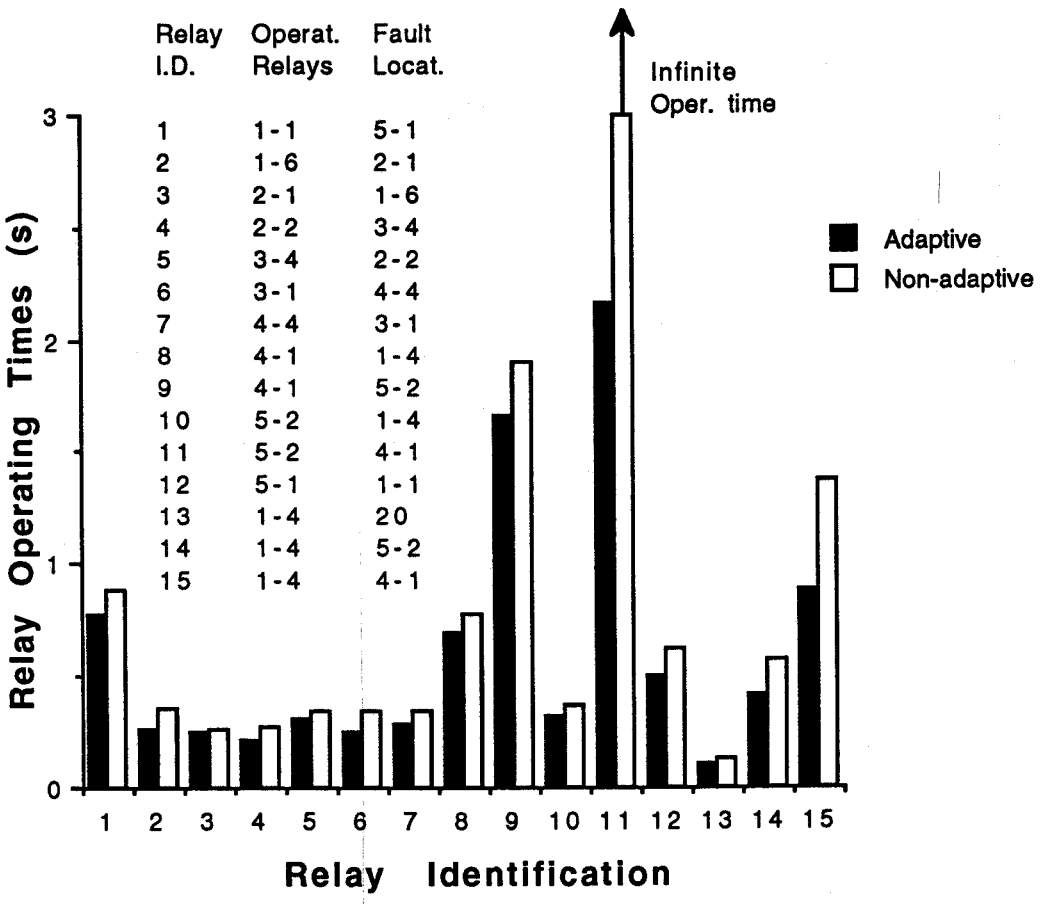

Figure 8.12: Primary relay operating times with and without adaptive settings of relays during MNLG-1.

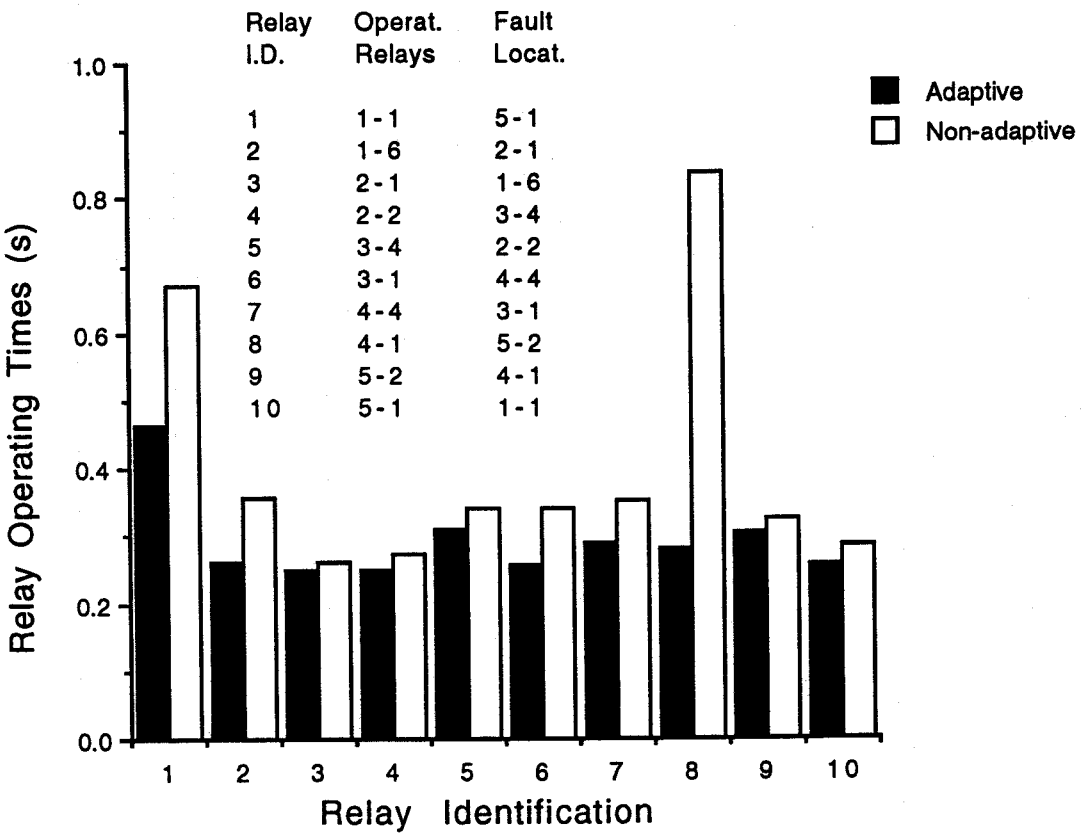

Figure 8.13: Primary relay operating times with and without adaptive settings of relays during MNLG-2.

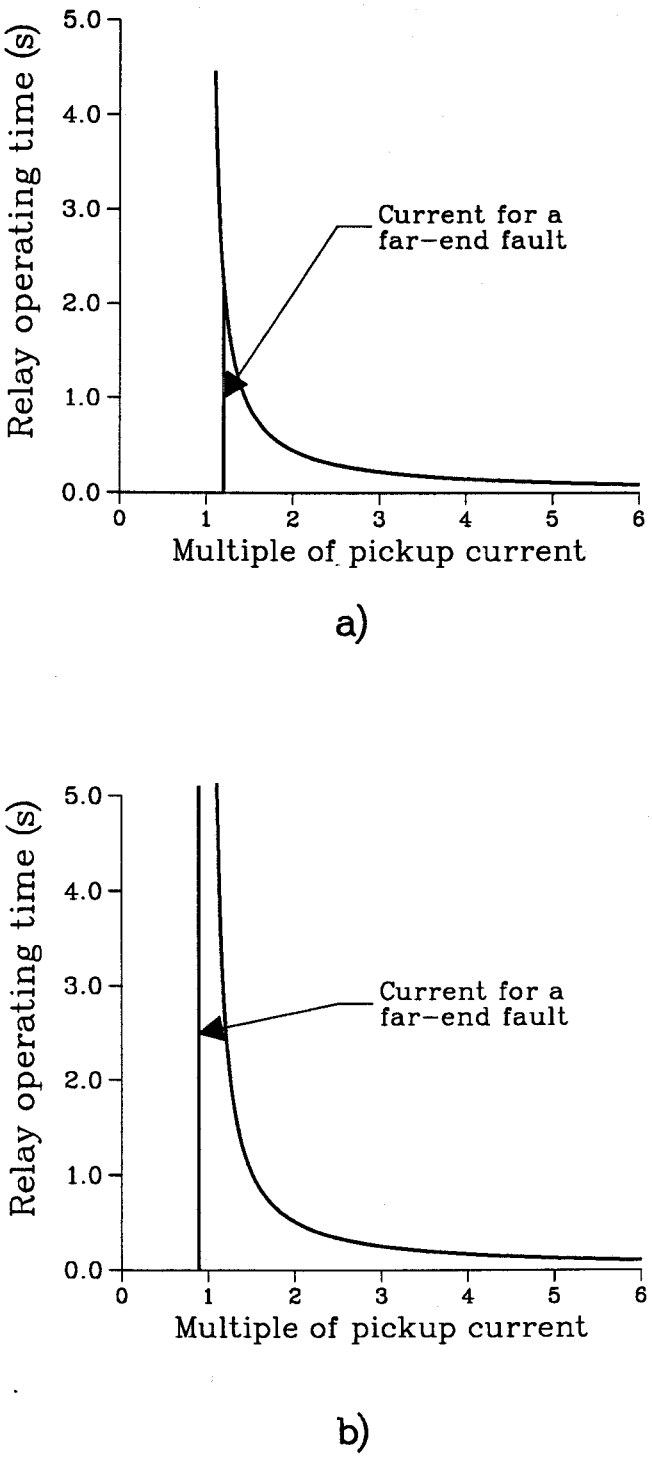

Figure 8.14: Operating states of relay 5-2 for a far-end fault during condition MNLG-1: (a) Adaptive setting, (b) Non-adaptive setting.

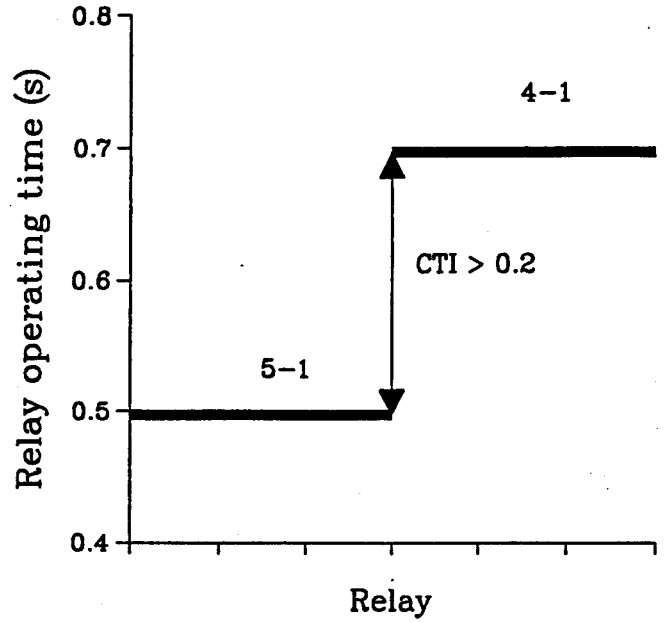

a)

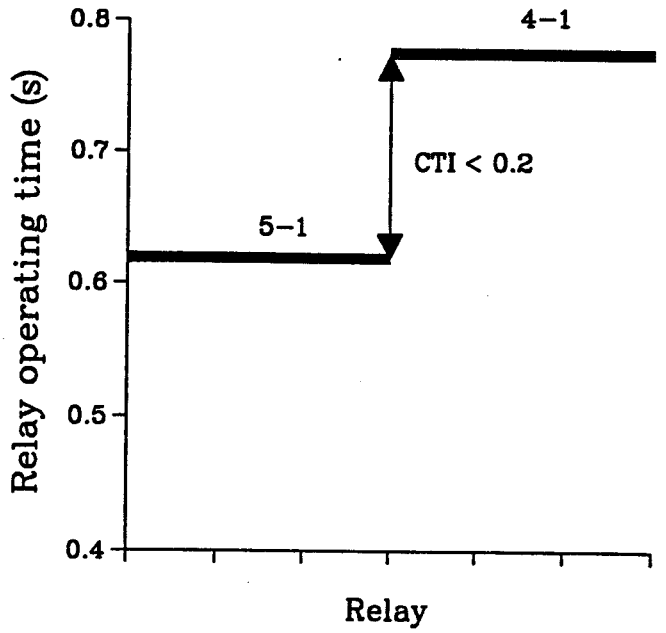

b)

Figure 8.15: Coordination between relays 5-1 and 4-1 during MNLG-1: (a) Adaptive setting, (b) Non-adaptive setting.

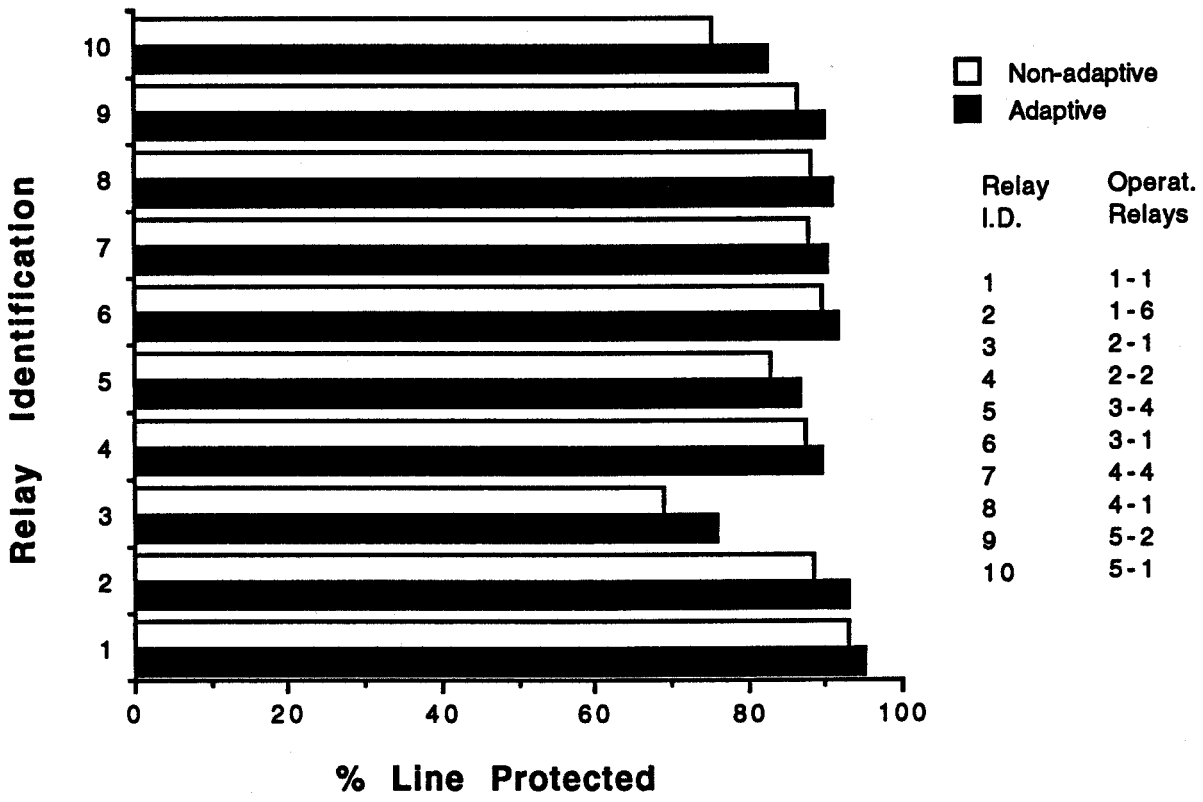

Figure 8.16: Percentage line protected with and without adaptive settings of instantaneous overcurrent relays during MNLG-1.

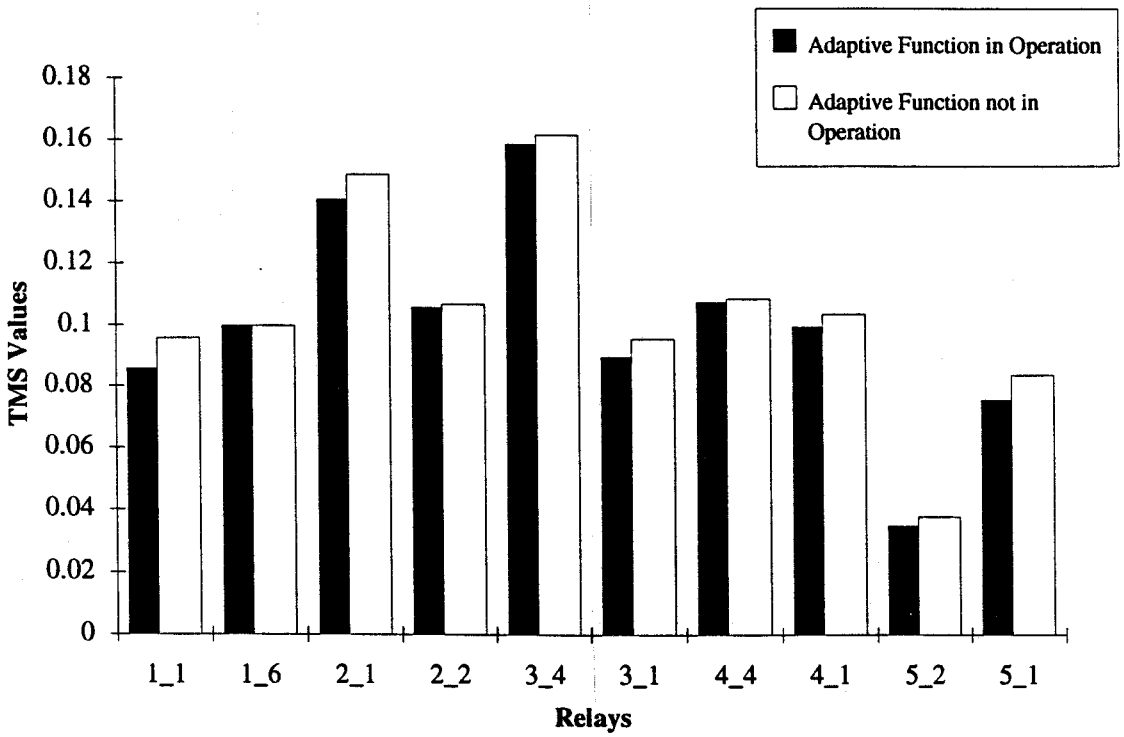

Figure 8.17: Locally Vs. centrally estimated TMS values.

9. SUMMARY AND CONCLUSIONS

9.1. Summary and Conclusions

Electric power systems experience faults and abnormal operating conditions. A fault can cause extensive damage to the system equipment. The equipment should, therefore, be protected to limit the damage. Protective relays used to perform this function have intelligence to detect faults and initiate opening of circuit breakers for isolating the faulted section.

The concepts of protecting power systems from faults and abnormal conditions have been described in the first chapter. Changing trends in power system protection leading to the development of microprocessor-based relays have been discussed. Recent trends of adaptive protection have also been described. The literature survey of adaptive relaying has been reported in that chapter. The major objectives of the work reported in this thesis were to design and implement in the laboratory a microprocessor-based adaptive protection system for a distribution network.

A typical distribution network has been described Chapter 2. Presently available protection schemes for distribution system are reviewed in that chapter. The commonly used protection schemes include overcurrent, directional overcurrent, instantaneous overcurrent, distance and pilot protections. The principles of each scheme and its advantage are discussed. The current-time scheme is preferred over the time-graded and current-graded schemes in protecting distribution networks. Directional inverse time overcurrent schemes are generally used to protect loop circuits so that relay coordination is achieved. The instantaneous relays are used to reduce the overall tripping time. These relays can be used if there exists an appreciable difference in currents during far and near-end faults. The distance and pilot relaying are commonly used in transmission

system protection. But many subtransmission and distribution systems use distance and pilot protection.

Overcurrent relaying algorithms, proposed in the past, have been reviewed in Chapter 3. Several models for representing time-current characteristic of overcurrent relays using polynomial and exponential equations are discussed. Both the polynomial and exponential equations accurately model the relay characteristics. However, exponential equations are simpler to implement in a microprocessor based relay. The least error squares (LES) technique, used for estimating the fundamental frequency components of currents and voltages, is discussed. Also, a fixed window recursive discrete Fourier transform (DFT) technique, for estimating currents and voltages, has been discussed. Since LES models the decaying dc component, it provides better estimates when a decaying dc component is present in a fault current.

Adaptive protection and its expected benefits in distribution systems are discussed in Chapter 4. Sensitivity and selectivity, the two most important issues, are subsequently addressed. The functional description of an adaptive protection, illustrated in that chapter, represents an hierarchical structure. The selected distribution network requires a special consideration for its instrumentation scheme because the ratio of fault and load currents experienced in the system is high. It is demonstrated in that chapter that two separate A/D converters along with two separate cts can alleviate the problems of saturations of cts and A/D converters.

Two software packages were needed for developing an adaptive protection system. The fifth chapter describes the first software package which performs relaying functions. In modelling the time-current characteristics, the exponential equation suggested by the IEC has been used. A presently available model of time-current characteristic has been modified for adaptive application. A mathematical model for directional relays has been developed which provides simpler implementation in a microprocessor. A 13-point least error square algorithm was used for estimating the fundamental frequency components of currents and voltages. The relaying software was implemented in a TMS320C25 microprocessor and is reported in this chapter. It is demonstrated in that chapter that it correctly emulates the overcurrent characteristics.

Another adaptive relaying software used for on-line determination of relay settings and their coordination is discussed in Chapter 6. This software has four modules. The development of each module has been discussed in details in the chapter. Previously proposed relay coordination techniques have been briefly reviewed in that chapter. The designed coordination software was developed based on an optimization technique. The development of the algorithm based on the optimization techniques has been described in the chapter. The coordination technique first selects the pickup settings which linearizes the current-time equation. It then employs the linear programming technique to optimize the *TMS* values. This technique has been developed in such a way that any infeasible constraint can be identified. The *TMS* values obtained in this technique are optimum which is one of the most important advantage over the other available coordination techniques.

A prototype system was designed in the power system laboratory at the University of Saskatchewan. This is discussed in the seventh chapter. The hardwares for implementing the scheme are described. The major hardwares consists of microcomputers, digital signal processing microprocessors, a local area network and a RS 232 link. Two application software, developed for communication between the substation controller and the central control computer, are discussed and described in the chapter.

System studies have been reported in Chapter 8. Several operating conditions were considered for conducting the studies. The relay setting criteria are illustrated in that chapter. The comparison of relay operating times and relay selectivity between the adaptive and non-adaptive approaches are reported. The results using the adaptive approach show that the relay sensitivities are better compare to the non-adaptive approach under selected operating conditions. The results also show that all the relays coordinate among themselves and achieve desired coordination margin for all operating conditions that were studied. The results show that the coverage of the instantaneous overcurrent relays is better if the adaptive approach is employed. Since the selected operating conditions are based on extreme operating states of the network, it is apparent that other conditions will exhibit similar results.

9.2. Suggestion for Future Work

It has been demonstrated in the thesis that the adaptive approach offers better protection compared to the conventional non-adaptive approach. In a distribution network, there are certain aspects which should be investigated for adaptive implementation. Future work should include the change in relay settings as the tap settings of transformers change. The cold-load inrush is another aspect that needs to be addressed. A relay should automatically change its settings during cold-load inrush period to prevent undesirable trippings. Many distribution networks use auto-reclosing features; reclosing of breakers can be made adaptive depending on the system operating conditions.

A protection system demands a high degree of reliability. Before applying to a real system, a reliability analysis of an adaptive system is important. Since adaptive protection requires the communication links between various devices, the possibility of developing a high fault tolerant communication network should be investigated. Finally, protection engineers would like to see the cost-benefit ratio. A study of cost is, therefore, required to be addressed. This should be carried out in conjunction with more work on implementation of the system.

REFERENCES

1. Mason, C. R., *The Art and Science of Protective Relaying,* John Wiley and Sons, Inc., New York; Chapman and Hall, Ltd., London, 1956.

2. Warrington, A.R. Van C., *Protective Relays,* Chapman and Hall, Ltd., London, 1968.

3. Rockefeller, G.D., "Fault Protection with a Digital Computer", *IEEE Transactions on Power Apparatus and Systems, Vol. PAS-88,* April 1969, pp. 438-462.

4. Gilcrest, G.B., Rockefeller, G.D. and Udren, E.A., "High Speed Distance Relaying Using A Digital Computer. Part I System Description", *IEEE Transactions on Power Apparatus and Systems, PAS-91, No.3,* May/June 1972, pp. 1235-1243.

5. Sachdev, M.S. (Coordinator), *Microprocessor Relays and Protection Systems,* IEEE Tutorial Course Text, Publication No. 88 EH0269-1-PWR, Piscataway, New Jersey, 1988.

6. Sachdev, M.S. (Coordinator), *Computer Relaying,* IEEE Tutorial Course Text, Publication No. 79 EH0148-7-PWR, New York, 1979.

7. Sachdev, M.S. and Wood, H.C., "Future Trends in Digital Relaying", *Conference on Digital Relaying- Future directions and Impact, Blacksburgh, VA, 1987, paper no. II-4,* pp. 1-8.

8. Rockefeller, G.D., Wagner, C.L., Linders, J.R., "Adaptive Transmission Relaying Concepts for Improved Performance", *IEEE Transaction on Power Delivery, Vol.3, No.4,* October 1988, pp. 1446-1458.

9. Horowitz, S.H., Phadke, A.G., Throp, J.S., "Adaptive Transmission System Relaying", *IEEE Transaction on Power Delivery, Vol.3, No.4,* October 1988, pp. 1436-1445.

10. Shah, K.R., Detjen, E.D., Phadke, A.G., "Feasibility of Adaptive Distribution Protection System Using Computer Overcurrent Relaying Concept", *IEEE Transaction on Industry Application, Vol.24, No.5,* Sept./Oct. 1988, pp. 792-797.

11. Jampala, A.K., Venkata, S.S., Domborg, M.J., "Adaptive Transmission Protection: Concepts and Computational Issues", *IEEE Transaction on Power Delivery, Vol.4, No.1,* January 1989, pp. 177-185.

12. U.S. Department of Energy, "The National Electric Relaibility Study", *DOE EP-003 Dist Category UC-97C,* April 1981.

13. Blackburn, J.L., *Protective Relaying Principles and Applications,* Marcel Dekker, Inc., New York, 1987.

14. Hieber, J.E., "Empirical Equations of Overcurrent Relay Curves for Computer Applications", *IEEE CP 31-CP-90*, 1965.

15. I.E.C. Standard, Publication No. 255-4, *Single Input Energizing Quantity Measuring Relays With Dependent Specified Time,* 1976.

16. Albrecht, R.E., Nisja, M.J., Peero, W.E., Rockefeller, G.D., and Wagner, C.L., "Digital Computer Protective Device Coordionation Program - I General Program Description", *IEEE Transactions on Power Apparatus and System, Vol. PAS-83*, April 1964, pp. 402-411.

17. Radke, G.E., "A Method for Calculating Time-Overcurrent Relay Settings by Digital Computer", *IEEE Transactions on Power Apparatus and System-Special Supplement, Vol. PAS-82*, 1963, pp. 189-205.

18. Singh, J., Sachdev, M.S., Fleming, R.J. and Krause, A.E., "Digital IDMT Directional Overcurrent Relay", *IEE Conference, Developments in Power System Protection, Publication No. 185*, April 1980, pp. 84-87.

19. Damborg, M.J., Ramaswami, R., Venkata, S.S. and Postforoosh, J.M., "Computer Aided Transmission Protection System Design, Part I: Algorithm", *IEEE Transaction on PAS, Vol. PAS-103*, 1984, pp. 51-59.

20. Sachdev, M.S. and Baribeau, M.A., "A New Algorithm for Digital Impedance Relays", *IEEE Transactions on Power Apparatus and Systems, Vol. PAS-98*, November/December 1979, pp. 2232-40.

21. Westinghouse Electric Corporation, *Instruction, Type CO Overcurrent Relay,* I.L.41-101 ed., 1973.

22. Luckett, R.G., Munday, P.J., Murray, B.E., "Substation Based Computer for Control and Protection", *IEE Conference, Developments in Power System Protection, Publication No. 125*, March 1975.

23. Brooks, A.E., "Distance Relaying Using Least Error Squares Estimates of Voltage, Current and Impedance", *Proceedings of the 10th Power Industry Computer Application Conference Publication No. 77 CH1131-2-PWR*, May 1977.

24. Ramamoorty, M., "A Note on Impedance Measurement Using Digital Computer", *IEE-IRE Proceeding (India), Vol.9, No.6*, November/December 1974.

25. Phadke, A.G., Hlibka, T. and Ibrahim, M., "A Digital Computer System for EHV Substation: Analysis and Field Tests", *IEEE Transactions on Power Apparatus and Systems, Vol. PAS-95, No.1*, January/February 1976, pp. 291-301.

26. Hope, G.S. and Umamaheswaran, V.S., "Sampling for Computer Protection of Transmission Lines", *IEEE Transactions on Power Apparatus and Systems, Vol. PAS-93, No.5*, September/October 1974.

27. Schweitzer, E.O., "The Design and Test of a Digital Relay for Transformer

Protection", *IEEE Transactions on Power Apparatus and Systems*, May/June 1979, pp. 795-805.

28. Hope, G.S., Malik, O.P. and Dash, P.K., "A New Algorithm for Impedance Protection of Transmission Lines", *Summer Meeting of the IEEE Power Engineering Society, Vancouver, B.C.*, July 1979.

29. Phadke, A.G., Throp, J.S., Adamiak, M.G., "A New Measurement Technique For Tracking Voltage Phasors, Local System Frequency, And Rate of Change of Frequency", *IEEE Transactions on Power Apparatus and Systems, Vol. PAS-102, No.5*, May 1983, pp. 1025-1038.

30. Sachdev, M.S. and Shah, D.V., "Transformer Differential and Restricted Earth Fault Protection Using A Digital Processor", *Transactions of the Engineering and Operating Division of the Canadian Electrical Association, Vol.20*, March 1981, pp. 1-11.

31. ANSI/IEEE Std.100-1988, *IEEE Standard Dictionary of Electrical and Electronics Terms*, 1988.

32. American National Standards Institute, *Requirements for Instrument Transformers*, ANSI Standard C57.13-1978 ed., 1978.

33. Sheingold, D.H. (edited), *Analog-Digital Conversion Handbook*, Prentice-Hall, 1986.

34. IEEE Working Group, Relaying Committee, "Relay Performance Considerations with Low Ratio Cts and High Fault Currents", *IEEE PES, paper no.92 SM 382-2 PWRD*, 1992.

35. IEEE Committee Report, "Computer Representation of Overcurrent Relay Characteristics", *IEEE Transaction on Power Delivery, Vol.4, No.3*, July 1989, pp. 1659-1667.

36. Westinghouse, *Applied Protective Relaying*, Westinghouse Electric Corporation, Relay Instrument Division, Newark, N.J.

37. Sachdev, M.S. and Wood, H.C., "Introduction and General Methodology of Digital Protection", *Canadian Electrical Association, Engineering and Operating Division Power System Planning and Operation Section*, March 1986.

38. Kernighan, B.W. and Ritchie, D.M., *The C Programming Langauge*, Prentice-Hall Inc., Englewood Cliffs, New Jersey, 1978.

39. Ariel Corporation, Highland Park, New Jersey, *Operating Manual For The DSP-C25 TMS320C25 DSP Board*, ed., 1989.

40. Sasson, A. M., Ehrmann, S.T., Lynch, P., Slyck, L.S.V., "On-Line Monitoring", *IEEE PES Summer Meeting, San Francisco, California, paper no. T 72 466-1*, July 9-14 1972, pp. 610-618.

41. Couch, G.H., and Morrison, I.F, "Data Validation and Topology Determination for Power System Monitoring and Control", *IEEE PES Summer Meeting & Energy Resources Conferences, Anaheim, California, paper no. C 74 361-2*, April 1974.

42. Stott, B., "Review of Load-Flow Calculation Methods", *Proceedings of the IEEE, Vol.62, No.7*, July 1974.

43. Elgerd, O.I., *Electric Energy Systems Theory: An Introduction,* McGraw Hill Book Company, New York, 1971.

44. IEEE Committee Report,, "Computer Aided Coordination of Line Protection Schemes", *IEEE Transaction on Power Delivery, Vol.6, No.2*, April 1991, pp. 575-583.

45. Knable, A.H., "A Standardised Approach to Relay Coordination", *IEEE Winter Power Meeting*, 1969.

46. Dwaraknath, M.H and Nowitz, L, "An Application of Linear Graph Theory for Co-ordination of Directional Overcurrent Relays", *Electric Power Problems: The Mathematical Challenge, Proceedings of the SIAM Conference, Seattle, Washington*, 1980, pp. 104-114.

47. Jenkins, L., Khincha, H., Shivakumar, S., Dash, P., "An Application of Functional Dependencies to the Topological Analysis of Protection Schemes", *IEEE Transaction on Power Delivery, Vol.7, No.1*, January 1992, pp. 77-83.

48. Urdaneta, A.J., Nadira, R., Jimerez, L.G.P., "Optimal Co-ordination of Directional Overcurrent Relays in Interconnected Power Systems,", *IEEE Transaction on Power Delivery, Vol.3, No.3*, July 1988, pp. 903-911.

49. Bradley S.P., Hax, A.C. and Magnanti, T.L., *Applied Mathematical Programming,* Addison-Weseley Publishing Company, California, 1977.

50. Jeter Melvyn W., *Mathematical Programming, An Introduction to Optimization,* Marcel Dekker Inc. New York, 1986.

51. Proteon Inc., Westborough, MA, USA, *High Performance Token Ring NetworkInterface Cards* .

52. Proteon Inc., Westborough, MA, USA, *The Series 70 Intelligent Wire Centers,* .

53. DigiBoard Incorporated, St. Louis Park, MW, USA, *DigiWare for PC/X,* .

54. Lefebvre, T., Nourris, M., Bornard, P., "A Local Area Network for Control Functions in EHV Substation", *Electricity de France*, 1986, pp. 270-274.

55. Suzuki et. al, "Development of a Substation Digital Protection and Control System using Fiber Optic Local Area Network", *IEEE Transactions on Power Delivery, Vol.4, No.3*, July 1989, pp. 1668-1775.

56. Puri, D., Hardy, H.R.S., Davall, P.W., Kennedy, W.O., McCuskee, L.B., Misskey, W.J., "A Local Area Network for an Electrical Substation", *IEEE Transactions on Power Apparatus and Systems, Vol. PAS-103, No.9*, September 1984, pp. 2399-2404.

57. Greenfield, David, "Into The Ring, Token Ring Gains Speed and Adherents", *Local Area Network Magazine*, 1989, pp. 134-142.

58. Novell Incorporated, Austin, Texas, USA, *Btrieve Record Management System* .

59. Greenleaf Software, Dallas, Texas, USA., *Greenleaf CommLib, Asychronous Communications Library for C,* 1992.

60. Westinghouse Electric Corporation, Product 42-86A, *Type SCV-D Current Transformers,* Westinghouse Electric Corporation, Measurement and Control Divison, Raleigh, Carolina, USA, .

A. Selection of Current Transformers

The current transformers for phase fault protection were selected based on maximum fault currents that the cts experience. The maximum fault currents at all relay locations are given in Table 4.2 in Chapter 4. Initially 2000/5 A cts were selected for fault currents between 20 to 50 kA and 1000/5 A cts for for fault currents between 10 to 20 kA. It was then examined whether these ratings are appropriate to sustain the fault currents. The first step was to determine the burdens on cts. Since the ANSI curve provides information concerning exciting voltage up to 1200/5 A ct, Westinghouse's ct excitation curve, shown in Figure A.1 was used for selecting 2000/5 A ct. Considering a ct rating of 2000/5 A, ct secondary burden of 0.96 ohm (from the curve), a lead burden of 0.30 ohm and relay burden of 0.50 ohm, a total burden of 1.8 ohm was estimated. For a fault current of 50 kA, ct secondary current is 125 A. Therefore, the voltage required to sustain the fault is 225 volts for a burden of 1.8 ohm. Since 2000/5 A ct can provide more than 300 volts (from the curve), this rating is in order for a fault current up to 50 kA.

In case of 1000/5 A ct, secondary burden is 0.70 ohm from the curve. Assuming the lead burden and relay burden are same, a total burden of 1.50 ohm was estimated. For a fault current of 20 kA, ct secondary current is 100 A. Therefore, the voltage required to sustain the fault is 150 volts. Since 1000/5 A ct can provide more than 200 volts, this rating is in order up to 20 kA fault current.

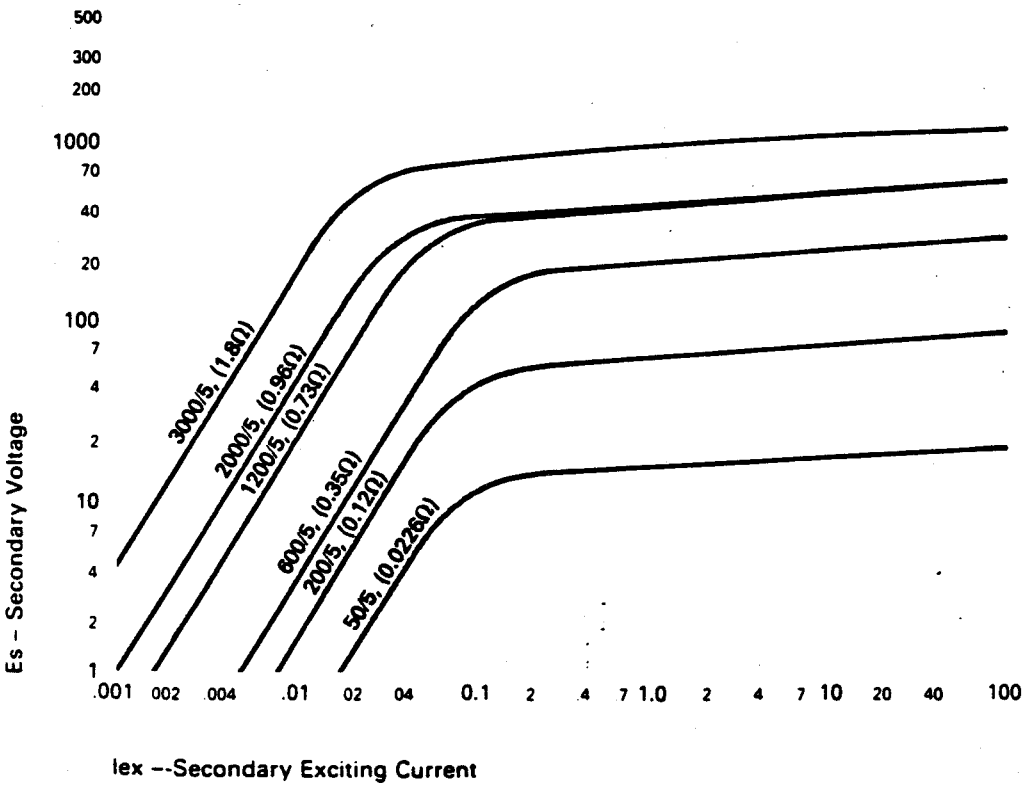

Figure A.1: Current transformer excitation curve [60].

B. Selection of Auxiliary Transformers

Auxiliary transformers are used to reduce the current levels before applying input signals to the A/D converters. Figure B.1 shows the arrangement of an auxiliary transformer with an A/D converter.

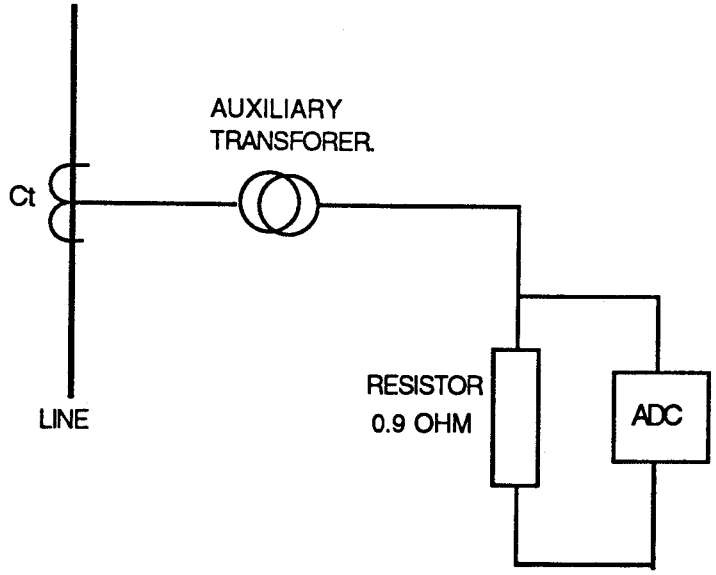

Figure B.1: Arrangement of an auxiliary transformer with an A/D converter.

During selection of an auxiliary transformer for phase faults, a dc offset factor of 2 was considered. With this dc offset, a 10 volt A/D converter would be inputed by 5 volts peak i,e $5/\sqrt{2}$ volts *rms*. For relay 1-1, current in the secondary side, corresponding to maximum fault current, is 117 A. This would require an auxiliary transformer ratio of $(117\times \sqrt{2}/5)$, which is 33:1. Considering a rating of 35:1, the maximum *rms* current to the input is 117/35, i.e. 3.90 A. Using a 0.9 ohm resistor to convert current into voltage, the applied voltage to the A/D converter would be 3.51 volts, i.e. 4.96 volts peak. Hence, 1 *LSB* of A/D converter would represent $(46800/4.96)\times (10/2^{12})$, i.e. 23 A which is quite reasonable resolution for this range of current.

For relay 1-4, the maximum current in the secondary side is 106.6 A. This would require an auxiliary transformer ratio of ($106.6\times\sqrt{2}/5$) which is 30.2:1. Considering a rating of 30:1, the maximum current to the input would be 106.6/30, i.e. 3.55 A. So the applied voltage to the converter is 3.2 volts, i.e. 4.53 volts peak which would provide a resolution of ($42642/4.53)\times (10/2^{12}$); 23 A. The currents at the secondary side of relay 1-6 and 2-2 are 106 A and 93 A respectively for which the rating of auxiliary transformer as 30:1 was selected.

The currents at the secondary side of relay 3-1, 4-4 and 5-1 are 81 A, 78 A and 82.5 A respectively for which the similar rating of auxiliary transformers were considered. For a secondary current of 82.5 A, the auxiliary transformer ratio is ($82.5\times\sqrt{2}/5$), i.e. 23.3:1. Considering a rating of 25:1, the maximum input current is 82.5/25, i.e. 3.3 A. So the applied voltage to the converter is 2.97 volts, i.e. 4.2 volts peak. This would provide a resolution of ($16207/4.2)\times (10/2^{12}$), i.e. 9.42 A. For relay 2-1, 3-4, 4-1 and 5-2, the secondary currents are 76.7, 74.6, 73 and 70.6 A respectively for which the same auxiliary transformer was considered. For 76.7 A secondary current, the rating of auxiliary transformer would be ($76.6\times\sqrt{2}/5$), i.e. 21.6:1. Let, 20:1 be the transformer ratio, then maximum input current is 76.6/20 which is 3.83 A. So the voltage applied to the A/D converter is 3.45 volts which is 4.87 volts peak. This would provide a resolution of ($15331/4.87)\times (10/2^{12}$), i.e. 7.68 A.

During selecting the A/D converters for metering and for moderate overload, no dc offset was considered. Three times of primary ct rating was considered as the maximum current that the cts for overload and metering will handle after which cts for phase faults will take over. So the secondary current at this condition is 15 A. The auxiliary transformer rating was selected as ($15 \times \sqrt{2}/10$), i.e 2:1. Therefore, maximum *rms* current to the input circuit is 15/2 volts which is 7.5 A *rms*, i.e. 10.6 A peak. Considering 0.9 ohm resistor, voltage applied to the A/D converter is 9.5 volts. Hence, 1 *LSB* of A/D converter represents ($2400/9.5) \times (10/2^{12}$) which is 0.62 A. This resolution is quite reasonable for this range of current.

C. Noise Amplification in a Nonrecursive Filter

The presence of noise affect the accuracy of the measurements. Depending on the magnitude of the filter coefficients, the adverse effect of noise on the measurements can be reduced. This can be demonstrated using a mathematical approach.

Suppose that some measurements are made. Let x_1 be a true measurement with an added noise n_i whose expected value $E(n_i) = 0$. The recorded measurement is $x_i + n_i$. Furthermore, let this noise n_i have a variance of σ^2. It is also assumed that for the actual measurements, $x_i + n_i$, the errors n_i are uncorrelated. Thus it is assumed that $E[n_i n_j] = \sigma^2$ for $j=i$, otherwise, 0. The condition of a zero mean is $E[n_i]=0$ and implies that there is no bias in the measurements. In both the cases the averaging over the ensemble of the noise is n_i.

A nonrecursive filter is defined by the formula

$$y_i = \sum_{k=-k}^{K} c_k (x_{i-k} + n_{i-k}). \qquad (C.1)$$

Since the E operator is applied only to the n_i and not to the c_k or x_{i-k}, the expected value is

$$E[y_i] = \sum_{k=-k}^{K} c_k (x_{i-k} + E[n_{i-k}]) = \sum_{k=-k}^{K} c_k x_{i-k}. \qquad (C.2)$$

The variance can be calculated with the following expression:

$$E[(\sum_{k=-k}^{K} c_k (x_{i-k} + n_{i-k}) - E(y_i))^2]. \qquad (C.3)$$

This expression can be rewritten as

$$E[\sum_{k=-k}^{K} c_k n_{i-k}]^2 = E[(\sum_{k=-k}^{K} c_k n_{i-k})(\sum_{j=-k}^{K} c_j (_{i-j})]^2. \qquad (C.4)$$

Since $E(n_i)=0$ and for $j \neq i$, $E(n_i n_j) = 0$, multiplying out and applying the operator E to the n_i leave only the terms given below.

$$\sum_{k=-k}^{K} c_k^2 E[n_k^2] = \sum c_k^2 \sigma^2 = \sigma^2 \sum_{k=-k}^{K} c_k^2. \qquad (C.5)$$

Thus the sum of the squares of the coefficients of a filter measures the amplification of the filtering process. It is for this reason that the sum of the squares of the coefficients of a nonrecursive filter plays a significant role.

D. Decoupled Load Flow Technique

Decoupled load flow method is similar to Newton-Raphson technique except that decoupled technique neglect the interdependence of MW flows and voltage magnitudes, and Mvar flows and phase angles in a power system.

The active and reactive powers flowing into any bus p of an n bus system can be written as

$$P_p = |V_p| \sum_{q=1}^{n} |V_q|(G_{pq}cos\delta_{pq} + B_{pq}sin\delta_{pq}), \qquad (D.1)$$

$$Q_p = |V_p| \sum_{q=1}^{n} |V_q|(G_{pq}sin\delta_{pq} - B_{pq}cos\delta_{pq}). \qquad (D.2)$$

Where:

$G_{pq} + jB_{pq}$	is the $(p,q)^{th}$ element of the bus admittance matrix,
δ_{pq}	is the phase angles of voltages at buses p and q,
V_p	is the voltage at bus p and
V_q	is the voltage at bus q.

For each bus, a similar pair of nonlinear equations are established. Equations D.1 and D.2 indicate that P_p and Q_q are functions of the magnitudes and phase angles of system bus voltages. An iterative solution of the equations is initiated by estimating the solution vector $[\delta^0 \ |V^0|]^T$ and expanding each function in the neighbourhood of this estimate using the Taylor series. Neglecting second and higher order terms of the series, Equations D.3 and D.4 are the first two terms of the Taylor series of Equations D.1 and D.2.

$$P_p(\delta_1^0 + \Delta\delta_1^0, \delta_2^0 + \Delta\delta_2^0, \ldots\ldots, \delta_n^0 + \Delta\delta_n^0,$$
$$|V_1^0| + \Delta V_1^0, |V_2^0| + \Delta V_2^0, \ldots\ldots, |V_n^0| + \Delta V_n^0)$$
$$= P_p(\delta_1^0, \delta_2^0, \ldots\ldots, \delta_n^0, |V_1^0||V_2^0| \ldots\ldots, |V_n^0|) +$$
$$\sum_{q=1}^{n} \frac{\partial P_p}{\partial \delta_q} \Delta\delta_q + \sum_{q=1}^{n} \frac{\partial P_p}{\partial |V_q|} \Delta V_q, \qquad (D.3)$$

$$Q_p(\delta_1^0 + \Delta\delta_1^0, \delta_2^0 + \Delta\delta_2^0, \ldots\ldots, \delta_n^0 + \Delta\delta_n^0,$$
$$|V_1^0| + \Delta V_1^0, |V_2^0| + \Delta V_2^0, \ldots\ldots, |V_n^0| + \Delta V_n^0)$$
$$= Q_p(\delta_1^0, \delta_2^0 \ldots\ldots, \delta_n^0, |V_1^0||V_2^0| \ldots\ldots, |V_n^0|) +$$
$$\sum_{q=1}^{n} \frac{\partial Q_p}{\partial \delta_q} \Delta\delta_q + \sum_{q=1}^{n} \frac{\partial Q_p}{\partial |V_q|} \Delta V_q. \qquad (D.4)$$

The left hand side of Equation D.3 is the scheduled active power injection into bus p and the first term of right hand side is the active power injection calculated using the estimated voltages. The difference between the scheduled and calculated power is known as active power mismatch and can be written as

$$\Delta P_p = \sum_{q=1}^{n} \frac{\partial P_p}{\partial \delta_q} \Delta\delta_q + \sum_{q=1}^{n} \frac{\partial P_p}{\partial |V_q|} \Delta V_q. \qquad (D.5)$$

Similarly, from Equation D.4 the reactive power mismatch can be written as

$$\Delta Q_p = \sum_{q=1}^{n} \frac{\partial P_p}{\partial \delta_q} \Delta\delta_q + \sum_{q=1}^{n} \frac{\partial P_p}{\partial |V_q|} \Delta V_q. \qquad (D.6)$$

Expressing Equation D.5 for all system buses except the swing bus and Equation D.6 for all load buses, the following set of Equations is obtained:

$$\begin{bmatrix} \Delta P \\ \Delta Q \end{bmatrix} = \begin{bmatrix} J_1 & J_2 \\ J_3 & J_4 \end{bmatrix} \begin{bmatrix} \Delta\delta \\ \Delta V/|V| \end{bmatrix}, \qquad (D.7)$$

where:

J_1, J_2, J_3 and J_4 are the submatrices of the Jacobian matrix.

$\Delta\delta$ is the vector increments in phase angles and

ΔV is the vector of increments in the voltage magnitudes.

The first step in decoupling is to neglect the submatrices J_2 and J_3 in Equation D.7. This procedure provides the following equations:

$$[\Delta P] = [J_1]\ [\Delta\delta], \tag{D.8}$$

$$[\Delta Q] = [J_4]\ [\Delta V/|V|]. \tag{D.9}$$

The elements of the submatrices J_1 and J_4, obtained from the Equations D.1 and D.2 are as follows:

$$J_1(p,p) = \frac{\partial P_p}{\partial \delta_p} = \sum_{q=1,q\neq p}^{n} |V_p V_q|(-G_{pq}sin\delta_{pq}+B_{pq}cos\delta_{pq}),$$

$$= -B_{pp}|V_p|^2 - Q_p. \tag{D.10}$$

$$J_1(p,q) = \frac{\partial P_p}{\partial \delta_q} = |V_p V_q|(G_{pq}sin\delta_{pq}-B_{pq}cos\delta_{pq}). \tag{D.11}$$

$$J_4(p,p) = |V_p|\frac{\partial Q_p}{\partial |V_p|} = |V_p| \sum_{q=1,q\neq p}^{n} |V_q|(G_{pq}sin\delta_{pq}-B_{pq}cos\delta_{pq})-2|V_p|^2 B_{pp},$$

$$= -B_{pp}|V_p|^2 + Q_p. \tag{D.12}$$

$$J_4(p,q) = |V_q|\frac{\partial Q_q}{\partial |V_p|} = |V_p V_q|(G_{pq}sin\delta_{pq}-B_{pq}cos\delta_{pq}). \tag{D.13}$$

In practical power systems, the following assumptions may be made:

$$\cos\delta_{pq} \approx 1;\ G_{pq}\sin\delta_{pq} << B_{pq}\ \ and\ \ Q_p << B_{pp}|V_p|^2.$$

With these assumptions, the terms of the Jacobian reduces to

$$J_1(p,p) = J_4(p,p) \approx -B_{pp}|V_p|^2, \qquad (D.14)$$

$$J_1(p,q) = J_4(p,q) \approx -B_{pq}|V_pV_q|. \qquad (D.15)$$

From Equations D.8 and D9 and using above assumptions, the following equations are obtained:

$$[\Delta P] = [B'_{pq}|V_p||V_q|]\,[\Delta\delta], \qquad (D.16)$$

$$[\Delta Q] = [B''_{pq}|V_p||V_q|]\,[\Delta V/|V|]. \qquad (D.17)$$

Where B'_{pq} and B''_{pq} are the elements of [-B] matrix.

These equations can be further simplified by incorporating the following modifications and assumptions:

1. Omit from [B'] the representation of those network elements that predominantly affect Mvar flows, such as shunt reactances and off-nominal transformer taps.

2. Omit from [B''], the angle shifting effects of phase shifters.

3. Neglect the series resistances when calculating the elements of [B'_{pq}]. Use the elements of the matrix [B'] for calculating the second order terms of Equation D.14.

4. Divide Equations D.14 and D.15 by $|V_p|$, and set $|V_q|$ terms to 1 *p.u.*

Incorporating the above modifications, and letting $V_p = V$ the simplified equations are

$$[\Delta P/|V|] = [B']\,[\Delta\delta], \qquad (D.18)$$

$$[\Delta Q/|V|] = [B'']\,[\Delta V]. \qquad (D.19)$$

In the above equations, matrices [B'] and [B''] are real, sparse and have the structures of [J_1] and [J_4] respectively. Since [B'] and [B''] contain only network admittances, they are constant and need to be trangularized only once at the beginning of the iterative process. The matrix [B''] is symmetrical and its upper triangular factor is stored. The matrix [B'] is also symmetrical, if there is no phase shifters in the network.

E. Simplex Method

The Simplex method iterates (pivots) by moving from one extreme point to another in search of an optimal extreme point. The method begins its search for an optimal extreme point from the origin. Before describing the Simplex method, some terminologies are defined as follows.

Euclidean Space: An m-dimensional Euclidean space, symbolized by E^m, is defined as the collection of all vectors $a = [a_1, \ldots\ldots a_m]$. For these vectors, addition and multiplication by a scalar are defined by the rules of matrix operations. Furthermore, associated with any two vectors in the collection is a non-negative number, called the distance between two vectors.

Basis: A basis for E^m is a set of m linearly independent vectors. Any vector in E^m can be expressed uniquely as a linear combination of the vectors of a given basis. The set of m unit vectors (1,0,.....0), (0,1,.....0), ..., (0, 0, ..., 1) is a basis for E^m.

Basic Solution: Given a system of m simultaneous linear equations in n unknowns, $Ax = b$, $m < n$ and rank of the matrix is m. If any $m \times m$ non-singular matrix is chosen from A, and if all the $n - m$ variables not associated with the columns of this matrix are set equal to zero, the solution to the resulting system of equations is called a basic solution. The m variables which can be different from zero are called basic variables.

The linear programming model can be written in general form as follows:

Objective: Minimize

$$z = \sum_{j=1}^{n} c_j x_j, \qquad (E.1)$$

Subject to

$$\sum_{j=1}^{n} a_{ij} x_j \geq b_i \ (i=1, 2,...m), \qquad x_j \geq 0, \tag{E.2}$$

where:

c_j	are the coefficients of objective function,
x_j	are the decision variables and
a_{ij}	are the constraint coefficients.

They can also be written as follows:

$$z = \bar{c}\,\bar{x}, \tag{E.3}$$

Subject to

$$A\,\bar{x} \geq \bar{b}, \qquad x \geq 0, \tag{E.4}$$

where:

A	is an m x n matrix,
$\bar{x}$	are n-vectors and
$\bar{b}$	is an m-vector.

The j^{th} column of matrix A is denoted as $\bar{a}_j$, $j=1,2,....n$. A matrix B will constitute of m linearly independent columns A and therefore, it will consist a basis for E^m. B will therefore be called a basis matrix. From the properties of a basis, any other vector in E^m can be written as a linear combination of the vectors in B. Therefore, any column of matrix A can be written as linear combination of the column in B as follows:

$$\bar{a}_j = y_{1j}\bar{a}_1 + y_{2j}\bar{a}_2 + ... + y_{mj}\bar{a}_m = \sum_{i=1}^{m} y_{ij} a_i. \tag{E.5}$$

For convenience, it is assumed that the basis B consists of $\bar{a}_1 \bar{a}_2 \ldots\ldots \bar{a}_m$ the first m columns of A. This can be assumed since the numbering of the vectors can be made arbitrarily. If $\bar{y}_j$ is an m component vector with components y_{ij}, then

$$[y_j] = \begin{bmatrix} y_{1j} \\ y_{2j} \\ . \\ . \\ y_{mj} \end{bmatrix}$$

Therefore, Equation E.5 can be written as $\bar{a}_j = B\bar{y}_j$. Since B is a basis for E^m and hence is a nonsingular matrix, $\bar{y}_j$ can also be written as $\bar{y}_j = B^{-1}\bar{a}_j$.

If matrix A is partioned into the basis matrix B and a non basic matrix, N, and $\bar{x}$ is partitioned into $\bar{x}_B$ and $\bar{x}_N$ then

$$A\bar{x} = (B,N)\bar{x} = (B,N) \begin{matrix} \bar{x}_B \\ \hline \bar{x}_N \end{matrix} = \bar{b}. \qquad (E.6)$$

Rearranging Equation E.6,

$$B\bar{x}_B + N\bar{x}_N = \bar{b}. \qquad (E.7)$$

However, by the definition of a basic solution corresponding to the basis matrix B, $\bar{x}_N = 0$. Therefore, $B\bar{x}_B = \bar{b}$, *or*, $\bar{x}_B = B^{-1}\bar{b}$. In this equation, $\bar{x}_B$ is a basic solution to $A\bar{x} = \bar{b}$ and variables in $\bar{x}_B$ are called basic variables.

Also, a scalar quantity is associated with each $\bar{x}_B$vector as follows:

$$z_j = \sum_{i=1}^{m} x_B c_i. \qquad (E.8)$$

With the preceding notation and definitions, the Simplex theory is developed. Considering some basic feasible solution exist, it is examined whether this solution is the optimal basic feasible solution or determine an improved basic feasible solution. Let's first attend to the latter. If a basic feasible solution to $A\bar{x} = \bar{b}$ exists and since it is assumed that the first m columns of A were a basis B, then

$$\sum_{i=1}^{m} x_{Bi}\bar{a}_i = \bar{b}. \qquad (E.9)$$

For obtaining a new basic feasible solution, one or more vectors $\bar{a}_i$ from B have to be removed and replace them with some other vectors $\bar{a}_j$ from N. In Simplex method, one vector is replaced at a time from the basis matrix and replaced, in order to generate a new basis matrix and its associated basic feasible solution. Each basic feasible solution corresponds to an extreme point of the convex set of feasible solutions. By replacing one vector at a time, it moves from one extreme point to an adjacent extreme point. The following section discusses how to find an improved adjacent extreme point or equivalently an improved basic feasible solution by replacing one basis vector with another.

Assume the basic feasible solution is in the form of Equation E.9. Consider the vectors of A which are not in the basis, they can be expressed in terms of the basis vectors as follows:

$$\bar{a}_j = \sum_{i=1}^{m} y_{ij}\bar{a}_i, \qquad j = m+1, \ldots\ldots, n. \qquad (E.10)$$

If some vector, $\bar{a}_j$, which is to enter the basis, then let us single out from the basis vectors, a vector $\bar{a}_r$ such that $y_{rj} > 0$. Then using Equation E.10,

$$\bar{a}_j = y_{rj}\bar{a}_r + \sum_{i=1}^{m} y_{ij}\bar{a}_i, \qquad i \neq r. \qquad (E.11)$$

Solving for $\bar{a}_r$ from Equation E.11,

$$\bar{a}_r = \frac{1}{y_{rj}} \bar{a}_j - \sum_{i=1}^{m} \frac{y_{ij}}{y_{rj}} \bar{a}_i, \quad i \neq r. \tag{E.12}$$

Substituting $\bar{a}_r$ from Equation E.12 into the basic solution given by Equation E.9,

$$\sum_{i=1}^{m} x_{Bi} \bar{a}_i + \frac{x_{Br}}{y_{rj}} \bar{a}_j - x_{Br} \sum_{i=1}^{m} \frac{y_{ij}}{y_{rj}} \bar{a}_i = \bar{b}, \quad i \neq r. \tag{E.13}$$

Rearranging Equation E.13, the following equation is obtained:

$$\sum_{i=1}^{m} (x_{Bi} - x_{Br} \frac{y_{ij}}{y_{rj}}) \bar{a}_i + \frac{x_{Br}}{y_{rj}} \bar{a}_j = \bar{b}. \tag{E.14}$$

The above equation is a new basic solution. Although it satisfies the constraints $A\bar{x} = \bar{b}$, it is not ensured that the basic solution is feasible. Examining Equation E.14, it is seen that the new values of x_{Bi}, x^{new}_{Bi}, is in the form,

$$x^{new}_{Bi} = x_{Bi} - x_{Br} \frac{y_{ij}}{y_{rj}} \geq 0 \qquad i \neq r, \tag{E.15}$$

$$x^{new}_{Br} = \frac{x_{Br}}{y_{rj}} \geq 0. \tag{E.16}$$

If $x_{Br} > 0$, then it must be required that $y_{rj} > 0$. If all the $y_{ij} \leq 0$, then the x^{new}_{Bi} will be non-negative. However, if some of the $y_{ij} > 0$, then whether or not $(x_{Bi} - x_{Br}) \frac{y_{ij}}{y_{rj}}$ be non-negative would depend upon which particular $\bar{a}_r$ had been chosen to remove from the basis. Let us now examine how to chose the correct $\bar{a}_r$.

If some $y_{ij} > 0$, Equation E.15 can be divided by y_{ij} to obtain

$$\frac{x_{Bi}}{y_{ij}} - \frac{x_{Br}}{y_{rj}} \geq 0. \tag{E.17}$$

To guarantee that Equation E.17 always holds, then column r can be chosen to be removed from the basis B as follows:

$$\frac{x_{Br}}{y_{rj}} = \min_{i} \{\frac{x_{Bi}}{y_{ij}},\ y_{ij} > 0\}. \qquad (E.18)$$

If r is chosen according to Equation E.18, then Equation E.17 will always be true.

It can be mentioned here that minimum in Equation E.18 may not be unique. In this case, one or more variables in the new basic solution will be zero and hence a degenerate basic feasible solution is obtained. If it were started with a degenerate solution, and x_{Br} was zero, then new basic solution would also be degenerate, since $x^{new}_{Br} = \frac{x_{Br}}{y_{rj}} = 0$. However, it is possible to have started with a degenerate solution and not have the new solution be degenerate. This can be found out by examining Equation E.18. If none of the y_{ij} were greater than zero for $x_{Bi} = 0$ in the degenerate solution, then x_{Br} would not be determined from the degenerate x_{Bi}. Hence the new solution might not be degenerate.

It is now summarised how to determine the vector $\bar{a}_r$ which is to leave the basis, B and the new basic variables are obtained.

1. Compute $\frac{x_{Br}}{y_{rj}}$ from Equation E.18 and this shows which column r of the basis matrix B is to be removed.
2. A new basis matrix, B^{new} consisting of columns $\bar{a}_i$, $i \neq r$ and a new column $\bar{a}_j$ is obtained.
3. The new basic solution is given by $\bar{x}^{new}_{B} = B^{new-1}\,\bar{b}$.
4. The new values of the basic variables are given by Equations E.15 and E.16.

The main concern in the preceding was to ensure that if a vector $\bar{a}_j$ came into the basis and a vector $\bar{a}_r$ was removed from the basis, the new solution would be a feasible solution.

It is now to be examined how to select the vector $\bar{a}_j$ which is to enter the basis in

order to give a new basic feasible solution. The following section illustrates how to find a new basic feasible solution that will give a greatest immediate decrease in the value of the objective function.

While searching for a new vector to enter the basis, theoretically any vector can be selected whose corresponding $z_j - c_j > 0$. However, a reduction in number of iteration can be achieved by selecting the one that gives the greatest immediate decrease in the value of the objective function. Hence the vector a_j to be selected which corresponds to

$$\bar{a}_j = \max_j (z_j - c_j). \qquad (E.19)$$

If there are ties, the rule is to select the vector with the lowest index j. This process of leaving and entering into the basis continues until there are no vector $\bar{a}_j$ with $z_j - c_j > 0$. This means for all vectors $\bar{a}_j$,$j=1,2,...m$, $z_j - c_j \leq 0$. It shall now be proved that when this occurs, z_0 is the minimum value of the objective function.

Let $x'_j \geq 0$, $j=1,2,....n$ be any feasible solution to $A\bar{x} = b$. Therefore,

$$\sum_{i=1}^{n} x'_j a_j = \bar{b}. \qquad (E.20)$$

The value of the objective function for this solution is

$$z' = c_1 x'_1 + c_2 x'_2 + ... + c_n x'_n. \qquad (E.21)$$

Any vector a_j in A can be expressed as a linear combination of the basis vector as follows:

$$\bar{a}_j = \sum_{i=1}^{m} y_{ij} \bar{a}_i. \qquad (E.22)$$

Substituting Equation E.22 into Equation E.20 and rearranging,

$$[\sum_{i=1}^{n} x_j' y_{1j}]\,\bar{a}_1 + [\sum_{i=1}^{n} x_j' y_{2j}]\,\bar{a}_2 + [\sum_{i=1}^{n} x_j' y_{mj}]\,\bar{a}_m = \bar{b}. \qquad (E.23)$$

Equation E.23 expresses the vector $\bar{b}$ in terms of the basis vectors, $\bar{a}_i$. If Equation E.20 and E.23 are compared, it is clear that

$$x_{Bi} = \sum_{i=1}^{m} x_j' y_{ij}, \quad i=1,2,.....,m. \qquad (E.24)$$

Since $z_j - c_j \leq 0$ for all j, so that replacing c_j by z_j in Equation E.21 yields

$$\sum_{i=1}^{n} x_j' z_j \leq z'_j, \quad j=1,2,.....,n, \qquad (E.25)$$

$$z_1 x'_1 + z_2 x'_2 + ... + z_n x'_n \leq z'. \qquad (E.26)$$

By definition, $z_j = \sum_{i=1}^{m} y_{ij}\, c_i$. Substituting this definition into above equation,

$$[\sum_{j=1}^{n} x_j' y_{1j}]c_1 + [\sum_{j=1}^{m} x_j' y_{2j}]c_2 + ... + [\sum_{j=1}^{m} x_j' y_{mj}]c_{Bm} \leq z'. \qquad (E.27)$$

Finally, substituting from Equation E.24 into Equation E.27,

$$c_1 x_{B1} + c_2 x_{B2} + ..+ c_m x_{Bm} = z_0 \leq z'. \qquad (E.28)$$

Equation E.28 reveals that a solution x_B is achieved for which all $z_j - c_j \leq 0$. Its value of z_0 is at least as small as any other feasible solution. Therefore, z_0 is the minimum value of the objective function.

The Algorithm

The algorithm has been developed based on Simplex method and is reported in Section 6.6.1. This section demonstrates a scenario when Phase I of Simplex method is not successfully achieved. This section also discusses the minimization of original z function, although it is similar to minimization of w function, described in Section 6.6.1.

It has been stated in Section 6.6.1 that if w cannot reduces to zero, no feasible solution exists to the original problem. One or more artificial variables at this stage will still be in basis with positive values. This is shown in Table E.1. In such case, at the end of Phase I, infeasible constraints corresponding to these positive artificial variables are withdrawn from the original problem and Phase I starts again.

The following procedure is followed to minimize the z function.

Step 1 If $\bar{z}_j \leq 0$ for $j = 1,2,....,n$ then stop, feasible solution is obtained. Where $\bar{z}_j$ is the current coefficient of column j in the z row. If it is not, then continue because there exists some $\bar{z}_j > 0$.

Step 2 Select the column to pivot in, i.e. the variable to introduce into the basis as

$$\bar{c}_l = \max_j \{\bar{z}_j\}$$

Such that $\bar{z}_j > 0$.

Step 3 Choose the row r to pivot in (i.e. the variable to drop from the basis) by the ratio test:

$$\frac{\bar{b}_r}{\bar{a}_{rl}} = \min_i \{\frac{\bar{b}_i}{\bar{a}_{il}}\}, \quad \bar{a}_{il} > 0.$$

Where $\bar{b}_i$ and $\bar{a}_{il}$ are the current values of row i and current coefficient of column l in row i respectively.

Step 4 Replace the basic variables in row r with variables l as follows:

Table E.1: Tableau showing end of Phase I with positive value in w and artificial variable in basis.

Basis	Current Values	x_1	x_2	.....	x_n	x_{s1}	x_{s2}	.....	x_{sm}	x_{t1}	x_{t2}	.....	x_{tm}
x_g	b_g	a_{g1}	a_{g2}	....	a_{gn}	a_{gs1}	a_{gs2}	.....	a_{gsm}	a_{gt1}	a_{gt2}	.....	a_{gtm}
x_h	b_h	a_{h1}	a_{h2}	.....	a_{hn}	a_{hs1}	a_{hs2}	.....	a_{hsm}	a_{ht1}	a_{ht2}	.....	a_{htm}
...	....												
...	....												
x_{tk}	b_k	a_{k1}	a_{k2}	....	a_{kn}	a_{ks1}	a_{ks1}	.....	a_{ksm}	a_{kt1}	a_{kt2}	.....	a_{ktm}
...	....												
x_r	b_r	a_r	a_{r2}	....	a_{rn}	a_{rs1}	a_{rs2}	.....	a_{rsm}	a_{rt1}	a_{rt2}	.....	a_{rtm}
z	b'	c'_1	c'_2	....	c'_n	c'_{s1}	c'_{s2}	.....	c'_{sm}	c'_{t1}	c'_{t2}	.....	c'_{tm}
w	b"	w_1	w_2	....	w_n	w_{s1}	w_{s2}	....	w_{sm}	w_{t1}	w_{t2}	....	w_{tm}

Note: b_k and b" are positive; w_1, w_2, ... in w row are either 0 or less than 0.

$$\bar{b}_r^{new} = \frac{\bar{b}_r}{\bar{a}_{rl}},$$

$$\bar{b}_i^{new} = \bar{b}_i - \frac{\bar{b}_r}{\bar{a}_{rl}} \geq 0, \quad i \neq r.$$

Step 5 Go to Step 1.

F. Record Management Software

In Btrieve record management software, file is the highest level database. It consists of series of pages. A page is the unit of storage which Btrieve transfers between memory and disk. A file is composed of a header page, data pages, and index pages. In creating a file, a fixed size for each page is specified. The page size is always a multiple of 512 bytes, up to 4096 bytes.

The Position Block

Btrieve uses an area of memory called the position block to maintain logical positioning information for use in accessing records. It maintains positioning and other necessary information associated with each open file. It stores this information in a 128-byte block of memory which passes between Btrieve and the application program. Some of the information contained between Btrieve and the application program are given below.

1. The current index path identifier, i.e. key number.
2. Three record pointers reflecting the logical currency based on the current key number. These records pointers are, previous pointer, current pointer points to the most recently accessed record and next record pointer.

Data Buffer Length

While using data buffer, application program must pass the length of the data buffer in an integer variable. For a file with a fixed length record, this parameter should match the record length specified the file first created. When records are inserted or a file is updated with variable record length, this parameter should equal the record length specified that has been specified during creating the file plus the number of characters included beyond the fixed length portion. While retrieving a variable length records, this parameter should be large enough to accommodate the longest record in the file.

Record Length

To calculate the record length, two steps are performed. Firstly, the logical record length is determined by calculating how many bytes of data needs to be stored in the fixed length portion of each record. This value is specified while creating the file. Second the physical record length is determined by calculating how many bytes of data including Btrieve's overhead are required to store the fixed length portion of each record. For files with fixed length records and no duplicate keys, the physical record length equals the logical record length. Compressed records always have a fixed record length of five bytes.

Key

In accessing the records, keys are used. Since Btrieve has no way of knowing the structure of the records in each file, each key is defined by identifying its offset in bytes from the beginning of the record and specifying the number of bytes to be used for that key. For example, suppose a particular key begins at the eighth byte of the record and extends for four bytes. Now, if a record is inserted into the file, Btrieve will extract four bytes, beginning at the eighth byte and use this extracted value to position the record in the index. Six key attributes, duplicate, modifiable, segmented, descending, null and manul, can be specified. When a key is specified with no duplicates, Btrieve does not allow an application to add multiple records to the file with the same value in this key field. Btrieve stores duplicate key values in the chronological order of insertion into the file. If one segment of a segmented key allows duplicates, all of the segments must allow duplicates.

G. Test Results

Test results for maximum load and generating condition with line 1-20 open (MXLG-2) are reported in Chapter 7. In this appendix, test results for other conditions are demonstrated.

Table G.1: Output from the topology detection module showing the circuits that are in operation during line 1-20 closed.

Circuit No.	Breaker No.	From	To	Line Parameter *p.u*
1	CB 1-6	1	6	0.723+j0.270
2	CB 1-1	1	28	0.386+j1.048
3	CB 1-4	1	28	0.585+j0.817
4	CB 2-1	2	8	1.218+j0.861
5	CB 2-2	2	9	1.047+j3.333
6	CB 3-1	3	12	0.555+j1.734
7	CB 3-4	3	11	0.591+j1.841
8	CB 4-1	4	16	0.688+j1.842
9	CB 4-4	4	15	1.042+j3.248
10	CB 5-1	5	21	0.427+j1.065

Table G.1 continued.

11	CB 5-2	5	22	0.536+j1.241
12	-	6	7	0.683+j1.064
13	-	7	8	0.243+j0.374
14	-	9	10	0.209+j0.653
15	-	10	11	0.077+j0.240
16	-	12	13	0.663+j2.160
17	-	13	14	0.357+j1.163
18	-	14	15	0.149+j0.463
19	-	16	17	1.024+j3.180
20	-	17	18	0.400+j0.616
21	-	18	19	0.165+j0.498
22	-	19	20	0.165+j0.498
23	-	20	21	0.804+j1.759
24	-	22	23	0.251+j0.407
25	-	23	24	0.337+j0.653

Table G.1 continued.

26	-	24	25	0.110+j0.171
27	-	25	26	0.173+j0.266
28	-	26	27	0.521+j0.801
29	-	27	28	0.464+j1.402

Table G.2: Output file from the state estimation module during condition MXLG-1.

Bus No.	Generated P *p.u*	Voltage Magnitude *p.u*	Phase Angle *rad.*	From	To	Line Flow P	Q
1	0.39285	1.02000	0.00000	1	6	0.961	-0.289
2	1.35213	1.02000	-0.02389	1	28	0.863	0.528
3	0.69892	1.02000	-0.01349	1	20	1.016	0.153
4	0.98084	1.02000	-0.00861	2	8	0.285	0.543
5	0.79092	1.02000	-0.00360	2	9	0.133	0.156
6	-	1.01526	-0.00870	3	12	0.229	0.112
7	-	1.00947	-0.01898	3	11	0.531	0.053
8	-	1.01202	-0.01986	4	16	0.308	0.239
9	-	1.01355	-0.02661	4	15	0.394	0.077
10	-	1.01555	-0.02376	5	21	0.749	0.332
11	-	1.01600	-0.02262	5	22	0.877	0.459
12	-	1.01686	-0.01671	6	7	0.954	-0.055
13	-	1.01332	-0.02046	7	8	-0.145	-0.594
14	-	1.01215	-0.02171	9	10	-0.497	-0.151
15	-	1.01360	-0.02022	10	11	-0.498	-0.032
16	-	1.01361	-0.01251	12	13	0.210	0.102
17	-	1.00764	-0.01497	13	14	0.129	0.062
18	-	1.00811	-0.01403	14	15	-0.392	-0.191
19	-	1.01083	-0.01069	16	17	0.127	0.149

Table G.2 continued.

20	-	1.01297	-0.00717	17	18	-0.143	0.017
21	-	1.01342	-0.00995	18	19	-0.780	-0.291
22	-	1.00984	-0.01178	19	20	-0.781	-0.175
23	-	1.00710	-0.01339	20	21	0.125	-0.083
24	-	1.00524	-0.01360	22	23	0.594	0.313
25	-	1.00478	-0.01358	23	24	0.143	0.213
26	-	1.00454	-0.01325	24	25	0.115	0.199
27	-	1.00464	-0.01177	25	26	-0.047	0.120
28	-	1.01133	-0.00679	26	27	-0.137	0.076
-	-	-	-	27	28	-0.468	-0.323

Table G.3: Output file from the state estimation module during condition MNLG-1.

Bus No.	Generated P *p.u*	Voltage Magnitude *p.u*	Phase Angle *rad.*	From	To	Line Flow P	Q
1	-0.40046	1.02000	0.00000	1	6	0.480	-0.303
2	0.62313	1.02000	-0.01093	1	28	0.446	-0.118
3	0.28811	1.02000	-0.00603	1	20	0.488	0.020
4	0.43802	1.02000	-0.00397	2	8	0.140	0.244
5	0.02418	1.02000	-0.00115	2	9	0.070	0.053
6	-	1.01741	-0.00336	3	12	0.118	0.032
7	-	1.01488	-0.00869	3	11	0.262	-0.010
8	-	1.01627	-0.00921	4	16	0.158	0.105
9	-	1.01757	-0.01264	4	15	0.193	0.000
10	-	1.01871	-0.01129	5	21	0.392	0.080
11	-	1.01868	-0.01072	5	22	0.421	-0.056
12	-	1.01882	-0.00783	6	7	0.477	-0.063
13	-	1.01753	-0.00994	7	8	-0.071	-0.331
14	-	1.01721	-0.01069	9	10	-0.245	-0.100
15	-	1.01804	-0.01000	10	11	-0.246	0.019
16	-	1.01705	-0.00609	12	13	0.109	0.027
17	-	1.01448	-0.00759	13	14	0.069	0.007
18	-	1.01479	-0.00718	14	15	-0.192	-0.119
19	-	1.01621	-0.00555	16	17	0.068	0.060

Table G.3 continued.

20	-	1.01705	-0.00373	17	18	-0.072	-0.005
21	-	1.01753	-0.00485	18	19	-0.390	-0.160
22	-	1.01848	-0.00648	19	20	-0.391	-0.040
23	-	1.01830	-0.00788	20	21	0.044	-0.048
24	-	1.01885	-0.00861	22	23	0.281	-0.126
25	-	1.01901	-0.00881	23	24	0.056	-0.115
26	-	1.01950	-0.00898	24	25	0.042	-0.122
27	-	1.02137	-0.00925	25	26	-0.039	-0.161
28	-	1.01954	-0.00493	26	27	-0.084	-0.183
-	-	-	-	27	28	-0.249	0.216

Table G.4: Output file from the state estimation module during condition MNLG-2.

Bus No.	Generated P *p.u*	Voltage Magnitude *p.u*	Phase Angle *rad.*	From	To	Line Flow P	Q
1	-0.72207	1.02000	0.00000	1	6	0.612	-0.446
2	0.73101	1.02000	-0.01818	1	28	0.811	-0.276
3	0.28751	1.02000	-0.02150	2	8	0.011	0.391
4	0.49944	1.02000	-0.03137	2	9	0.198	0.014
5	0.19742	1.02000	-0.02647	3	12	0.247	-0.007
6	-	1.01685	-0.00470	3	11	0.133	0.028
7	-	1.01496	-0.01234	4	16	0.287	0.126
8	-	1.01658	-0.01368	4	15	0.064	0.041
9	-	1.01753	-0.02441	5	21	0.753	0.085
10	-	1.01867	-0.02396	5	22	0.060	0.113
11	-	1.01872	-0.02396	6	7	0.608	-0.207
12	-	1.01879	-0.02566	7	8	0.059	-0.476
13	-	1.01753	-0.03070	9	10	-0.117	-0.140
14	-	1.01723	-0.03303	10	11	-0.117	-0.020
15	-	1.01805	-0.03297	12	13	0.238	-0.013
16	-	1.01580	-0.03563	13	14	0.197	-0.034
17	-	1.01132	-0.04090	14	15	-0.064	-0.160
18	-	1.01102	-0.04118	16	17	0.196	0.080

Table G.4 continued.

19	-	1.01214	-0.04012	17	18	0.056	0.014
20	-	1.01267	-0.03888	18	19	-0.263	-0.141
21	-	1.01599	-0.03386	19	20	-0.263	-0.021
22	-	1.01831	-0.02660	20	21	-0.315	-0.046
23	-	1.01833	-0.02619	22	23	-0.079	0.045
24	-	1.01898	-0.02409	23	24	-0.304	0.056
25	-	1.01924	-0.02351	24	25	-0.318	0.049
26	-	1.01989	-0.02248	25	26	-0.400	0.009
27	-	1.02227	-0.01912	26	27	-0.445	-0.013
28	-	1.01981	-0.00919	27	28	-0.611	0.385

Table G.5: Output of the fault analysis module for condition MXLG-1.

Relay Location	Fault Location	Fault Current *Amps*
1-1	2-1/2-2	-267
1-1	3-1/3-4	243
1-1	4-1/4-4	404
1-1	5-1/5-2	4945
1-1	20	-955
1-1	1-1	46860
1-6	2-1/2-2	8967
1-6	3-1/3-4	2336
1-6	4-1/4-4	121
1-6	5-1/5-2	-1521
1-6	1-6	42898
2-1	1-1/1-6	6690
2-1	3-1/3-4	-1951
2-1	4-1/4-4	-340
2-1	5-1/5-2	1921
2-1	20	3498
2-1	2-1	15243

Table G.5 continued.

2-2	1-1/1-6	-1641
2-2	3-1/3-4	4806
2-2	4-1/4-4	943
2-2	5-1/5-2	-353
2-2	20	-690
2-2	2-2	18568
3-1	1-1/1-6	530
3-1	2-1/2-2	-837
3-1	4-1/4-4	3531
3-1	5-1/5-2	388
3-1	20	895
3-1	3-1	16192
3-4	1-1/1-6	1798
3-4	2-1/2-2	4561
3-4	4-1/4-4	-777
3-4	5-1/5-2	483
3-4	20	809
3-4	3-4	14956
4-1	1-1/1-6	3548
4-1	2-1/2-2	532
4-1	3-1/3-4	-748
4-1	5-1/5-2	1809
4-1	20	4215
4-1	4-1	14529

Table G.5 continued.

4-4	1-1/1-6	358
4-4	2-1/2-2	997
4-4	3-1/3-4	3505
4-4	5-1/5-2	-233
4-4	20	-732
4-4	4-4	15619
5-1	1-1/1-6	2783
5-1	2-1/2-2	804
5-1	3-1/3-4	415
5-1	4-1/4-4	250
5-1	20	-132
5-1	5-1	16549
5-2	1-1/1-6	3259
5-2	2-1/2-2	905
5-2	3-1/3-4	608
5-2	4-1/4-4	1272
5-2	20	5791
5-2	5-2	13236
1-4	2-1/2-2	-835
1-4	3-1/3-4	799
1-4	4-1/4-4	3940
1-4	5-1/5-2	6440
1-4	20	20619
1-4	1-4	42772

Table G.6: Output of the fault analysis module for condition MNLG-1.

Relay Location	Fault Location	Fault Current *Amps*
1-1	2-1/2-2	-506
1-1	3-1/3-4	-114
1-1	4-1/4-4	92
1-1	5-1/5-2	4442
1-1	20	-488
1-1	1-1	42583
1-6	2-1/2-2	8760
1-6	3-1/3-4	2303
1-6	4-1/4-4	62
1-6	5-1/5-2	-1677
1-6	1-6	39100
2-1	1-1/1-6	6382
2-1	3-1/3-4	-2116
2-1	4-1/4-4	214
2-1	5-1/5-2	1865
2-1	20	3442
2-1	2-1	13962

Table G.6 continued.

2-2	1-1/1-6	-1709
2-2	3-1/3-4	4669
2-2	4-1/4-4	928
2-2	5-1/5-2	-419
2-2	20	-769
2-2	2-2	17367
3-1	1-1/1-6	481
3-1	2-1/2-2	-921
3-1	4-1/4-4	3410
3-1	5-1/5-2	357
3-1	20	865
3-1	3-1	14719
3-4	1-1/1-6	1760
3-4	2-1/2-2	4366
3-4	4-1/4-4	-873
3-4	5-1/5-2	462
3-4	20	805
3-4	3-4	13563
4-1	1-1/1-6	33393
4-1	2-1/2-2	484
4-1	3-1/3-4	-859
4-1	5-1/5-2	1741
4-1	20	4047
4-1	4-1	13252

Table G.6 continued.

4-4	1-1/1-6	422
4-4	2-1/2-2	974
4-4	3-1/3-4	3380
4-4	5-1/5-2	-304
4-4	20	-811
4-4	4-4	14373
5-1	1-1/1-6	2306
5-1	2-1/2-2	541
5-1	3-1/3-4	159
5-1	4-1/4-4	30
5-1	20	-132
5-1	5-1	15414
5-2	1-1/1-6	2978
5-2	2-1/2-2	793
5-2	3-1/3-4	487
5-2	4-1/4-4	1124
5-2	20	5426
5-2	5-2	12345
1-4	2-1/2-2	-1023
1-4	3-1/3-4	645
1-4	4-1/4-4	3728
1-4	5-1/5-2	6104
1-4	20	19603
1-4	1-4	388875

Table G.7: Output of the fault analysis module for condition MNLG-2.

Relay Location	Fault Location	Fault Current *Amps*
1-1	2-1/2-2	-897
1-1	3-1/3-4	100
1-1	4-1/4-4	1199
1-1	5-1/5-2	5273
1-1	1-1	36503
1-6	2-1/2-2	8638
1-6	3-1/3-4	2393
1-6	4-1/4-4	464
1-6	5-1/5-2	-676
1-6	1-6	34605
2-1	1-1/1-6	6471
2-1	3-1/3-4	-2190
2-1	4-1/4-4	-235
2-1	5-1/5-2	893
2-1	2-1	13971
2-2	1-1/1-6	-1900
2-2	3-1/3-4	4693
2-2	4-1/4-4	1056
2-2	5-1/5-2	-91
2-2	2-2	17278

Table G.7 continued.

3-1	1-1/1-6	-198
3-1	2-1/2-2	-997
3-1	4-1/4-4	3442
3-1	5-1/5-2	776
3-1	3-1	14812
3-4	1-1/1-6	1953
3-4	2-1/2-2	4387
3-4	4-1/4-4	-1002
3-4	5-1/5-2	82
3-4	3-4	13502
4-1	1-1/1-6	1117
4-1	2-1/2-2	119
4-1	3-1/3-4	-645
4-1	5-1/5-2	3180
4-1	4-1	13299
4-4	1-1/1-6	228
4-4	2-1/2-2	1049
4-4	3-1/3-4	3319
4-4	5-1/5-2	-725
4-4	4-4	12838
5-1	1-1/1-6	3983
5-1	2-1/2-2	915
5-1	3-1/3-4	40

Table G.7 continued.

5-1	4-1/4-4	-1164
5-1	5-1	10958
5-2	1-1/1-6	-891
5-2	2-1/2-2	-250
5-2	3-1/3-4	884
5-2	4-1/4-4	3212
5-2	5-2	13171

Table G.8: Operating times of adaptive relays for primary and backup protection during MXLG-1.

Fault Locat.	Relay Location	Primary Protection			Backup Protection		
		Relay	Type of Prot.	Relay Operat. Time (s)	Relay	Type of Prot.	Relay Operat. Time (s)
1-1	Near-end	1-1	Inst.	0.033	2-1 5-2 4-1	O/C O/C O/C	0.250 0.300 0.608
	Far-end	5-1	O/C	0.408	4-1	O/C	0.608
5-1	Near-end	5-1	Inst.	0.033	4-1 1-4	O/C O/C	1.484 0.518
	Far-end	1-1	O/C	0.250	2-1 4-1	O/C O/C	1.251 1.484
1-6	Near-end	1-6	Inst.	0.033	5-1 4-1 5-2	O/C O/C O/C	0.408 0.608 0.300
	Far-end	2-1	O/C	0.250	3-4	O/C	0.944
2-1	Near-end	2-1	Inst.	0.033	3-4	O/C	0.303
	Far-end	1-6	O/C	0.290	5-1 4-1 5-2	O/L O/L -	8.10 12.06 -
2-2	Near-end	2-2	Inst.	0.033	1-6	O/C	0.290
	Far-end	3-4	O/C	0.303	4-4	O/C	2.326
3-4	Near-end	3-4	Inst.	0.033	4-4	O/C	0.290
	Far-end	2-2	O/C	0.220	1-6	O/C	4.701
3-1	Near-end	3-1	Inst.	0.033	2-2	O/C	0.220
	Far-end	4-4	O/C	0.283	5-2 1-4	- -	- -
4-4	Near-end	4-4	Inst.	0.033	5-2 1-4	O/L O/C	2.984 1.210
	Far-end	3-1	O/C	0.329	2-2	O/C	4.601
4-1	Near-end	4-1	Inst.	0.033	3-1	O/C	0.329
	Far-end	5-2 1-4	O/L O/C	2.984 0.8878	1-1 2-1 1-1	- - -	- - -
5-2	Near-end	5-2	Inst.	0.033	1-1	O/C	0.250
	Far-end	4-1 1-4	O/C O/C	1.484 0.416	3-1 2-1 1-1	O/L O/C O/C	17.50 1.251 0.742
1-4	Near-end	1-4	Inst	0.033	5-1 2-1	O/C O/C	0.408 0.250
	Far-end	5-2 4-1	O/C O/C	0.327 0.608	3-1	O/L	3.260

Table G.9: Operating times of adaptive relays for primary and backup protection during MNLG-1.

Fault Locat.	Relay Location	Primary Protection			Backup Protection		
		Relay	Type of Prot.	Relay Operat. Time (s)	Relay	Type of Prot.	Relay Operat. Time (s)
1-1	Near-end	1-1	Inst.	0.033	2-1 5-2 4-1	O/C O/C O/C	0.250 0.327 0.698
	Far-end	5-1	O/C	0.498	4-1	O/C	0.698
5-1	Near-end	5-1	Inst.	0.033	4-1 1-4	O/C O/C	1.665 0.490
	Far-end	1-1	O/C	0.772	2-1 4-1	O/C O/C	1.255 1.667
1-6	Near-end	1-6	Inst.	0.033	5-1 4-1 5-2	O/C O/C O/C	0.498 0.698 0.327
	Far-end	2-1	O/C	0.250	3-4	O/C	0.939
2-1	Near-end	2-1	Inst.	0.033	3-4	O/C	0.307
	Far-end	1-6	O/C	0.264	5-1 4-1 5-2	- O/L -	- 11.430 -
2-2	Near-end	2-2	Inst.	0.033	1-6	O/C	0.264
	Far-end	3-4	O/C	0.307	4-4	O/C	2.161
3-4	Near-end	3-4	Inst.	0.033	4-4	O/C	0.290
	Far-end	2-2	O/C	0.210	1-6	O/C	3.044
3-1	Near-end	3-1	Inst.	0.033	2-2	O/C	0.210
	Far-end	4-4	O/C	0.290	5-2 1-4	- -	- -
4-4	Near-end	4-4	Inst.	0.033	5-2 1-4	- O/C	- 1.105
	Far-end	3-1	O/C	0.253	2-2	O/C	3.637
4-1	Near-end	4-1	Inst.	0.033	3-1	O/C	0.253
	Far-end	5-2 1-4	O/L O/C	2.168 1.105	1-1 2-1 1-1	- - -	- - -
5-2	Near-end	5-2	Inst.	0.033	1-1	O/C	0.772
	Far-end	4-1 1-4	O/C O/C	1.665 0.490	3-1 2-1 1-1	O/L O/C O/C	6.364 1.255 1.334
1-4	Near-end	1-4	Inst.	0.033	5-1 2-1	O/C O/C	0.498 0.250
	Far-end	5-2 4-1	O/C O/C	0.326 0.698	3-1	O/L	2.050

Table G.10: Operating times of adaptive relays for primary and backup protection during MXLG-2.

Fault Locat.	Relay Location	Primary Protection			Backup Protection		
		Relay	Type of Prot.	Relay Operat. Time(s.)	Relay	Type of Prot.	Relay Operat. Time (s)
1-1	Near-end	1-1	Inst.	0.033	2-1	O/C	0.250
	Far-end	5-1	O/C	0.252	4-1	O/C	1.200
5-1	Near-end	5-1	Inst.	0.033	4-1	O/C	0.281
	Far-end	1-1	O/C	0.486	2-1	O/L	5.630
1-6	Near-end	1-6	Inst.	0.033	5-1	O/C	0.252
	Far-end	2-1	O/C	0.250	3-4	O/C	0.881
2-1	Near-end	2-1	Inst.	0.033	3-4	O/C	0.304
	Far-end	1-6	O/C	0.257	5-1	O/C	2.762
2-2	Near-end	2-2	Inst.	0.033	1-6	O/C	0.258
	Far-end	3-4	O/C	0.304	4-4	O/C	1.750
3-4	Near-end	3-4	Inst.	0.033	4-4	O/C	0.285
	Far-end	2-2	O/C	0.250	1-6	O/C	2.091
3-1	Near-end	3-1	Inst.	0.033	2-2	O/C	0.250
	Far-end	4-4	O/C	0.285	5-2		-
4-4	Near-end	4-4	Inst.	0.033	5-2	O/C	0.285
	Far-end	3-1	O/C	0.267	2-2	O/C	3.300
4-1	Near-end	4-1	Inst.	0.033	3-1	O/C	0.267
	Far-end	5-2	O/C	0.285	1-1	O/L	7.095
5-2	Near-end	5-2	Inst.	0.033	1-1	O/C	0.487
	Far-end	4-1	O/C	0.281	3-1	O/L	1.230